The Creation of Long Distance Directional Plasma Discharges via the Exploding Wire Technique

David Smith

A thesis submitted in partial fulfilment
of the requirements for the degree of
Master of Engineering
in
Electrical and Computer Engineering
at the
University of Canterbury,
Christchurch, New Zealand.

2008

ABSTRACT

This thesis describes the work completed to create long distance directional discharge using the exploding wire technique.

A historical literature review gives the previous works completed on exploding wires dating back to 1780. The review also gives the current understanding of the exploding wire phenomena.

The design and construction of a test set to create long distance exploding wires is outlined. A capacitor bank, high voltage switch, charging circuit, hand earths design and construction methods are given.

The measurement of the impulse and charging voltage and current is explored and solutions found. Design and construction of a Rogowski Coil and associated circuitry is outlined. Development of software made for reconstruction of rogowski signals is outlined.

Results of testing of different wire explosions is given. It is found that if the charge voltage of the capacitors is to high the wire explodes to fast to remove all charge from the capacitors. If the charge is too low the wire may not have enough energy to explode. Conditions for maximum energy discharged by a plasma shrouded exploding wire are found for varying wire diameters and lengths up to 10m.

ACKNOWLEDGEMENTS

I would like to express my thanks to the many people that have helped with this project. Firstly and foremost Dr Wade Enright, for his support and guidance through out the project. Wade your friendship and mentoring has enlightened me to the joys of electrical engineering. You have helped make me into a moral engineer. Your guidance over the last few years will stay with me for the rest of my career.

I would also like to thank the Electric Power Engineering Centre (EPE Centre) and Mr. Joseph Lawrence. The financial support given has allowed for my studies to be conducted without the additional pressure of increasing debt or part time work.

Many thanks must go to the friendship and support I have got from the Academic and Technical staff within the department. Cheers Ken Smart for getting things done and giving me grief about not coming to soccer. Cheers Jac Woodburg for putting up with all my equipment in your lab and your awesome technical advice. Cheers to the late Ron Battersby for your help in the workshop.

I would also like to thank my close friends made over the years whose guidance, support and distraction has been welcome. Cheers Lance, Nick, Simon, John, and Clayton... I told you I'd finish!

I would also like to thank my Mum and Dad for understanding that being a student for a couple more years wasn't the worst idea I have ever come up with. Your guidance and assistance was awesome.

Finally I would thank Davinia. Thanks for all the support and encouragement that you have given me.

PUBLISHED PAPERS

The following paper was published as a result of the work associated with that presented in this thesis.

D. W. R. Smith, W. Enright, and P. Bodger. A Test Circuit for Long Distance Directional Plasma Discharge Using the Exploding Wire Technique. *15th International Symposium on High Voltage Engineering*, August 2007, Ljubljana , Slovenia. T3-489. pg122.

CONTENTS

LIST OF FIGURES

LIST OF TABLES

Chapter 1

INTRODUCTION

1.1 GENERAL

Wires may explode when a large current is conducted through them. Due to the inductance of a wire the current must initially increase from zero. In the initial stages of a wire explosion the relatively low current will cause heating of the wire. This heating will in turn force the wire to expand. Time continues and the current through the wire may increase to high levels if the supply allows. As the wire expands it produces stress upon itself due to the speed of expansion. This stress forms a stress wave which may flex and break the wire into pieces.

Generally to force a substantial current through a fine wire high voltages are used. As the wire fractures the voltage between fractures maybe enough to force an arc between them. The arc is a form of plasma that will grow as it heats with conduction of current. The plasma arc may grow to envelope the segments of fractured wire creating a plasma conduction path independent of the wire. The conduction path in plasma results in a long distance arc sustained as long as the energy of the supply allows. With the use of exploding wires long distance arcing can occur with relatively low voltages.

In order to produce an exploding wire two elements are required; the wire and a current source able to deliver the thousands of amps required to fracture the wire. Current sources can be capacitor banks. These are slowly charged and then quickly discharged through the wire. DC generator sets have also been used to produce the current required.

To the observer a long distance plasma path produced via the exploding wire technique is a loud, instantaneous flash of brilliant light. With the use of equipment within the University of Canterbury (UoC) Electrical and Computer Engineering Departments High Voltage Laboratory discharges of up to 70 meters have been produced using 60kV.

Exploding wires have been reported as early as 1780. Understanding has been gleamed from physical experimentation and theoretical models. In the years of research conducted to date no model has accurately been able to predict the outcome of an exploding wire discharge from the initial conditions.

1.2 THESIS OUTLINE

Chapter 2 gives a historical review of the available literature to date. Efforts are made to give the current state of understanding in the exploding wire field.

Chapter 3 describes the design and construction of a high voltage high current test set. The design and construction of a capacitor bank with the use of 15kV oil filled capacitors is given. A high voltage, high current, sliding electrode switch was designed and constructed. The switch allows for safe discharge of the charged capacitors through the wire. A set of hand earths was designed and built. All equipment testing to international standards is noted.

Chapter 4 describes the selection of current and voltage measurement equipment. Charging voltage and current can be measured via commercially available equipment. To measure current a Rogowski Coil was produced with associated circuitry and software.

Chapter 5 describes testing conducted to find measured results for exploding wires. The results give insight into the maximum energy dissipation possible for a wire.

Chapter 6 summaries the research described within the thesis and describes the proposed direction for future research and development.

Chapter 2

LITERATURE REVIEW

2.1 INTRODUCTION

This chapter presents some previous work given in the literature which is necessary to appreciate this thesis. In order to create a long distance directional plasma discharge using the exploding wire technique, an exploding wire needs to be produced. This chapter gives a short history of the discovery and early research into exploding wires. Current research offers many dynamic processes involved in an exploding wire. Much work has been conducted as to which of these processes is important to the overall wire explosion. This chapter gives a brief overview as to these processes and their effects on the exploding wire.

2.2 LITERATURE REVIEW

While wire explosion has been known for many years it remains a relatively poorly understood phenomena. Several dynamic processes occur during the explosion mechanism all encompassed by the term "exploding wire". The aim of this chapter is not to explain the exploding wire mechanism completely but give a understanding of the current state of the field. Also of interest to the Author is electrical high energies research and pulsed power applications. The purpose of these applications are different from the goals of this work, much can be drawn from the measurementation and methods of observation used. This allows for the author to apply theses methods to the field of exploding wire.

Exploding wire is a phenomena researched under many different guises and for various purpose's. The literature is not abundant in its depth but there are a several groupings of papers;

- Theoretical - Literature regarding one or more of the dynamic mechanisms of

exploding wire. This literature is more common as exploding wires are a "test case" for magnetohydrodynamics, and magneto-elasticity. [22, 34, 21, 23, 24]

- Purely Empirical - Literature outlining experimentation conducted and the results found [16, 14, 15]
- Theoretical and Empirical - Usually a attempt to explain a phenomena with the use of physical theory. [17]

Literature sources can be hard to find due military applications of exploding wires. In some cases information is limited or not re-workable. It is common to find exploding wire cited for the following research applications;

- Pressure vessel testing with reference to high rise-time shock waves or to failure. [37]
- Use of exploding wires as a method of propulsion.[19]
- Use of exploding wires as a controlled ignition system for solid fuelled ammunitions[32]
- The use of exploding wires as an ignition system for confined fusion research [16]
- The use of exploding wire for thin film production. [18]

The first observation of exploding wires can be dated to Nairne's experiments in 1780 [25]. Nairne used a static charge generator to charge a capacitor and "shorten" an iron wire significantly without melting it. This phenomena was observed 3 years later by Nairne in 1783. In this case an exploding wire was produced by a lighting strike on a farmhouse. The lighting strike appeared to of entered the top of a lead downpipe and then proceed into the house via a "night bolt" or door lock made from a wire. This wire door lock had been shortened significantly. [26]. Nairne latter utilised this phenomena to prove that electrical current was the same in all parts of a single conductor

During the early 20th century research into exploding wires increased due to military interest. Anderson began the first modern experimentation in the 1920's. His research found that temperatures in exploding wires could reach those of the sun [12]. This ignited interest in the topic until the late 1950's when the field held its first official meeting of researchers. A series of four conferences was held titled "Exploding Wire Phenomenon" and a of a set of proceedings was produced for each. With the use of analog oscilloscopes voltage and current waveforms where found for lower energy, short wire explosions(under 30cm, up to 50kJ of energy). One of the most important findings was that of Nasilowski's; some wires where fracturing in the solid state, rather than

locally vaporising as previously thought. This repelled a strictly thermodynamic model of exploding wire and allowed for a new physical process to be considered [12].

It became apparent during this time that no two wire explosions are the same. It was found that the mechanisms where highly dependent upon the local experimental conditions, furthermore slight differences hindered the absolute repeatability of the experiments[12].

These dependencies on the local conditions where addressed some years latter by a in-depth analysis of the state of the field and accompanying experimentation conducted by Bennett et al in 1974 [9]. He found a bevy of reasons behind the differences in repeated experimentation;

- Crystal size and orientation of metal wire.
- Orientation of the cold pre-drawn metal wire.
- Pressure surrounding the metal wire.
- Circuit differences.
- Initial temperature differences.

Also cited around this time, with the advent of high speed x-ray photography, is the appearance of mechanical vibrations along the wire. An example of x-ray photography is given in Figure 2.1 from [31]. With this new technology it was also found that electromagnetic skin effect has no effect on the actual thermal explosion mechanism [12]. This was proven via experiments repeated with different metals with different magnetic permeability. The photography of steel and copper wires with vastly different skin depths showed that both have clear density striations of similar appearance. This experiment reiterated that wire shattered in the solid state.

Imperial work in the field has reduced in its quantity since the heavily experimental period of the 1920's - 1970's. A much more theoretical approach was taken by researchers to the mechanism. Much of the more recent literature has been dealing with the mechanisms using analytical physic's. Electrodynamics, electromagnetic, thermal, elasto-plastic and mechanical theories are the current focus of research. [24]

Not all experimentation has ceased at this time. The opening of the Sandia National Laboratories z machine in June 1980 allowed for high energy experimentation. Based in Albuquerque, New Mexico the machine produces the highest energy wire explosions ever produced. The purpose of this machine is to create very high pressures in

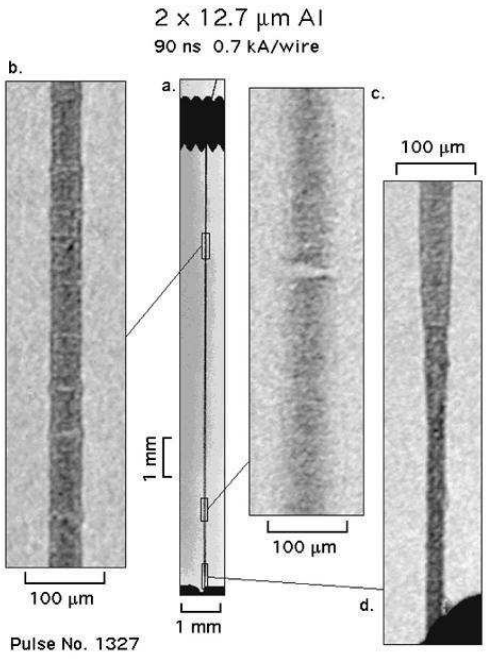

Figure 2.1 An example of an exploding Al wire radiograph. Note the eruption of the metal

plasma to study fusion. An array of tungsten wires is placed in the machine and a current of 20 million amps conducted through the tungsten. The wires explode and the resulting plasma compresses with the electromagnetic pinch effect. As the plasma is so compressed, temperatures of up to 3 million Kelvin, and a instantaneous power of 230TW have been achieved. The machine is also the most powerful x-ray source ever produced. The machines electromagnetic field induces high voltages in all of the surrounding metallic structures as shown in 2.2.

Discussions on the mechanism of exploding wire have become vastly more involved in recent years via the use of modern physics and computer modelling for verification. It is necessary to mention certain mechanisms which are thought to be involved in the exploding wire process.

One of the most obvious mechanisms of exploding wire is the thermodynamic process that occurs during the explosion. The wire undergos a thermodynamical mechanism during the various stages of explosion. Initially when the current is relatively low the wire undergos standard resistance heating. The wire is essentially a resistor at this point.

Expanding on this initial process, the model can be simplified by assuming the surrounding environment as a perfect thermal insulator. This assumption holds due to the relative speed of heating. The energy installed into the wire is found using Equation 2.1.

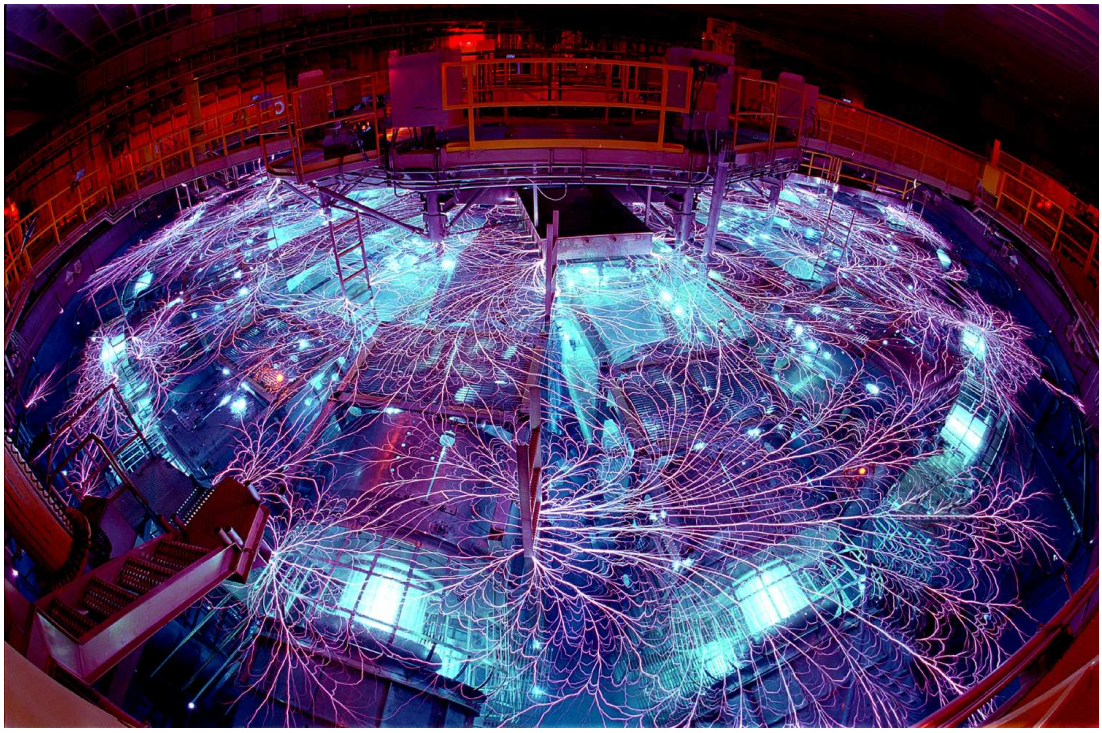

Figure 2.2 Electrical arcing and corona caused by electromagnetic fields in the Sandia National Laboratories Z-Machine

$$E_{installed} = \int_0^t (I(t)^2 \times R(t))dt \tag{2.1}$$

Where I(t) = current in the wire and R(t) = resistance of the wire.

Equation 2.1 is only correct at the very first stages of the wire explosion when only wire heating is occurring and the voltage is below that of the corona inception. It is important to note that the resistance of the wire is dynamic. Until the point of corona inception, or the first fracture, the only contributor to the energy input of the wire is resistive heating. From Equation 2.1 the temperature of the wire can be found hence resistance of the wire can also be found. To find the temperature change over a period of energy installation Equation 2.2 can be used.

$$T_f = \frac{q}{m \times C_g} + T_i \tag{2.2}$$

Where T_f is the final temperature, T_i is the initial temperature, C_g is the specific heat of the material, and m is the mass

Using Equation 2.1 and Equation 2.2 we can find the temperature of the wire in the initial heating stage.

$$T(t) = \frac{(\int_0^t (I(t)^2 \times R(t))dt)}{c_p \times m} \times T_0 \tag{2.3}$$

To further elaborate, resistance is found with regard to temperature: α is the temperature coefficient of resistance, R_0 is the standard resistance at a known temperature T_{std}.

$$R(t) = R_0 \times [1 + \alpha \times (T(t) - T_{std})] \tag{2.4}$$

Where R_t is the resistance with respect to time, resistivity (p), length (l) and area (A)

$$R_0 = \frac{p \times l}{A} \tag{2.5}$$

But this formulation denies the skin effect of the impulse. The skin effect should be taken into account for larger wires or high frequencies where it will have a effect. Taking this into account in a good conductor;

$$\alpha \cong \sqrt{\pi \times f\mu\sigma} \tag{2.6}$$

Where α = the attenuation constant of the conduction medium, f is the frequency, μ is the permeability, σ is the electrical conductivity;

This leads to a skin depth.

$$\delta_s = \frac{1}{\alpha} \tag{2.7}$$

Where δ_s is the skin depth

Using Equation 2.6 and Equation 2.7 the equivalent conductor resistance for a cylindrical wire can be found This equivalent resistance is the equivalent of three skin depths, hence working for 95% of the current.

$$R_{eqiv} = l \times (\pi \times (\delta_s * 3)^2) \times p \tag{2.8}$$

where R_{eqiv} = The equivalent resistance and l is the length.

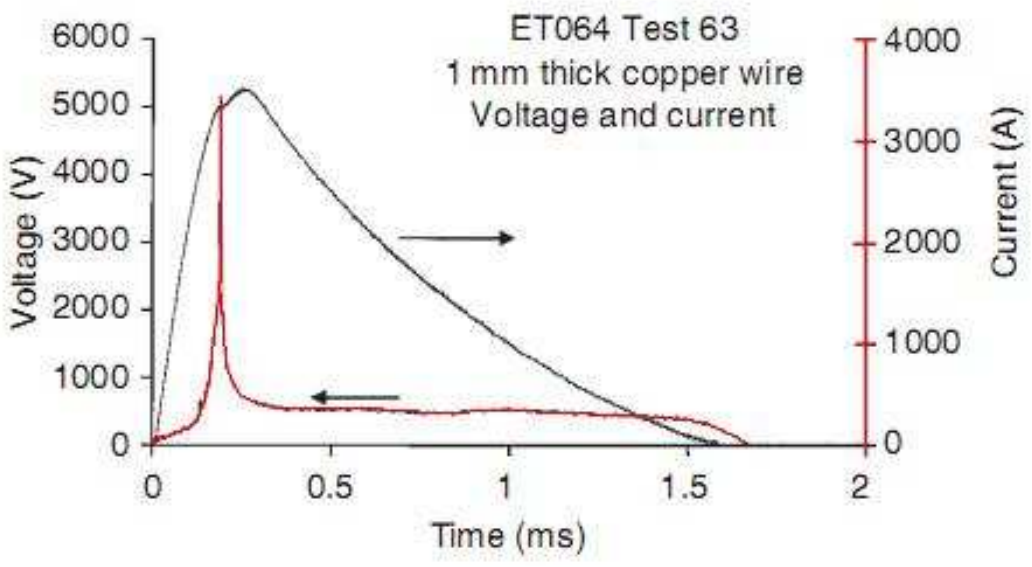

Figure 2.3 An example of a typical voltage and current waveform for a exploding wire. Current is the lower trace. [32]

So during this heating stage if the current flowing through the wire is known the resistance and hence voltage can also be found. Inversely if the voltage over the wire is known then the current in this heating stage can be found. By measuring both voltage and current finding the resistance simply comes from ohms law;

$$V = IR \tag{2.9}$$

It is important to remember that the sole resistive heating of the wire would only apply if all other mechanisms lye dormant. Generally it is accepted that in the initial stages of wire explosion the wire will undergo resistive heating alone without the interference of other mechanisms. This can be shown by the voltage and current waveforms of Figure 2.3 as the initial area where the current is linear before the current spike.

As soon as the first fracture appears the resistance of the explosion stops relying solely on the wire temperature but also on that of the plasma arc. The size of the plasma arc between conductor fragments is related to the temperature of the plasma, and the time given for it to expand whilst current is flowing. The plasma between conductor fragments will envelop the ends of these fragments and alow for radial and axial current components.

The plasma will continue to expand from the fractures and begins to shroud the wire fragments as shown in Figure 2.4. The plasma will continue to grow from these fragments and begin to envelop the wire fragments. The plasma surrounding the wire

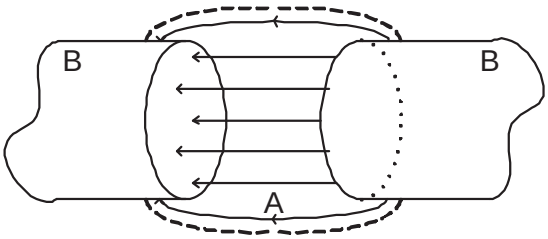

Figure 2.4 An example of a plasma between wire segments enveloping the ends. (A) indicates the plasma shroud, (B) indicates the wire segments. The arrows suggest the current path.

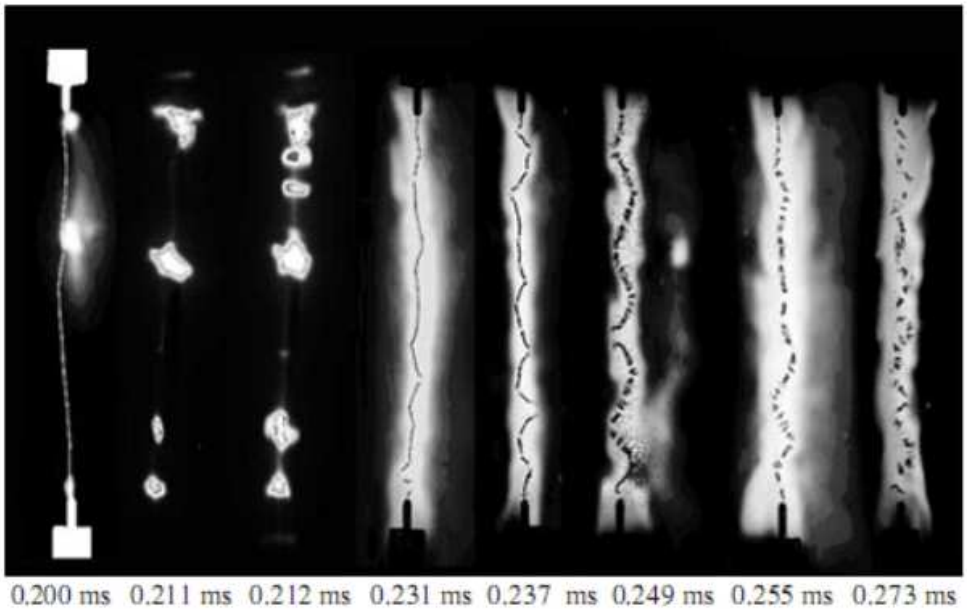

Figure 2.5 A xray and photograph montage. This is a example of plasma between and enveloping wire segments [32]

expands over the exploding wire process due to the increasing voltage and presence of fine or vaporised conductor and increased ionisation of the air. The plasma will continue to expand until it meets plasma from the next fragment. When the plasmas meet a conduction path will be formed through the plasma along the length of the wire. The amount of current flowing in this region will depend on the size of the plasma, its density and resistance.

During the wire explosion process the thermodynamic effects on the remaining will continue but now accompanied by other mechanisms. As the wire breaks or vaporises remaining segments of the wire will continue to heat with the current flow through them although this is now a fraction of total current flow due to plasma current flow I_{plasma}. Heat energy may also be added to the wire by the hot plasma via conduction.

As perviously discussed a large amount of energy is passed into the wire over a short period. In the common experience of slow resistive heating of a wire the wire will heat, elongate, and expand. In the situation of exploding wires these results will also occur but in a much shorter time frame. Most wire explosions are complete within $1\mu s$ to $300\mu s$ depending on the circuit configurations and test piece.

The frequency of energy deposition is also dependent on the test equipment and the test piece. As the energy delivered is generally an impulse, a range of frequencies will be present. The frequency range of energy input will be dictated by the LCR characteristics of the circuit, but as L and R are dynamic within the wire the dominant frequencies will be vary during the event.

The energy input will cause a standing stress wave in the test piece due to the rapid expansion of the wire. The thermal expansion processes will also be occurring whilst the wire begins to vibrate. This process was first put forward by Ternan [33]. He states that if the wire can be treated as a uniform conductor with elasticity then a stress wave can propagate. This stress wave will in turn vibrate the wire. If the vibrations are of great enough magnitude they will cause the wire to exceed its tensile strength and snap at a point. The reduction of the strength of the wire due to ohmic heating will also be prevalent, allowing smaller stress forces to break the wire than expected at room temperatures.

Once the wire has fractured circuit inductance should force a arc across the break to continue conduction. The wire parts will begin to build a stress wave again causing further breaking the wire. This process may repeat its self many thousands of times breaking the wire in to small pieces.

These theories are generally accepted but there is no defined model for the electrical wire parameters (R and L) during the wire explosion. As the wire breaking is assumed a exceptionably non-linear process it would be a challenge determine the initial conditions of the wire pieces after the first fracture.

Conductor standing waves have been investigated experimentally in a attempt to find current maximums for superconductors. Experimentalists noted that the natural mechanical frequency of the test piece is known to vary with the application of current. This may alow the stress waves to further influence the wire via resonance with the natural mechanical frequency.

The stress waves are also effected by the physical connections of the circuit they are in. For a wire with two clamped ends it is expected that the combination of stress waves and electromagnetic forces will first break the wire at one of the clamped ends. A wire with free ends the wire will break in the centre. A wire with a clamped and a free end

the wire is predicted to break at the clamped end.

Electromagnetic forces occur in any material that has current flow or contains a different charge with reference to other materials. In exploding wires the electromagnetic forces are prevalent due to current flow within the wire its self and the electric state of the surrounding environment (ie ground planes, return paths, and the supply circuit). Several related forces are relevant to the exploding wire mechanism. All of these forces are defined or use Maxwells equations

$$\nabla.\mathbf{E} = \frac{\rho_v}{\epsilon_0} \tag{2.10}$$

$$\nabla \times \mathbf{E} = -\frac{\partial \mathbf{B}}{\partial t} \tag{2.11}$$

$$\nabla.\mathbf{B} = 0 \tag{2.12}$$

$$\nabla \times \mathbf{B} = \epsilon_0 \mathbf{J} + \mu_0 \epsilon_0 \frac{\partial \mathbf{E}}{\partial t} \tag{2.13}$$

Where:

- $\mathbf{B}$ = Magnetic field
- $\mathbf{E}$ = Electric field
- ρ_v = Electric charge density
- ϵ_0 = Permittivity of free space
- $\mathbf{J}$ = Current density

Radial forces act on the all parts of the wire, with direction towards the centre of the wire, as shown in Figure 2.6. This force will have a effect of putting the wire under pressure. The only radial electromagnetic force is referred to the as the Lorenz Force (LF). In a current carrying conductor the LF is significantly small so that the observer does not notice the compression of the wire. In applications where the currents are large the force becomes larger and will have a more notable effect on the conductor.

Consider two parallel wires both with a current in the same direction. The wires will tend to attract. This is because the wires self and mutual magnetic fields. This force is defined by Lorentz force law.

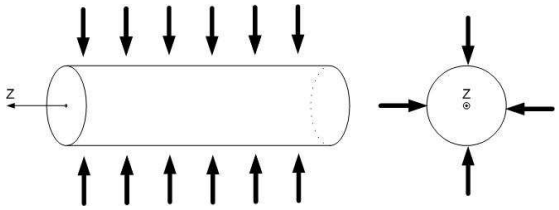

Figure 2.6 The lorenz forces acting on a wire

$$F_{mag} = q(\vec{v} \times \mathbf{B}) \tag{2.14}$$

Where F_{mag} is the force, q is the charge, v is the velocity of the conductor and $\mathbf{B}$ is the magnetic field.

Microscopically within a conductor the LF is present. A single conductor can be modelled by splitting it into small finite conductive elements all carrying a current. In this model each elements self and mutual magnetic fields will act upon one another causing the wire to have a radial force acting up on it.

During the wire explosion this force will compress the wire. The current is the same in all parts of the wire and therefore the force will be equally distributed along the length of the wire. It is not capable of breaking the wire unless there is an irregularity in the wire (i.e. a chemical or mechanical deformation). Also there may be other mechanisms, such as those previously stated, deforming the wire or amplifying the compression at a point. Several studies by Molokov and Allen [23, 24] have shown the forces to be large, but as the wire is a solid, the compression relatively small. Shown in Figure 2.7 [24] is a specific example of displacement of a wire due to Lorenz Force. Other studies have shown that while lorenz forces are large they are not large enough to break the wire [23, 24].

Tensile electromagnetic forces are those which act along the axis of a wire. Tensile electromagnetic forces have been theoretically and experimentally presented in the exploding wire mechanism. Two such forces have been debated in the literature are:

- Ampéré forces
- Lorenz forces

Ampéré forces are ones which Ampéré described in his book “Memoir on the Mathematical Theory of Electrodynamic Phenomena, Uniquely Deduced from Experience”. These mechanical forces act on the crystal latices of the metal with current flowing

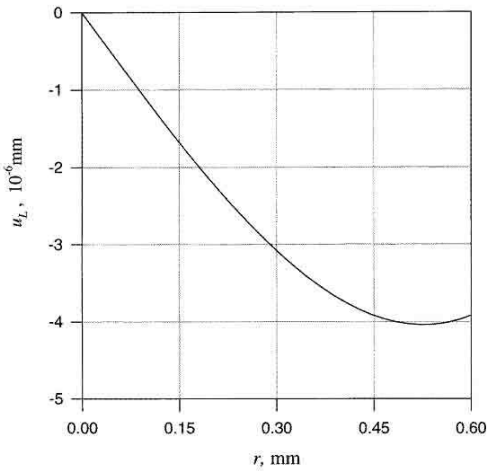

Figure 2.7 The lorenz displacement due to current in a wire. Calculated forces are for a aluminium wire of radius 0.6mm length 12mm, with a constant current of 5kA

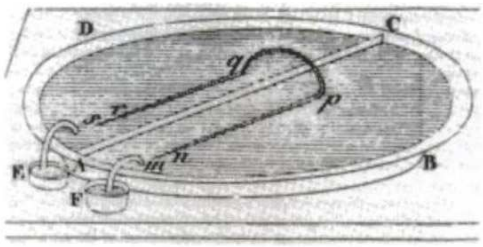

Figure 2.8 Ampéré drawing of the hairpin experiment

through them. This was famously shown by Ampéré using the "hairpin experiment". In this experiment a copper "hairpin" shaped conductor was floated in two baths of mercury as shown in Figure 2.8 [8]. The mercury bath has a insulating channel running through it ensuring that current flows through the hairpin. The hairpin itself is insulated apart from two ends (r and n in Figure 2.8) only allowing current to pass into these points from the mercury. Voltage was applied into one bath of mercury to the hair pin at point n. Current then flows through the hairpin to the other bath. The hairpin in turn floats away from the point source of current. Ampere explained this by the effect of longitudinal tension on the mercury conductor.

The force with reference to exploding wires is outlined by Graneau. This force can be expanded to the single conductor case, again by treating the solid conductor as a grouping of smaller conductors, hence each having a force on one another [14]. The summation of these forces would lead to a tension in the conductor itself.

This theory itself has been disputed, most obviously by Carpenter [11]. He cites that incorrect analysis and calculation elude to a different force other than the commonly

accepted longitudinal LF. Carpenter implies that LF is at work. In rebuttal Graneau challenges Carpenter to prove him wrong experimentally.

Longitudinal LF are the opposing thesis for the electromagnetic longitudinal forces. As explained previously these forces are of electromagnetic nature and can be conceptually extended to single conductor cases. The argument for Lorenz Forces is that they will be the same as amperes forces if only the magnetic component is considered if the divergence of the current is zero [33].

Once the wire has snapped at a point it will be come free at that point. From the theories put forward by Wall and Molokov et al, it is expected that the wire will then snap at the next fixed end [35, 24]. Once no fixed ends remain it is expected the wire fragments will act as free ended wires. Modelling has shown that the forces will be increased in the wire fragments due to their reduced lengths [35]. The increased forces will cause the wire to continue fracturing until a point when the current is reducing (capacitors become discharged) or the inductance of the circuit can no longer force conduction through the plasma paths between wires.

With all of the theoretical work that has been done on exploding wires one problem remains, they do not completely explain the mechanism to the point where it is known what the result of a experiment will be before it is conducted. The most advanced works by Wall and Allen et al, describe the mechanism as one which will break the wire at both clamped ends and then the middle, although if one puts this to Figure 2.5 they will see this is not the case. A lot of the mechanisms are not known perfectly and maybe so undefinable that it will never be known. What is known is that if high enough current is passed through a wire it will shatter. Further work contained in this document will empirically attempt to find some set initial conditions that will cause the wire to explode producing a plasma path with repeatability.

Chapter 3

DESIGN AND CONSTRUCTION OF A HIGH ENERGY, HIGH VOLTAGE TEST SET

3.1 INTRODUCTION

In the designing of a high energy, high voltage (HV), test set for the purpose of exploding wires there are many considerations. Of the upmost importance is operator safety. No equipment may be allowed to be used which may cause the operator harm. As high voltages are to be used there is a risk of electrocution. If such a electrocution were to take place the high energies would lead to a high likelihood of death. The electrocution hazard must be minimised in the design process.

Mechanical issues are another group of considerations. Thought must be given to how the equipment is to be set out and what is a acceptable physical size. Supports and framing must be able to handle static loads of equipment as well as dynamic failure loads. How the equipment can be transported and what are the maximum capacities of transportation mechanisms need to be considered.

Electrical issues are the final grouping of considerations. The designer must decide what is a acceptable energy source, and how to transmit this energy to the test piece. The designer must decide how should switching occur and what is a acceptable loss in the associated supply circuitry. Insulation design is also of great importance with regards to undesired flashovers and user safety.

This chapter outlines the requirements and processes involved in the design and construction of a high energy, high voltage test set for the explosion of wires and production of plasma paths.

3.2 ENERGY SUPPLY METHOD

In the literature there are two different methods given for supplying electrical energy to the load (an exploding wire):

1. A single or "bank" of capacitors charged then switched on to the load [31, 15, 37].
2. The use of a DC generator switched onto the load [27].

The DC generator has the benefit of current regulation over the experimental period. A specialist DC generator was not available at the time at the University of Canterbury and therefore this option was not pursued. The capacitor option was chosen because numerous high voltage capacitors were available.

Commonly HV dc capacitors are charged via a rectified HV ac source [31, 15, 37]. The circuit configuration for charging is set out in Figure 3.1. The mains voltage (230V ac) source is passed through a VariAC to control voltage magnitude. This gives the operator the ability to limit the current supplied to the capacitor load. An appropriate sized fuse is included so the supply was not over-loaded. From the VariAC current is then passed through a step up transformer to increase the voltage. A diode then rectifies the HV ac to a half-wave HV current. The capacitors will accept this current and charge appropriately. The diode maybe reversed to allow for negative charging of the capacitors. This method allows for controlled charging of capacitors from a readily available mains voltage ac source.

Once the capacitor bank is charged to the test voltage, the charging circuit is then disconnected and a switch from the capacitor bank may be closed. The capacitors will then discharge through the load as shown in Figure 3.2. The electrical equipment that must be assembled, connected and built for experimentation is known.

3.2.1 Electrical Considerations

3.2.1.1 Insulation Requirements

The insulation coordination design focussed upon two main categories of equipment. These were equipment which the operators will physically touch and equipment that the operators are acceptably isolated from. The operator touch equipment has a larger insulation safety margin than the non-contact equipment.

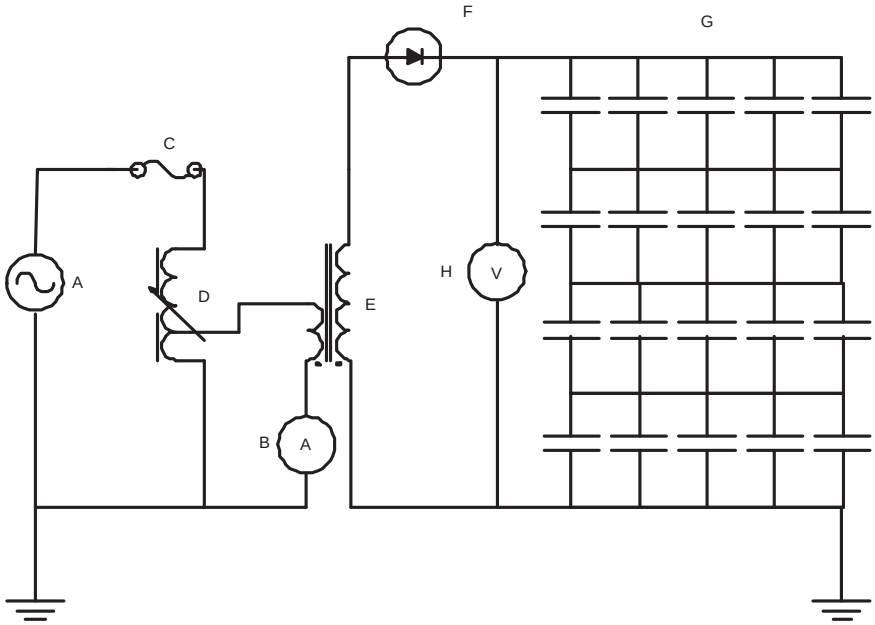

Figure 3.1 The commonly used circuit for charging of capacitors, A: Mains Voltage Source B: 10A Ammeter C: 20A Circuit Breaker D: 10A VariAC E: 230/80kV Step Up Transformer F: 150kV HV Diode G: Capacitor Bank

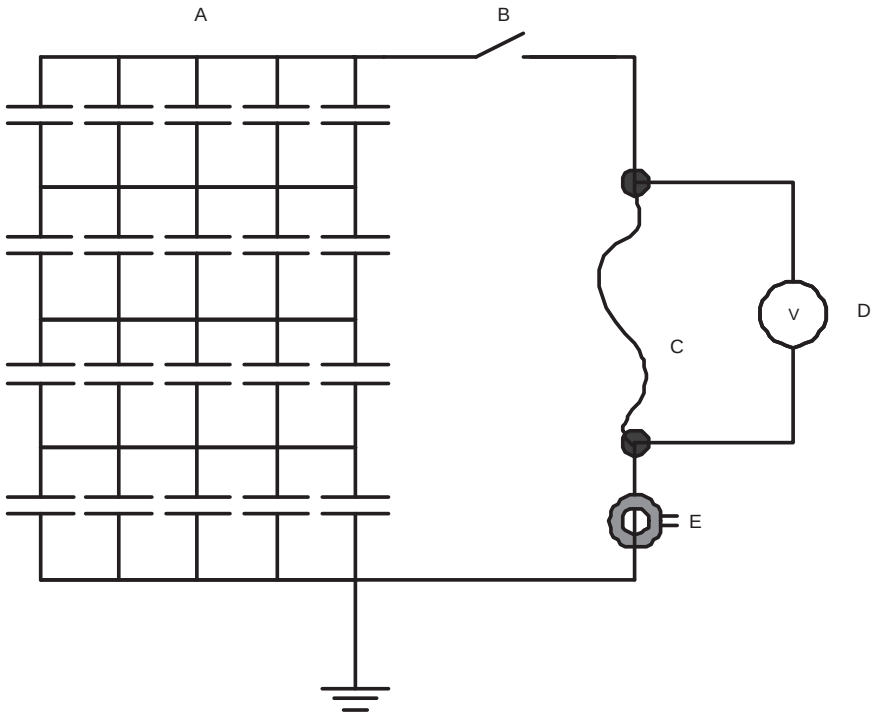

Figure 3.2 The commonly used circuit for loading the charged capacitors with an exploding wire, A: Capacitor Bank B: Switch C: Exploding Wire Load

Minimum Approach Distance (Metres)	Nominal Design Voltage (kV ac l-l)	Nominal Design Voltage (kV dc)
2.2	220	180
1.5	110	90
1.0	66	54
0.75	50	41
.60	33	27
.45	22	18
.30	11	9
.25	6.6	5
.15	1	0.8

Table 3.1 EEA SM-EI Minimum approach distances for live equipment work.

Physical touch and effective touch equipment is the VariAC, switching trigger, metering equipment, and hand earths. These pieces of equipment must be subjected to voltages in accordance with the manufactures specifications. If the equipment built in house then the insulation must be proven to an independent and recognised International Standard. The equipment must also ensure that a minimum approach distance is maintained by the operator as outlined in the Electricity Engineers Association of New Zealand (EEA) "Safety Manual - Electricity Industry" (rule 3.703 "Reduced Minimum Approach Distances For Certain Employees Near Exposed Live Conductors") [5]. These distances can also be applied to any instrumentation or low voltage leads which travel near hv equipment. The insulation relied upon by these rules is the air between the user and the hv equipment. The minimum approach distances shown in Table 3.2.1.1 are published for a.c. line to line voltages shown in column 2. The converted tables for dc use are given in Table 3.2.1.1 using Equation 3.1, these are shown in column 3.

$$V_{dc} = \frac{V_{ac-equiv} \times \sqrt{2}}{\sqrt{3}} \tag{3.1}$$

The equipment which the operator is not in contact with does not need such stringent insulation requirements. The purpose of this insulation is not operator safety but rather equipment protection from failure or damage caused by flashover. Commercially manufactured items can be relied upon within its specifications. In the case of specialist university designed and manufactured equipment careful consideration must be given to its insulation coordination.

3.2.1.2 Rising Earth Potentials

As a large amount of current will be released at high voltage during a wire explosion, it is possible that the laboratory earth plane will see a rising potential to that of other

external or remote earth planes and connections. If an external or remote earth is introduced via the local power supply to the laboratory this must be isolated from the user. In order to isolate this earth, an isolating transformer is used between the local supply and the user operated VariAC. The isolating transformer removes this external earthing and equipment is able to be only to the laboratory earth. Careful earth bonding removes the possibility of high touch potentials for the operator as all hand and foot contact is bonded to the local laboratory earth.

3.2.2 Physical Considerations

The test set design had to consider the following mechanical matters:

- The transportation of equipment to allow for storage.
- The static loading of equipment due to gravity.
- The dynamic loading of equipment due to failure.
- The physical volume of equipment.

All test set equipment must be transported over short distances within the laboratory to allow for storage and to let other testing take place. The University of Canterbury High Voltage Laboratory has: a 1 tonne pellet trolley and a 1 tonne single track remote controlled roof crane. The maximum weight of the test set or parts there of is therefore 1 tonne. It was desired that the equipment be easily and quickly moved or disassembled.

The supporting frames for the capacitor stack were required to withstand the static gravity load of the oil filled capacitors; they weigh around 60kgs each.

If equipment suffers a electrical failure then dynamic mechanical effects will be present. If a capacitor fails and ruptures its tank in a explosive manner then subsequent failure of other equipment needs to be avoided. A stack of capacitors could topple causing further catastrophic failures. The capacitor frame should be set up in a way that minimises the likelihood of subsequent failure modes.

The physical volume of the test set should be minimised to reduce laboratory space requirements. Physical size must be balanced against flashover distances and corona inception voltages.

3.3 CAPACITORS

Eighty oil filled 17.1uF 6.675kV capacitors were available for use in this project. Originally these capacitors were used as part of the 12th harmonic filter on the New Zealand HVDC link. The capacitors were gifted to the University of Canterbury after a upgrade of the HVDC link filtering rendered them obsolete. The capacitors are foil electrode type with oil impregnated paper as the dielectric. The capacitor cans are made of mild steel and have connection points to allow for bolting to framing. Inside the capacitors discharge resistors were originally fitted so that if the supply voltage was removed the capacitors would discharge internally. This allowed for maintenance on connected equipment without retaining voltage once isolations were in place. As the capacitors were to be used as a energy storage mechanism the discharge resistors were removed. This was achieved via drilling into the casing and clipping the resistor leads to disconnect them. Previous testing on these capacitors have shown that they are able to be used at a voltage of up to 20kV. A upper limit of 15kV was set. While the capacitors had passed a 20kV soak test for 60 seconds it was decided that the experiments should be carried out at a level of 85% below the over voltage test level. In hindsight this choice appears appropriate as there were no capacitor failures in more than 200 exploding wire tests.

The energy requirements for these experiments is variable. Half of the available capacitors are to be built in a modular racking system with the option of using the remainder if the energy was considered insufficient. The capacitor energy Equation 3.2 gives a energy storage of 77kJ at 15kV for the forty capacitors.

$$w_{capcitor} = \frac{1}{2}Cv^2 \tag{3.2}$$

A failed capacitor from experiments prior to this thesis was available to be examined. The steel capacitor tank welds had ripped open. The internal fault had power arced causing it to produce gas under the dielectric oil. Within the sealed tank the pressure increased rapidly, from the gas production, forcing the case to rip open. The capacitor tank had undergone some ballooning due to internal pressure rise (see Figure 3.4 (b)). Internally the capacitor had damage within its foil layers (see Figure 3.4(c)). From this dissection the electrical fault caused oil to spill from the tank and 20mm swelling of the casing in the horizontal axis. Given the failure mechanism of this capacitor is it clear that an air gap was therefore required between capacitors to allow for capacitor swelling in case of failure. Equipment is also required to be available to clean up oil. Fire fighting equipment is also needed to be available in case there is oil fire.

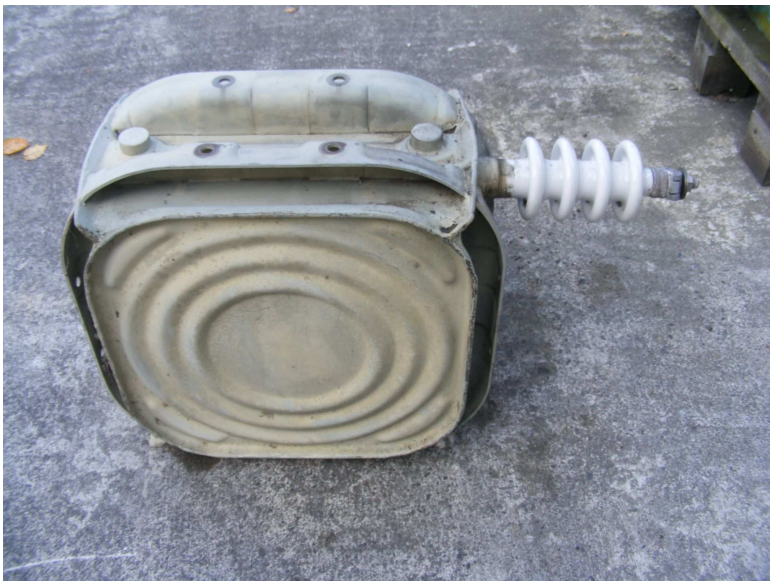

Figure 3.3 A single 6.75kV 17.6uF capacitor with connecting hardware

3.3.1 Capacitor Racking

Capacitor racking was employed to allow for the capacitors to be stacked in a usable formation. A review of commercially available systems was conducted, and despite most available units being 3 phase shunt connections, common themes emerged. The capacitors in commercial system always had spacing between one another regardless of the case potential. It is expected that manufacturers require an air-gap to allow for heat transfer and possibly in preparedness for a capacitor failure. Commercial capacitor banks are commonly stacked to allow for a reduced footprint. Insulation stands between each layer of capacitors is utilised to allow for different case voltages this can be seen in Figure 3.5. In building a capacitor stack it will be that many of the tanks will be at high voltage with respect to earth. The insulation between rows and between the lowest row and earth requires careful consideration.

A prototype capacitor row was built using 75mm by 25mm wooden framing. The row was constructed to gave an air-gap of 75mm between capacitor tanks of equal potential. Each capacitor was connected to the wooden frame via four M10 bolts on both the top and bottom to give a secure connection. A layer of 3mm polycarbonate plastic was placed on stand offs between the capacitors and the operator. The intention of this shield was to ensure that the operator would be protected from any oil or fragments that could expelled during a worst case capacitor failure.

During testing of this prototype row it was found that the wood was not suitable to hold the weight of the capacitors. Considerable flexing of the wooden structure was

(a) Multiple capacitor failure due to electrical fault of a single capacitor.

(b) Swelling of the capacitor case.

(c) Internal foil layers showing the area under fault.

(d) Removed foil layers showing result of a electrical fault.

Figure 3.4 The electrical failure of a capacitor bank and dissection of electrical capacitor failure.

Figure 3.5 A 115kV shunt, 3 phase capacitor bank. Note the insulation between layers of capacitors. [www.abb.com]

the main concern. Also the wood structure could not be stored outside in the hv laboratory compound due to moisture inception. The polycarbonate sheet was found to give limited protection due to a lack of structural support, if a large explosion were to occur the perspex would well rip from its connection bolts. Moreover the perspex did not allow for the application of hand earths to the capacitors. As the capacitors layers were to be situated on top of one another the horizontal outriggers were thought to be too short giving insufficient tip-over restraint. The wooden racking was unacceptable in many regards it was decided to move to a steel structure.

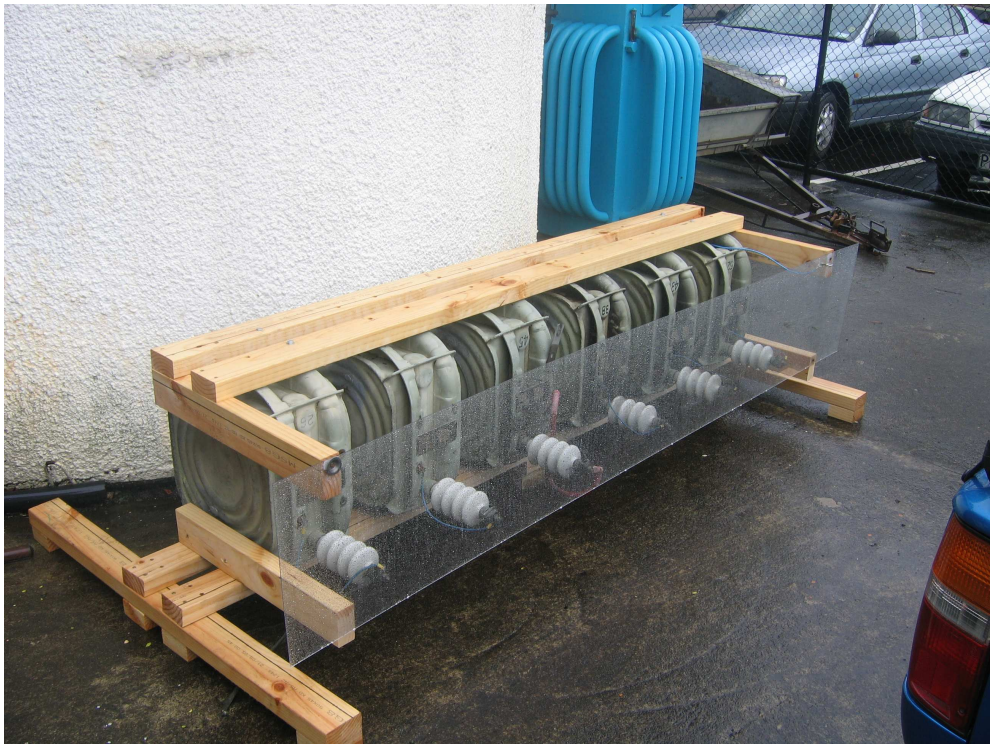

Figure 3.6 The first capacitor rack prototype

In the new design the capacitors were to be placed in gangs of 5 per layer. It was decided that the operator should be able to remove capacitors electrically from each of these layers without the need to remove them physically. Circuit parameter flexibility was the intention. The layers were to be placed on top of one another to a maximum height of four layers. The middle two layers were to have connected cases at equal potential, reducing the overall mechanical connections. It was decided that the operator should have the flexibility to connect each layer in series or parallel as required.

A second prototype capacitor rack was produced from 6mm mild steel angle section. Steel fabrication is much more difficult than wood, but the superior strength is needed. The insulating properties of the wood were not relied upon in the original prototype so the design was not drastically changed due to the conductivity of the steel. The steel

was cut to four 1500mm lengths and ten 10mm holes were drilled with the appropriate spacings. The mild steel lengths were prepared and painted with International PA-10 vinyl etch primer to avoid corrosion during outdoor storage. Four 25mm holes were drilled into the angle section lengths at the top corners of the capacitor rack as crane connection points for lifting. The four steel lengths were bolted to the capacitors with eight M10 bolts per capacitors via the capacitor mounting points on their tanks. The second prototype capacitor rack was successful, two four rack capacitor stacks were built.

The bottom layer of each capacitor stack was fitted with castors to aid movement. The castors needed to be able to withstand 1200kg of capacitors and an additional 107kg of angle section steel. Three castors are rated for 1300kg load so that if one were to fail the remaining three castors are still rated for the load. Industrial waste bin castors were selected, they have a 700kg rating. Made from cast iron, the castors are able to turn 360 degrees for manoeuvering. The castor-frames were arc-welded to the bottom capacitor rack.

The bottom capacitor rack needed to be fitted with supporting outriggers to steady the stack. The outriggers were fabricated from the 6mm angle section steel and are 3m long. At the ends of the outriggers screw down feet were added. The feet were produced from lengths of M12 threaded rod with a solid steel foot. A steel tube handle was welded to the top of the threaded rod so the operator can screw it into position. The rod is threaded to the outrigger via a M12 nut welded to the outrigger. A 25mm hole was drilled in each end of the outrigger for tie downs to be attached. These tie downs attach to the upper capacitor layers giving stability. The outriggers were also cleaned and painted with International PA-10 vinyl etch primer.

Between each layer of capacitors insulators must be inserted to isolate the different voltages of the capacitor tanks. The cost of commercial ceramic or polymer based insulators was prohibitive an alternative was required. The insulation is load bearing. The bottom layer of insulators must withstand approximately to 1000kgs of capacitors and steel. It was decided that plastic piping would meet the insulation requirements and (if of sufficient thickness) be able to withstand the load above it.

Culvert piping was chosen with a 250mm diameter and a wall thickness of 3mm. It is relatively inexpensive as it recycled from industrial grade tubing. The culvert piping is made from Polyvinyl Chloride (PVC) and the voltage withstand characteristics of this material was not known. The actual withstand voltage was found via HV testing of the PVC. Two aluminum straps were attached to the cleaned tubing as shown in Figure 3.7 with a 100mm gap between. One strap was earthed and increasing AC voltage was then applied to the other. While this would not be the final configuration for the

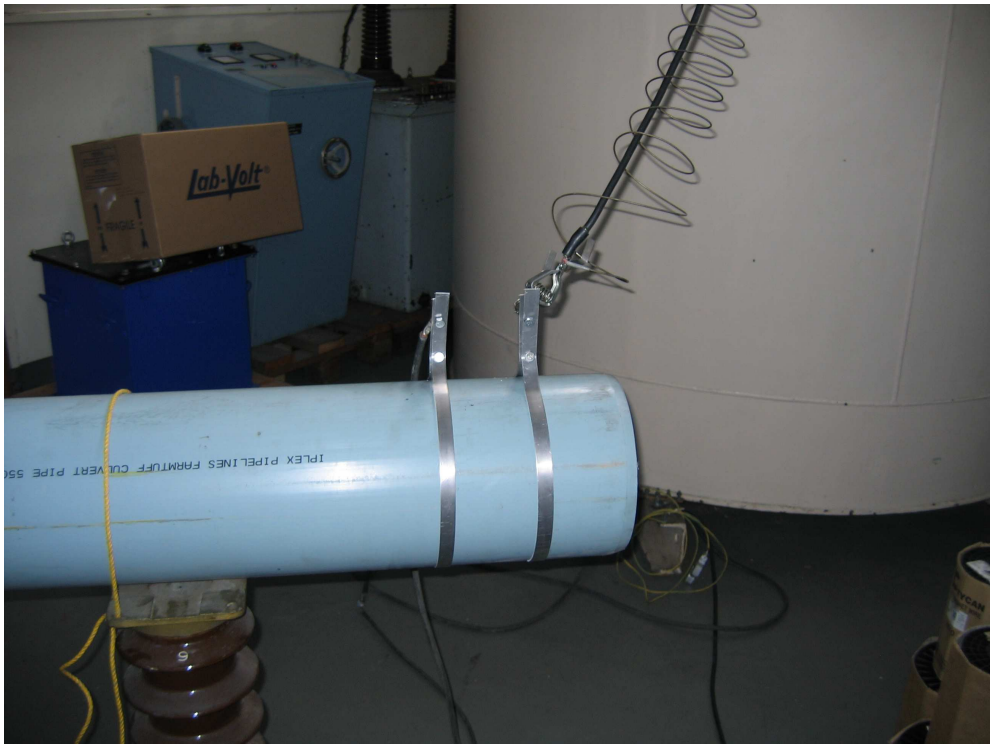

Figure 3.7 PVC tubing flashover test set up.

insulators it was used to give insight to the withstand voltage of the PVC surface. In this configuration the PVC withstood a minimum breakdown voltage of 46kV ac rms over 10 tests. This is the equivalent to a peak applied voltage of 65kV.

The PVC insulator tubing required slots to be cut so that they could interface with the angle steel of the capacitor racks. If the insulator lengths were 190mm this would give 100mm between the closest points of the section steel. The electrical strength of this arrangement is 65kV. The eight slots per insulator were cut on a table saw. The insulator and angle section steel arrangement was high voltage tested. An insulator was cut to length and slots cut. Angle steel was inserted in these slots as they would be in the test set up. This configuration is shown in Figure 3.8. A voltage was applied between these angle sections and increased until flashover was observed. A minimum breakdown voltage of 52kV ac rms over 10 tests was found. The flash overs appeared to occur in the air gap rather than the surface of the insulator. It was found that a slightly higher withstand of 7.3kV/cm was obtained in this proposed capacitor stacking configuration. The maximum anticipated operating voltage of the test set up is 15kV per layer and therefore the insulators give a safety factor of 4.9.

The capacitor racks were then set up in their final configuration. Insulating transport tie downs were used between each layer and the outriggers to give stability and to allow for building the upper layers in a square manner.

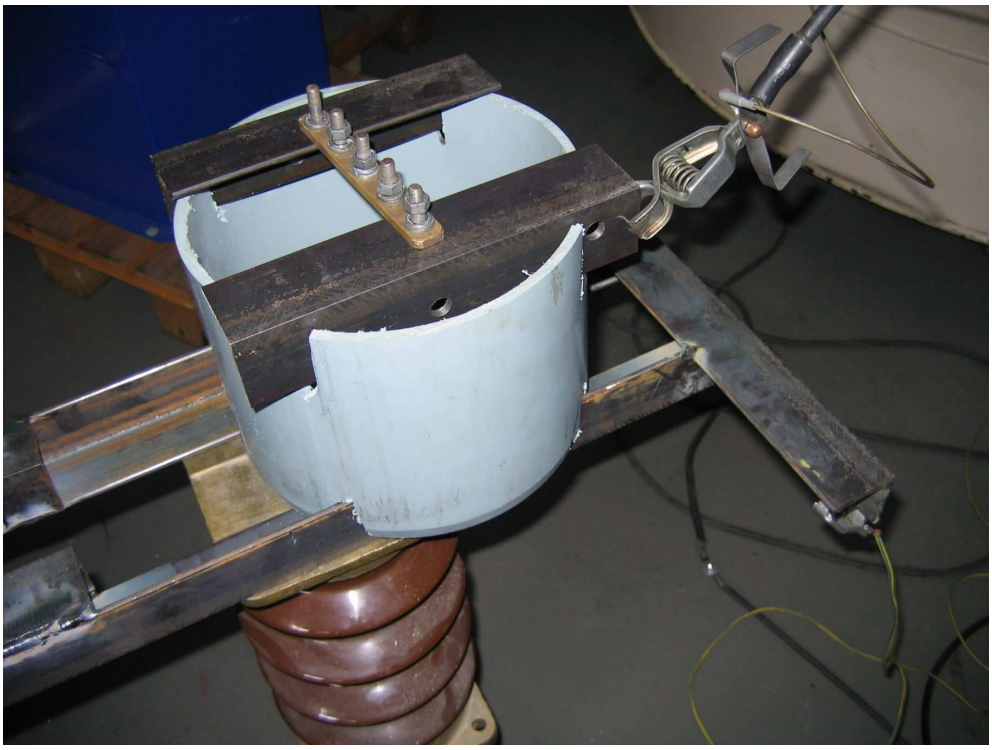

Figure 3.8 Insulator flashover type test set up.

3.3.2 Capacitor wiring

Consideration was given to ensure that electrical losses are minimised in the capacitor stack connections. The internal impedance of the capacitors can not be avoided, but the use of low resistance cabling in the capacitor interconnections reduces losses. In the capacitor arrangement of this work there are two types of connections: the connections between equipotential capacitors cases and bushings (parallel connection); and the connections between layers of different potentials (series connections). During charging a relatively low current will pass through the series connections into the capacitors. A small current may pass through the parallel connections during charging, equalising the paralleled capacitor potential. During discharge all currents maybe significant due to small electrical tolerance differences in the capacitors and the need for test current to pass between layers.

Between equipotential capacitors copper strapping conductors were cut, drilled, and bolted to the capacitors casing to avoid case potential differences. Flexible 16mm cable was used to connect the capacitor bushing terminals This cabling was stripped at connection points and at an end to allow for the application of hand earths. Each bushing head has a saddle clamp connection to allow for good cable connection. Between capacitor layer five 95mm flexible conductors were connected. These conductors were

terminated with tinned copper crimp lugs and bolted to the appropriate casings using M10 bolts.

3.4 SWITCHING MECHANISM

A suitable switching method is required to connect the capacitor source to the exploding wire load. The switch must be rated for the high voltage and high current. It is important to ensure that the switch does not flashover during charging; as this will place the charging circuit under over current stress possibly leading to equipment failure.

Commercial switching equipment that allows for both high voltage and high current switching is rare and expensive. Generally most high voltage and current impulse switches work on the concept of spark gap breakdown. The difference between spark gap switches is associated with the method of breaking down and the insulating gas between the electrodes. Generally the gaps are broken in three different ways;

- Difference in potential over the gap (Trigatron);
- Laser triggering;
- Physically closing the gap.

The first method "Trigatron" forces one of two electrodes to a different voltage that increases the potential between the two. During charging the electrode gap remains below breakdown voltage. Once the required voltage has been reached the user will trigger an applied voltage of a different polarity to one electrode hence exceeding the breakdown voltage, causing flashover. Generally the gap is triggered by a "spark-plug" system which flashes to one of the electrodes less than 10kV. Commercially available "Trigatron" switches are used in laboratory impulse generators as shown in Figure 3.10. Here the spark plug is shown on the left hand sphere.

Laser triggered gaps utilise a focused laser to force break down. The laser will generally be fired through a small hole in one of the electrodes and then hit the other. The laser will rapidly heat the electrode it shines upon causing a small plasma ball to be formed on the surface. The laser also ionises and heats the insulating gas in its path. This gas heats to the point of becoming a plasma in the position between the electrodes were the laser is most focused. The two plasmas will eventually join creating a plasma section extending from one electrode. As the plasma is conductive the plasma will assume the voltage of the laser receiving electrode. The gap is now reduced in spacing by the introduction of conductive plasma. With this reduced gap the electrode arrangement

(a) Completed capacitor bank with strops and wiring

(b) Bolted connections between racks and capacitors

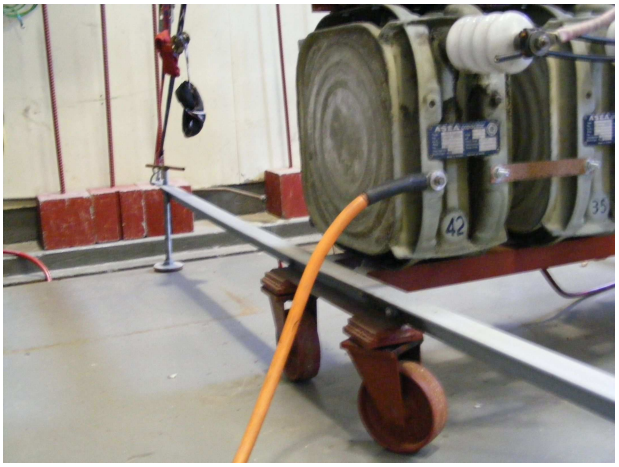

(c) The castors and outriggers with strops

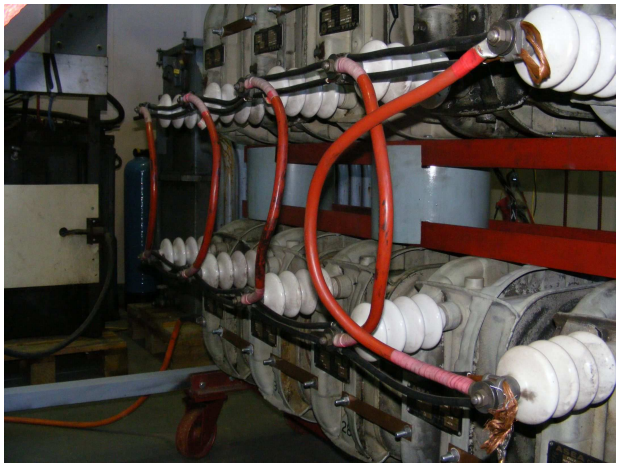

(d) 95mm wiring used for series connections and 6mm wiring for parallel connections

Figure 3.9 The completed capacitor bank racking system.

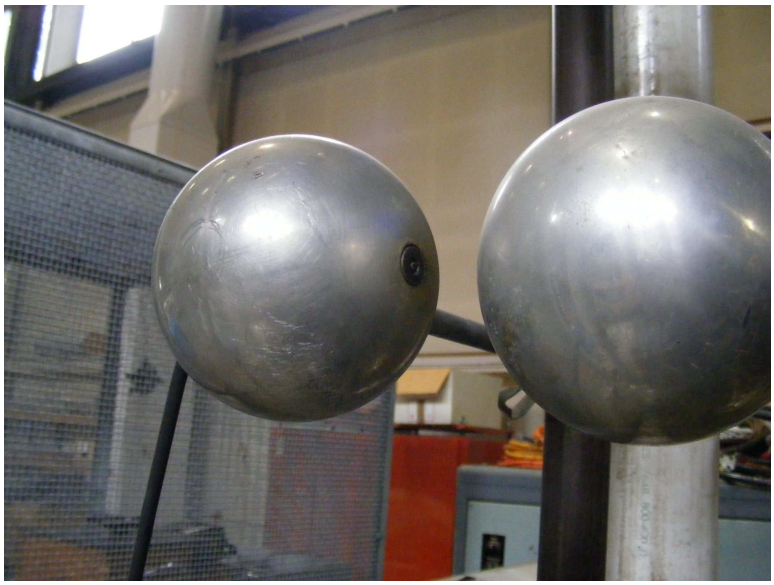

Figure 3.10 1.4MV Impulse generator triggering spark-gap.

will break down allowing conduction [20]. Generally pressurised gasses which are easily ionisable are used in laser triggered switches (such as N_2) [30]. The cost of sourcing a suitable laser and requirement for a pressure vessel to be constructed to house the electrodes made this method of switching impractical for this research.

The final method commonly used for switching high voltage is to flash-over a spark gap by reducing its width or using a foreign conductor to mostly bridge the spark gap. Commercial circuit breakers were considered unsuitable for this project, they were not rated for the d.c. voltages and current required by this research.

Previously a knife switch has be utilised in switching of capacitors onto an exploding wire load as seen in Figure 3.11. The switch worked by having a energised electrode fall in a pendulum motion onto the load connected electrode. The switch electrodes were separated via an insulated pole structure which held the top electrode at the horizontal position. When the user wished to activate the switch they would pull an insulated cord releasing the energised swinging electrode so that it swings down to the other electrode, making contact. This switching technique was considered inappropriate for this research. The number of mechanical components made it distracting during experiments.

It was decided that a three electrode switch would be constructed. The switch would close the gap between two hemi-spheres via a third electrode that would fall between them. This method allows for flexibility in voltage rating as the hemi-sphere separation could be adjusted. The third conductive electrode would be guided down to the hemi-sphere via an insulated tube. Openings in the insulated tube could be cut to allow for

Figure 3.11 A knife switch previously used for exploding wire research.

flash-over between the hemispheres.

Two 12.5cm aluminium hemi-spheres with steel shanks were used. The hemi-spheres allowed for some gap setting using the standard sphere-gap tables [4]. Using these tables it was found that the sphere separation required for the maximum 60kV d.c. voltage expected in testing would be greater than 50mm. For the minimum voltage of 15kV d.c. the gap would be less than 2mm. This gap data allowed for a prototype hv switch to be built. Actual gap breakdown would differ from the standard sphere gap due to the presence of the insulating tube.

The last 160mm of the 600mm long hemisphere shanks were threaded so the gap could be adjusted. To insulate the spheres and shanks from the ground plane two PVC 110mm tubes, 500mm long were used. The tubes had two 13mm holes drilled 20mm from the top to allow the semi-sphere shanks to be passed through them. The shanks could then be secured to the PVC tubing using M12 bolts on the threaded section. The hemispheres then had four 10mm holes drilled in the outer sections to allow for electrical connections: four $95mm^2$ conductors were then bolted through these holes. An aluminium bus-bar was cut and drilled to allow incoming connections to be connected to the four $95mm^2$ conductors. The bus-bar was mounted on a 500mm length of formica tubing to insulate from the ground plane. The bus bar allows for the operator to disconnect the supply cabling without having to move the spheres.

Brass tubing of 104mm outer diameter, wall thickness of 3mm, 130mm in height was used to make the third electrode. Brass gives a good combination of strength and conductivity. The strength is needed as this electrode will be dropped from a height of 2m down the guide tube to triggering the gap. Whilst copper tubing would be a better conductor and give less losses over the switch, but it would deform after many operations. Four M4 threaded holes were tapped into the brass to allow for an end plate to be attached. The endplate was made from steel was attached to the brass tubing so that an electro-magnet could be used to hold the electrode at the top of the guide tube. The steel end plate was drilled and countersunk to ensure the four M4 countersunk screws did not sit proud of the electrode top plane reducing the steel contact with the electromagnet and hence reducing the ability for the electromagnet to hold the electrode.

A 2m length of 110mm diameter PVC tubing was acquired for the falling electrode guide. The electrode guide had two slots 100mm wide by 125mm high cut at a height of 480mm to allow switch gap to breakdown. The length of the tube gives insulation between the high voltage hemisphere and the electromagnet at the top of the tube. A PVC sleave of height 50mm and inner diameter just bigger than the electrode guide was connected to the ground plane to allow the electrode guide to be removed. This

Table 3.2 Breakdown voltage for the High Voltage Switch to earth strap

Test Number	Breakdown Voltage (kV ac RMS)	Peak ac Breakdown Voltage
1	76	93
2	84	103
3	79	97
4	82	100

caters for loading the switch and transport. An earth strap was connected around the base of the electrode guide so that any flashover from the high voltage hemispheres would strike to this earth-bonded strap. When the unit is in use this strap is connected to laboratory earth with a 16mm copper cable.

The electromagnet for holding the sliding electrode consists of a winding of 400 turns of 0.6mm wire wound on a plastic former. This former is then placed onto a layered steel "E" type core. An end cap for the PVC guiding tube was then made from Medium Density Fiberboard (MDF) with a opening to allow the insertion of the electromagnet assembly. A block type connecter was screwed into the MFD end cap to allow connection from the electromagnet and a power supply. The 2 core supply wire was additionally held to the end cap with a brass plate to ensure the wire could not fall from the end cap. This plate reduces the possibility of the supply wire breaking free and contacting a high potential part of the circuit if it were to fall out of the block connector.

A 15m 2 core lead runs from the electromagnet end cap to the operators were it is connected to a low voltage DC power supply and switch. The DC power supply runs the electromagnet and associated wiring at 1 amp, 3 volts. This supply gives a firm hold on the electrode. The supply lead is held away from the high voltage using the minimum approach distance to avoid flashover. The switch is a push button type mounted in a plastic box. It is most important that the high voltage can not be transported to the operator via the electromagnet supply leads.

Testing of the switch was conduced with reference to the High Voltage Air Switch Standards produced by the IEEE [3] to ensure that the switch would not flash over under normal operating conditions. An ac power frequency voltage was applied to a sphere and increased until the point of flashover. The opposing sphere was left floating. The power frequency test can be considered a “hard” test as it allows for ionisation of the surrounding air while the voltage is increased to the point of flash over. This ac testing did prove that flashover occurs consistently to a earthed bond strap around the base of the electrode guide rather than the earth plane. Results of the four tests shown in Table 3.2 and an example of the flashover is shown in Figure 3.12

Figure 3.12 A flashover to the earth strap at the bottom of the electrode guide during testing

Table 3.3 Breakdown voltage for the High Voltage Switch to earth strap

Test Number	Breakdown Voltage (kV ac RMS)	Peak ac Breakdown Voltage
Largest sphere gap (mm)		
1	62	76
2	63	76
3	62	76
4	62	76
Smallest sphere gap (mm)		
5	45	55
6	45	55
7	47	58
8	45	55

Testing was conducted between the spheres to find the flashover voltage required to break the gap without the presence of the 3rd electrode. This testing was used to find the minimum distance between the spheres for applied voltages. If the spheres were too close together then the spheres would flash over as the capacitor bank was being charged. If the distance is too far for the capacitor voltage then the spheres may not flash over to the third electrode when dropped, not triggering the circuit. Four power frequency ac tests were conducted for the two extremities of sphere placement. The results of these tests are listed in Table 3.3 and Figure 3.13 shows the flashover. The flashover occurred on the surface of the insulating tube.

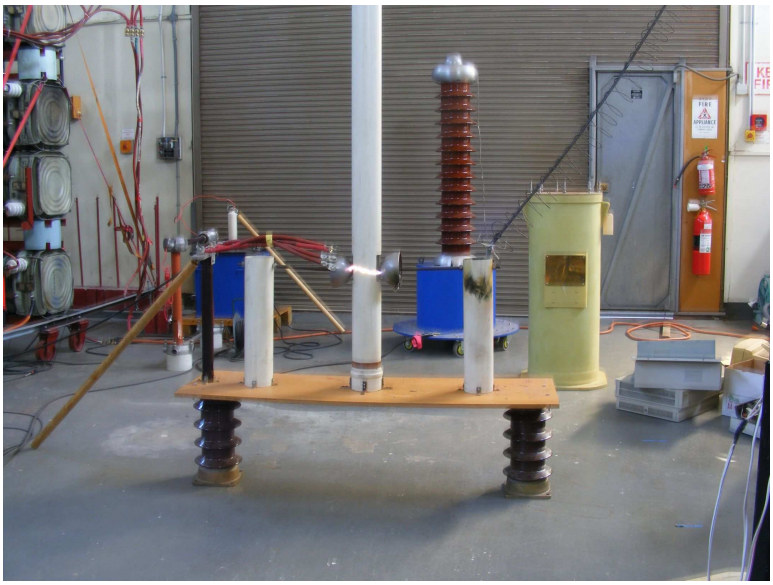

Figure 3.13 A test with a flashover between spheres

3.5 OPERATOR APPLIED HAND EARTHS

Hand held earth sticks were required so that HV equipment can be brought to laboratory earth potential before operator contact. All equipment which is brought to a high potential during testing is required to be earthed and isolated before a operator can approach. The minimum approach distance as in the EI-SM [5] which states;

> The application of isolation and earthing rules and procedures prevents hazard from causes that include but are not limited to the following:
>
> a Inadvertent connection to HV supply.
>
> b Interconnection with other parts of the power system.
>
> c Stored Charge in capacitors.
>
> d Induction from adjacent circuits, atmospheric conditions or direct lighting strike.
>
> e Backfeed from secondary circuits, e.g. via voltage transformers.

Of relevance from this section is all points with the exception of item b. The EI-SM [5] also states with special reference to capacitors:

> In addition, before work commences, individual capacitors and groups of parallel connected capacitors that are to be worked on, or that could be contacted during work, shall be discharged and earthed.

(a)

(b)

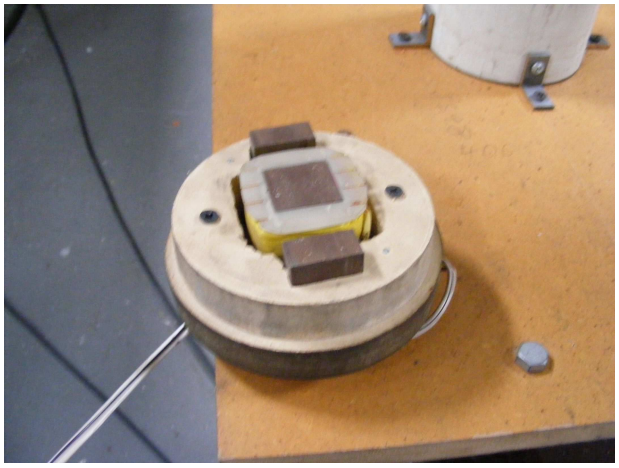

(c)

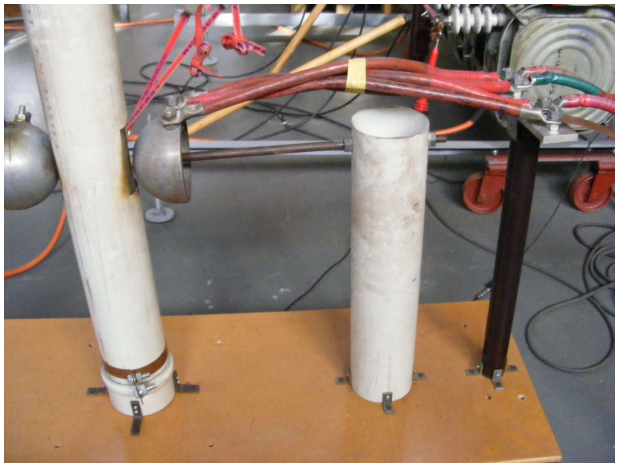

(d)

Figure 3.14 Completed High Voltage, High Current, Switch

Figure 3.15 A wooden commercial earth stick 4m in length.

Figure 3.16 A fiberglass type commercial earth stick.

From this section it can be seen that there is a requirement to discharge and earth all capacitors, and earth and isolate other HV equipment before work may commence on the equipment. As the exploding wire is usually disintegrated after a discharge the operator must isolate, discharge, earth the equipment after every test so that they may reload the test piece and the HV switch. In the power industry use of hand-applied earths is widespread to comply with the EI-SM.

Generally modern hand earthing equipment is made from hollow or foam filed reinforced fiberglass topped with an attached clamp and tail. The end clamp is placed over the conductor being earthed and then the pole is twisted screwing the clamp tight on the conductor. The tail, made of copper cable, needs to be able to withstand a full fault current from the system to which it is applied and is therefore generally substantial in size. On the free end of the tail another clamp is attached so that the operator may connect it solidly to earth. An Example of modern hand earths are given in Figures 3.15 and 3.16.

There are no International Standards for the design or production of live-line hand tools such as hand earths. There are two guides available for the testing of such equipment. The inspection of “The IEEE Guide for Field Testing Power Apparatus Insulation” and the “IEEE Guide for In-Service Maintenance and Electrical Testing of Live-Line Tools”

[2, 1] gives procedures for the testing of hand earth equipment. The testing described in these documents requires that the insulating pole must be able to withstand, 50kV per 300mm for wood and 75kV per 300mm for fiberglass for one minute. No reference to the length requirements of these poles for relative working voltages could be found. The IEEE testing limits convey no safety margin. From the EI-SM the minimum approach distances can be used as the absolute minimum length of the insulating pole. From the IE-SM for a 60kV dc (73.5Kv line to line rms ac equivalent) requires a distance of 750mm.

In this work dual four layer stacks of capacitors were built and therefore eight sticks were needed for the earthing. One insulated stick was required as a water resistor discharge probe. One hand earth was also required for the output of the HV transformer. In total 10 hand earth were required. The relative cost of wooden dowel in comparison to the equivalent fiberglass tubing the best option for use in the laboratory. To this end four lengths of 25mm diameter pine dowelling was obtained. The dowelling was cut making 12 1.2m sticks. The hand earths then had a channel routed around their circumference 200mm from one end to serve as a marker for the operator not to extend their hold over. The sticks were then coated with 3 coats of polyurethane to stop moisture ingression. Moisture ingression is to be avoided as it effects the breakdown properties of the wood.

Steel screw-in storage hooks were purchased as the connection point for the sticks. A 40mm by 15mm 5mm thick steel tab was drilled with a 10mm hole and then arc wielded to the hooks. The hole acts as a bolt point for the tail lead via a 20mm M10 through bolt. This hook and tab was then screwed into the end of the dowel poles.

$16mm^2$ wielding cabling was obtained for use as the tail conductor. The cabling was cut into 4m lengths and crimped with a 10mm connector. The cabling was required to be able to withstand full discharge from the capacitors. Temperature rise calculations were conducted for the cabling and it was found the power loss over the conductor would be enough to cause a 500 °C rise, which is below the copper tails melting point. However if an earth stick were applied to the fully charged capacitor bank the resulting electrical explosion at the point of application would be significant.

Once the sticks were complete, testing in accordance with IEEE Guide for In-Service Maintenance and Electrical Testing of Live-Line Tools [2] was conducted. In this testing spring electrodes 300mm apart are looped around the stick. Every second electrode is brought to a voltage of 75kV ac rms for one minute (as stated for new equipment) whilst the other electrodes are bonded to earth. Current is measured through the earth return path and was found to be constant (not increasing) and below the guides requirements. A racking system allows for many sticks to be tested at once as shown

in Figure 3.17. The hand earths passed this test.

Figure 3.17 Earth stick testing

Chapter 4

MEASUREMENT

4.1 INTRODUCTION

In the charging of the capacitors it is important that the operator know the voltage of the stack so not to damage equipment. Whilst charging the operator needs to know the charging current so that the charging circuit components are not overloaded. This chapter explains the process and equipment used to measure the charging current and voltage.

In order to understand the exploding wire it is important to make scientific observations over the period of explosion. Measuring the current and voltage across an exploding wire gives the instantaneous energy and resistance of the wire both vitally important in gaining an understanding of the mechanism. To this end this chapter explains the process of current and voltage measurement of the circuit. The voltage measurement is done with the use of commercial voltage divider. The current measurement is a much more challenging task due to the magnitude of the impulse current. This chapter gives the process for building and testing a high current impulse measurement device.

4.2 CHARGING VOLTAGE MEASUREMENTS

During the charging of the capacitor stacks the operator requires to observe the voltage of the capacitor layers. By knowing the charge voltage of the capacitors the operator can avoid over charging and reduce the risk of failure of equipment. As voltage of the capacitors is directly related to the energy stored within the operator can estimate the discharge energy into the exploding wire load before testing. This will allow them to prepare for the intensity of the explosion.

It's required is that the voltage be known for each layer of capacitors. This allows the operator to know if there is any unequal charging. As layers may differentiate from one

another in their electrical characteristics the layer voltages will also differ. Whilst it was expected that there will be some differentiation in voltages between layers a large difference in layer voltages will give a indication of a equipment fault. In the case of large differences in layer voltages, the operator can avoid a failure by stopping charging and inspecting equipment. If only the total stack voltage is known there is a possibility that one layer is charged to over-voltage compensating for another layer which is may of failed.

There are several options to measure the HV dc on the layers. Potential dividers are a option as they alow for the measurement on commonly available multimeters. Generally potential dividers are made by a series connection of resistors, capacitors or both. The voltage measured over one of the series connected components has a direct relationship to that of the total voltage measured due to voltage division. With knowledge of the impedance ratios of the divider elements the total voltage can be defined. High impedance elements are used to reduce the power losses in the divider. Resistive dividers can suffer from power losses and stray capacitance to earth at higher voltages and frequencies [6]. For this reason most high voltage impulse measurement is done with capacitive dividers. In the case of measuring the layer voltage (which is essentially steady state) a resistive divider will be of sufficient accuracy.

Six Fluke 80K-40 High Voltage Probe's were acquired (as shown in Figure 4.1). The probes have a 10MΩ input impedance. At a voltage of 15kV the probes will dissipate around 23Watts of power. The probe tips were originally pointed allowing for hand measurement. As the probes are hanging on the capacitor stack a clamp connection needed to be added. The point of the probes were threaded and a screw-on alligator clip attached. This clip allows for the probe to be clamped onto the measurement point and hang freely. The clamped ends were tied to the measurement points with a length of fuse wire. If the alligator clip were to slip off the fuse wire will still stay in place removing the possibility of the probe falling onto other live equipment. Some measurement points on the stack are the capacitor cases. To allow for measurement, paint is removed from the case at the point of contact. This avoids the paint giving any insulation at the measurement point. The probes are connected to standard multimeters and give a reading of 1000:1V.

The probes are rated for up to 40kV dc rms so not all measurements on a four layer stack at 60kV could be referenced to earth. The first two layers are measured between the capacitor bushings and earth. The leads from the probes are then connected to a coaxial cable via a connector and extend to the operator area. The operator can then have the multimeters nearby displaying the first two layers voltages. The upper two measurements (up to 45 and 60kV respectively) are referenced to the capacitor

Figure 4.1 The Fluke80k-40 high voltage resistive divider

case voltages. The multimeters are strapped to the capacitor cases and brought to case potential whilst the probe reads the bushing voltage (as shown in Figure 4.2. During energisation of the capacitor bank these multimeters can not be touched due to their voltage. With the aid of binoculars the operator can read the multimeters from the operator area. Layer voltages are monitored during charing to ensure that the capacitors are sharing charge equally. The user can find the total capacitor bank voltage by adding the individual layer voltages. After discharge the operator can see the remaining voltage on the layers and find the energy dissipated into the load and losses.

4.3 CHARGING CURRENT MEASUREMENTS

During charging the current regulated by the VariAC is measured by a 20A ammeter. A 20A charging current is used initially. This limit ensures that the mains supply is not overloaded during charging. As the mains supply is protected by a circuit breaker the supply could not be damaged. By avoiding tripping this breaker the operator will not have to leave the safety of the operator area to reset it. At voltages approaching the limit of 60kV charging current is reduced from 20A so to be more accurate in the final charge. As the capacitors are at positive dc voltage it is thought that the negative half of the ac waveform from the step-up transformer can cause corona noise. By reducing the current supplied the transformer it outputs a slightly lower voltage. The negative half of the ac wave-shape to positive capacitor potential is reduced, as is the corona.

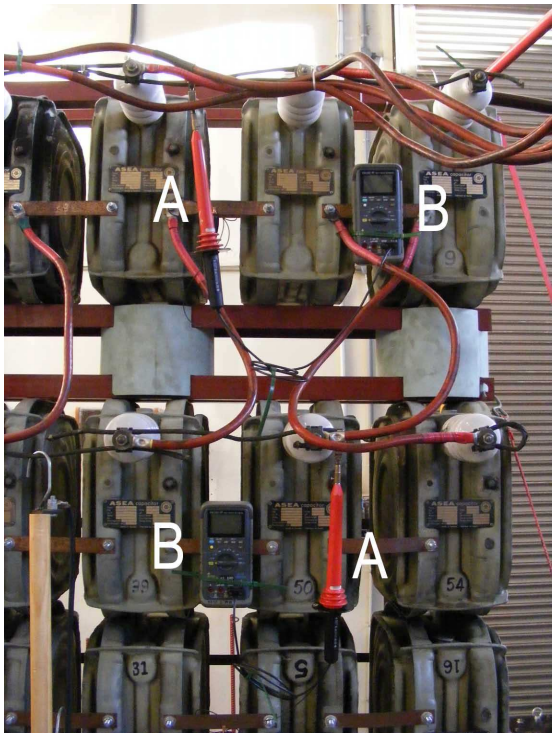

Figure 4.2 The voltage probes on the upper two layers of capacitors. The multimeters case voltage is brought to that of the capacitor case it is attached to. A:The voltage probes. B:The multimeters strapped to the capacitor cases.

4.4 IMPULSE VOLTAGE MEASUREMENT

As described previously there are two potential dividers which may be able to measure HV impulse voltages. The capacitive voltage divider is a ideal option as it avoids the previously stated downfalls of resistive dividers [6]. A Ferranti capacitive voltage divider was available with a rating of 600kV ac and 200pF. The divider measures between the exploding wire connection on the switch to the base of the capacitors. The divider gives a $10,000:1$ output allowing for measurement on common high speed oscilloscope's. The divider output signal is delivered by coaxial cabling with standard BMC connectors. The signal is delivered to a Tektronix TDS220 100MHz oscilloscope away from the wire explosion so the electromagnetic noise is reduced.

4.5 IMPULSE CURRENT MEASUREMENT

The measurement of high speed current impulses with large magnitudes is a challenging task. During testing the laboratory environment has high electromagnetic noise due to the arcing occurring. As with other measurements well shielded equipment with a strong output is desired. This ensures the signal output has a acceptable signal to noise

Figure 4.3 The Ferranti capacitive voltage divider used for voltage measurement over the exploding wires

ratio. Due to this noise devices must have a flexible output gain so that a signal above the noise floor can be given over the different testings magnitudes.

Commonly two different methods are used to measure high current fast impulses;

- The use of current shunts of low impedance.
- The use of current transformers or coils to measure the current.

In the first case the current is passed through a shunt of known resistance and the voltage is measured. From ohms law one can then derive the current. The shunt will have a inductive element giving it a impedance of $Z = R + j\omega L$. It is preferable to have minimised inductive impedance over the frequency range being measured. To avoid this shunts are designed for frequency ranges as well as current capability. As the frequency produces a skin effect on the shunts conductive elements it is desirable that shunt elements are thinner than two skin depths so the ac impedance is similar to that of the dc impedance i.e. $(\omega L)/R \ll 1$.

A current shunt was obtained for the purpose of current measurement. The shunt was originally used for a large synchronous machines excitation current measurement. The current used for this excitation is dc. The impedance of the shunt over the frequency range of 0 - 30kHz needed to be found to ensure that the ωL impedance was not dominant. The shunt was marked with 100mV at 2000A giving a dc resistance of $50\mu\Omega$. To find the frequency dependent impedance the shunt was tested with a signal generator through a 2kW valve amplifier. The amplifier purpose was to allow a voltage to be produced over the shunt of high enough level that it could be measured. The phase

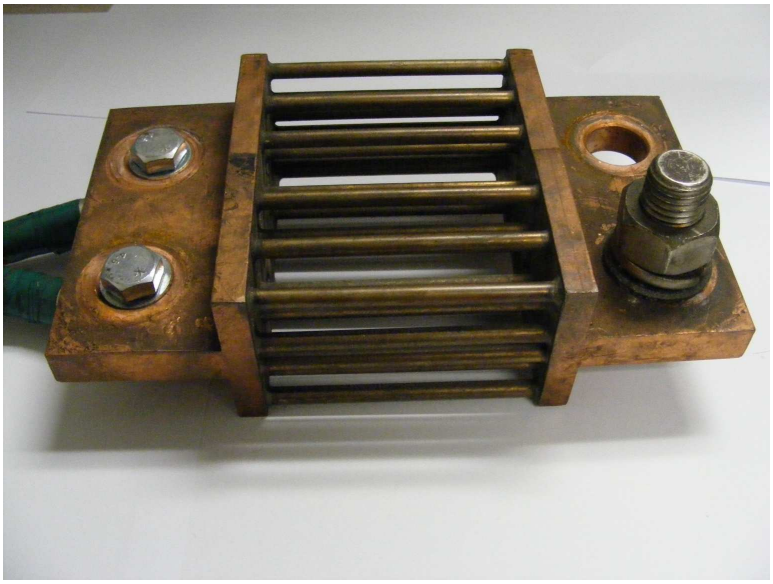

Figure 4.4 The dc current shunt used with connections

shift of the current verses the voltage was measured over the shunt to find the L values over the frequency range. Unfortunately the amplifier running at 2kW was only able to create a voltage of 12mV near the limits of the measuring instrumentation. Further due to the non-linear amplifier characteristics, frequencies beyond around 10kHz at 2kW gave a distorted sinusoidal waveforms. The distorted voltage waveform rendered the results inaccurate (as the frequency input is non-singular). Without the means to frequency test the shunt the use of it was abandoned.

With the use of induction one is able to find the current carried through a cable. This has the added benefit of not affecting the circuit characteristics by added impedance as a shunt would. Commonly Current Transformers (CT's) are used to measure currents in the power industry and laboratories. A CT works through a transformer action with the current carrying conductor acting as one turn on the primary. A toroidal steel core with helicoidal windings is placed around the measured conductor. From these windings a "burden" load is placed between their terminals. The voltage across the burden gives a indication of the current carried in the "primary" conductor. As a CT uses a steel core saturation can be reached giving inaccurate readings over the burden. In the case of impulse currents this saturation effect is of concern as the currents will be of large magnitude. Also as the impulse is of a single polarity it has the ability to drive the CT quickly to saturation. In the case of these experiments several thousand amps were expected so the core of the CT would have to be prohibitively large.

Another method of inductively measuring currents is by the use of a Rogowski Coil (RwC). This method uses a coil arrangement much the same as the secondary of a

CT except without the magnetic core. Instead the RwC it works by using the varying magnetic field of the current carrying conductor to induce a voltage proportional to the rate of change of current in its windings (as shown in Equation 4.1 given in [28]). The absence of the magnetic core also gives the coil output linearity over a range of amplitudes and frequencies.

$$v_{out} = M\frac{di}{dt} \tag{4.1}$$

Were v is the voltage output, M is the mutual inductance of the RwC, $\frac{di}{dt}$ is the change in current with change of time.

From the geometric design of the RwC the mutual inductance can be determined. By integrating v_{out} with the knowledge of the mutual inductance the current can be found. The RwC method was considered appropriate for exploding wire current measurement.

4.5.1 Rogowski Coil Design and Construction

As the mutual inductance of the RwC directly effects the output at its terminals it is of importance that the coil's geometry is designed for its end application. From Equation 4.1 we can see that the design lays in the mutual inductance term. The M term is described in Equation 4.2

$$M = -\mu_0 nA \tag{4.2}$$

Were M is the mutual inductance, μ_0 is the permeability of free space, n is the turns per metre, A is the cross sectional area.

We can see that much of the accuracy of the RwC comes from the geometry of its construction. To gain acceptable accuracy in the final coil the construction must be done within acceptable tolerances. Most RwC are wound linearly on a flexible non-magnetic former, then bent into a toroidal shape. Of particular importance is that the coil geometry and turns do not deform as this will effect the mutual inductance and the end measurements.

A prototype coil was constructed to test the characteristics of these devices. The first prototype used a 18mm diameter, 300mm long length of compressed air tubing as its coil former. As the tubing was flexible it could not be held taught and clamped into a winding machine without buckling. To over come this buckling a metal rod was passed through the tubing giving it rigidity. The tube and rod were then clamped in a winding machine and wound with 0.6mm wire. The windings were wound side by side giving

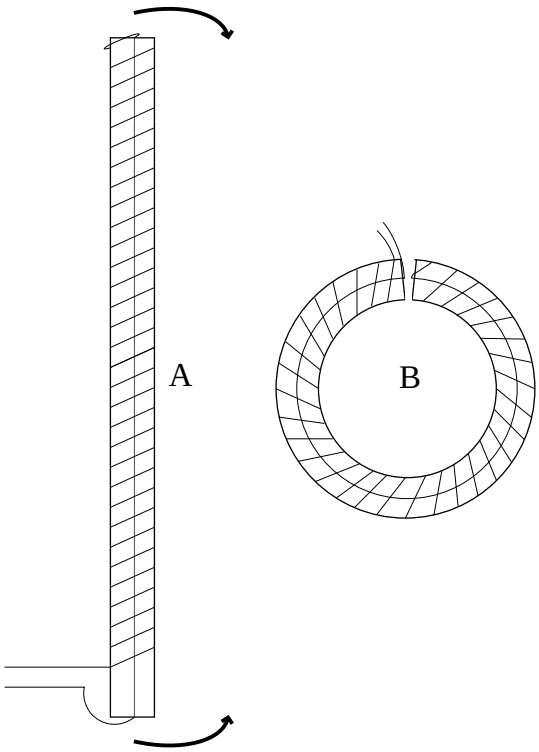

Figure 4.5 A: A rogowski coil linearly wound on a flexible former, B: The coil once bent into a toroidal shape

Table 4.1 Characteristics of Rogowski Coil "Prototype 1"

Prototype Rogowski Coil 1	
Length	300mm
Diameter	18mm
Cross sectional area	2.54e-4 m^2
Turns	500
Turns per metre	1667
Mutual Inductance	-5.32e-07

a total of 500 turns or 1667 turns per metre. Once the coil turns were complete the wire was passed back through the former. By returning the lead through the former any magnetic flux normal to the created loop is compensated for (such as noise). The expected electrical characteristics of the coil are given in Table 4.1 [7].

The winding leads were fitted with multistranded flexible leads and a connector to avoid breakage. The coil was then covered with heatshrink to give some external insulation to the windings. Unfortunately when the winding was bent into a toroid some windings were squeezed out of position due to compression on the interior of the toroid shape. Once the windings had moved it was assumed that the accuracy of the RwC was ruined and the prototype was abandoned.

Table 4.2 Characteristics of Rogowski Coil "Prototype 2"

Prototype Rogowski Coil 2	
Length	300mm
Diameter	23mm
Cross sectional area	$4.15 \times 10^{-4} m^2$
Turns	240
Turns per metre	802
Mutual Inductance	4.19×10^{-7}

Further investigation was conducted and a second prototype was designed for the purpose of testing. 23mm tubing was used as a former. As with prototype 1 a metal rod was inserted into the tube to ensure the former was ridged on the winding machine and did not crush with the winding compression. This prototype used separated windings to allow for the windings to gather on the interior and separate on the exterior when the RwC was bent to form a toroid. To ensure a consistent turns ratio two wires were wound onto the former and then one was removed leaving a single wire with consistent spacing. Every 25mm the windings were taped so that they would not move if tension was lost on the winding machine. The metal rod used for winding was removed leaving the coil. The nature of the former material was to crush when formed into a toroid. To allow the coil to be bent and not buckle the former was filled with sand and then bent. Once bent the two former ends were connected together. As the sand was not pure and of unknown composition it had to be removed before testing. To remove the sand and ensure the former not buckle the coil was placed in a freezer to cool. This hardened the former material so it would not deform when the sand was removed. After 4 hours the coil was removed from the freezer and the sand poured out leaving the empty toroidal coil as shown in Figure 4.7. The winding was then coated in NOMEX paper to give it insulation and mechanical strength. The two leads were then soldered onto a connector. The characteristics of this coil are given in Table 4.2

This RwC was then tested to find its electrical characteristics. In this testing a 3m 0.2mm diameter wire was exploded. The capacitors were charged to 15kV then the switch was released, loading the capacitors with the wire. The wire undergoes a small explosion as seen in Figure 4.8. The capacitors generally discharge with 12.1kV remaining giving a energy output of 0.8kJ over 50mS.

The coil was attached to the current return lead connected to the exploding wire so not to stress the insulation. The output of the RwC was saved to a Tektronix TDS220 100MHz oscilloscope. From this testing it was quickly apparent that the coil output voltage was too high. During this testing the coil had a peak voltage output of 60V while the capacitor bank was only running at 6% of its possible output. As it was expected that the currents would increase for higher energy explosions the coil would

Figure 4.6 The second prototype with insulation removed to expose windings for illustration.

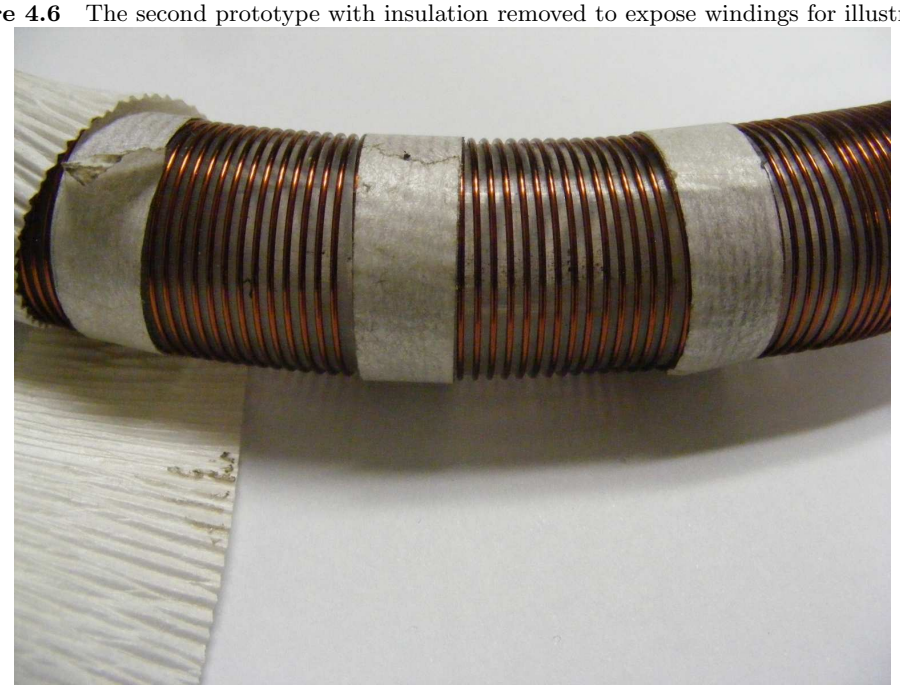

Figure 4.7 A close view of the second prototypes windings.

Figure 4.8 A small wire explosion used to test the Rogowski coils response. Coils are positioned at the bottom right of the picture on the current return lead.

Table 4.3 Characteristics of Rogowski Coil "Prototype 3"

Prototype Rogowski Coil 3	
Length	470mm
Diameter	8mm
Cross sectional area	$5.03 \times 10^{-5} m^2$
Turns	82
Turns per metre	174
Mutual Inductance	2.47×10^{-8}

quickly be putting out too much voltage for the measurement equipment.

As the prototype 2 RwC had not meet requirements another coil was designed and built. To reduce the output voltages of the new coil the mutual inductance was reduced by reducing the turns and the diameter of the former. 8mm air tubing was used for the former significantly reducing the cross sectional area. The former was wrapped in double sided adhesive tape sticking the wire to the former to allow for the turns to have bigger spacings without movement. Once the winding was made one end of the coil was pushed through the centre of the former so both terminations are at one end of the former. The coil was wound using the winding machines automatic feed. This allows for the turns to be automatically spaced on the coil. The coil was then dipped in a plastic coating to give external insulation and mechanical strength. The winding leads were soldered on to some more flexible leads and terminated with a connector.

To test this RwC the same configuration as the testing conducted for prototype 2. A 0.2mm, 3m wire was exploded with a 15kV voltage on the capacitors. 12.1kV remained on the capacitors after discharge. The peak output voltage for the new coil was 5.6V. The voltage maybe still considered high for such a low energy discharge, but the limits of fabrication made this the smallest mutual inductance coil possible to manufacture.

To assess the quality of the prototypes signal, it was compared to the output of a commercially available current measurement device. A Fluke i3000 flexible current clamp was used. This device is rated to measure frequencies from 10Hz to 50kHz and currents to 3000A, so is considered able to measure the current wave form. Both waveforms were captured using a 100MHz oscilloscope utilising single waveform capture. The rogowski output as measured is the derivative of the current waveform as per Equation 4.1. Significant noise was visible on the RwC output waveform as expected due to the high noise environment and relatively low signal levels. The waveform captures were transferred to computer with the use of the Tektronix WaveStar^{TM}software. Once a data-set was available it is converted to a Microsoft Excel^{TM}spreadsheet. The sheet is then processed using a simple MATLAB program. The program uses rectangular numerical integration to integrate the waveform. It can be seen that the integration

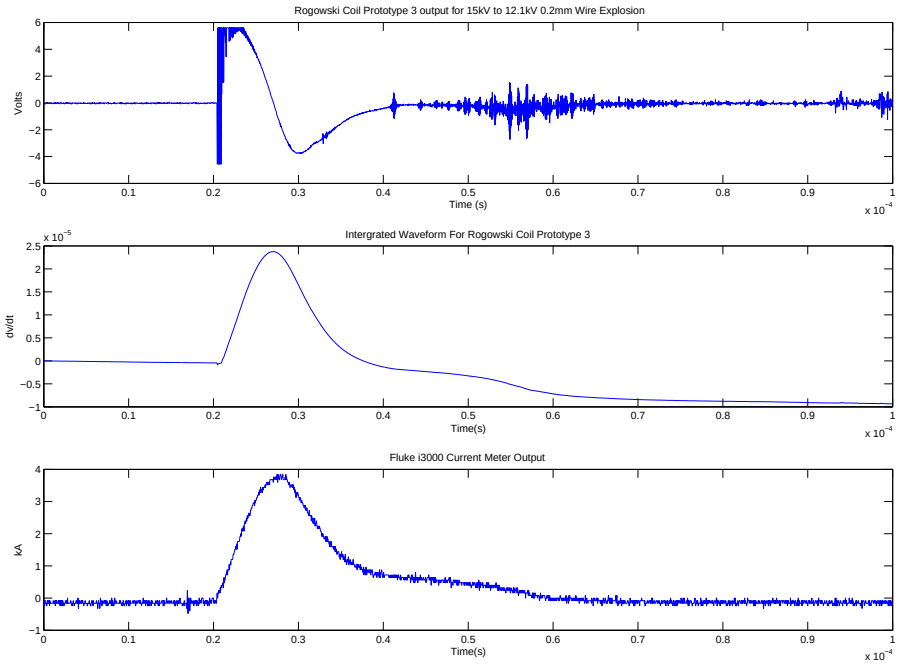

Figure 4.9 The Rogowski Coil raw output, intergraded output and the commercial probes measurement.

algorithm is working as a low pass filter removing some of the noise present in the original RwC output waveform. The waveforms are shown in Figure 4.9. We can see from Figure 4.9 that the integrated RwC wave shape matches the commercial current probe well. Scaling is needed to give the operator a understanding of the amplitude, but this could be done via a integration circuit or software at a later stage. Of concern is the DC offset remaining at the end of the impulse on the integrated waveform. This can only arise from a noise being induced in the coil, or associated circuits. The inclusion of common mode rejection may remove this if it is a common mode noise problem.

From this information we can estimate the "real" mutual inductance of the coil. From the data available the average mutual inductance is obtained from dividing the integrated RwC output by the commercially measured current as shown in Equation 4.3.

$$M = \frac{\int v_{RWC-out}}{i} \tag{4.3}$$

This gives a mutual inductance of 3×10^{-8}, close to the value of 2.74×10^{-8} calculated from the coils geometry. As this coil is the best of the three produced it was decided to use it as the current measuring device for later tests.

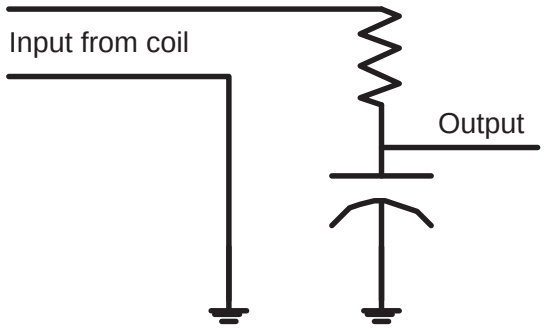

Figure 4.10 A resistor capacitor integrator

4.5.2 Rogowski Coil Integration Circuitry

To allow the user to see the current waveform immediately after a test it was decided to build an analogue circuit to integrate the incoming waveform from the RwC. There are several methods of analogue and digital integration available for this task. Generally analog systems are used as it allows immediate high speed integration to occur. As the author has little experience in digital hardware design it was decided to use analog equipment.

The simplest method of integration is the use of a resistor-capacitor passive integrator. Shown in Figure 4.10 the resistor-capacitor integrator works by the capacitor storing charge when voltage is applied giving a integration. Resistor-capacitor integrators can work well at high frequencies but generally have the requirement of a low voltage output coil [28]. As the amplitude of current impulses measured are high this method is less than ideal. The approximate response for a resistor-capacitor integrator is given in Equation 4.4.

$$v_{out} = \frac{1}{RC} \int V_{in} dt \text{ for } \omega \gg \frac{1}{RC} \tag{4.4}$$

Another method of integration is the use of a active analogue integrator, commonly using a operational amplifier (op-amp). The use of a op-amp allows for the integrator to give valid results for a range of frequencies and magnitudes limited by the op-amps inherent limits. This integrator gives consistent results over a large frequency range and allows the user to avoid often changing the circuit gain or post processing.

The third method of integration is using a computer to analyse and integrate the data. The data would have to be transferred to the computer then analysed. Due to this transfer this method unfortunately would not give instantaneous waveforms as the other methods would.

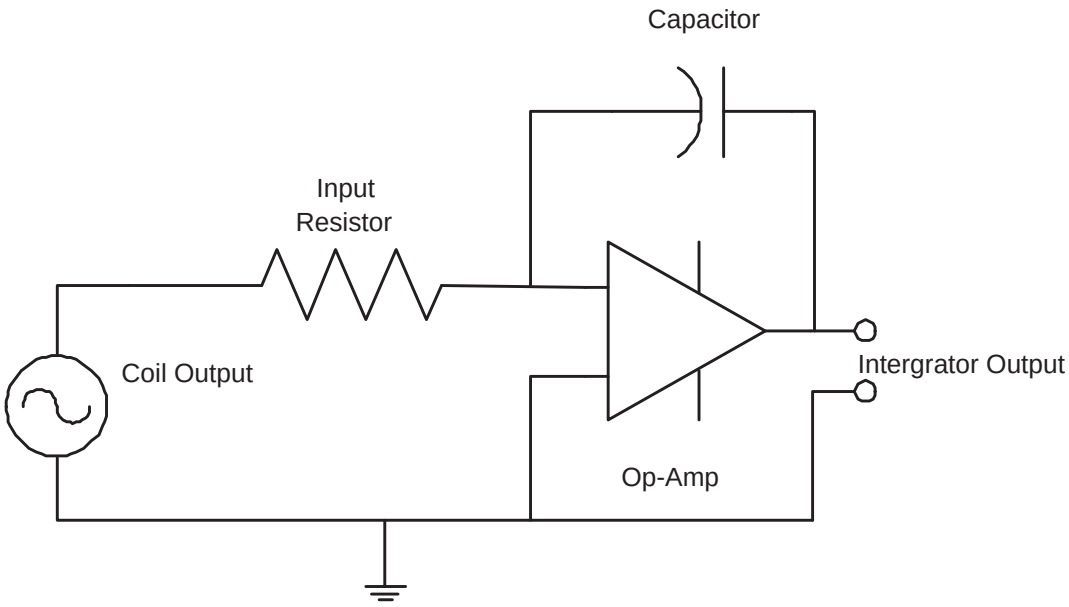

Figure 4.11 A op-amp integration circuit with RwC input

It was decided to build a analogue integration circuit to allow for the real time measurement of current. A review of the literature was conducted giving several different analog circuits which could achieve the required result. From the literature many variations on the standard op-amp integration circuit (as shown in Figure 4.11) are given [36, 7, 28]. The purpose of most the variations is to improve the integrators frequency response for high (100kHz+) frequencies. These high frequencies are not prevalent in the waveforms so these variations to the circuit were not considered. Other variations are used to reduce the gain of low frequency or dc inputs to the integrator. This is important in this application as the noise floor may have a dc bias inducing a run-away in the integration. When the circuits built as a "perfect integrator", such as in Figure 4.11, the integrator will quickly move to one of its voltage limits. This is because the circuit will pick up any random noise and zero frequency offset drift and integrate it out to the limits. To avoid this error a resistor is included in parallel with the capacitor so that the integrator is "leaky". By having a leaky integrator circuit will become stable at rest, and any dc bias will be removed with a RwC time constant [7].

To find acceptable values for the discrete components the op-amp integrator design formulas were used. As a op-amp integrator has a gain as given in Equation 4.5, this was used to find some intimal values for C and R. As a gain of 10,000 would give a 2 volt peak output for the waveform given in Figure 4.9 a resistor value of 10kΩ and capacitor value of 1nF is used.

$$G = \frac{-1}{R \times C} \tag{4.5}$$

An integration circuit was first modelled in the PSpice circuit simulation software. The software allows the input of the measured waveforms from testing as in Figure 4.9. Using the pure integration op-amp circuit the output was a biased version of the real integration as the integrator had intergraded to the -9V rail. With the addition of the "lossy" resistor the waveform is non-biased and brought back up to the 0V axis. Once again visible in this models output is the dc bias on the waveform from the RwC. As with the other dc inputs the lossy integrator will decay the RwC dc signal in the active part of the waveform. Some post-integration analysis will need to be done to remove this resistor-capacitor decay from the waveform leaving the real integration. With the addition of this resistor the new open loop gain is as given in Equation 4.6.

$$G = -\frac{R_f}{R_g} \times \frac{1}{R_f \times C_s + 1} \tag{4.6}$$

With the modelling successfully complete a circuit was built on a breadboard to test the response. The circuit was powered by two 9V batteries to give the ± 9V rails for a Texas Instruments TL071 op amp. The circuit was built and tested in the laboratory connected to the 3rd prototype RwC with 5m of co-axial 50 Ω cabling. Using the same test circuit as for the previous RwC testing (15kV 3m 0.2mm wire explosion) It was found that the circuit would only output noise. As the environment for this testing is high noise it seemed that the breadboard was particularly good at picking up this noise making the output unreadable. To give the breadboard some shielding the board and measuring oscilloscope was placed in a sealed faraday cage box connected to laboratory earth. Whilst this gave some improvement in the results they were still less than acceptable due to the induced noise. Further shielding was required and the breadboard discarded.

A circuit was built on copper plating to provide a earth plane to give better shielding. The components were glued to the copper plate and soldered together. Two holes were drilled into the plate and two BNC connecters screwed into place to allow for input (from RwC) and output (to oscilloscope) from the integration circuit. A further hole was drilled allowing a earthing bolt connection to be placed through the plate. A LED was included to indicate the integrators power is connected.

With the unit built it was then tested on a high current ac source to prove its integration capabilities before being exposed to the high noise environment of the laboratory. A step down, partial core, transformer was used to give a current output of 200A into a

Figure 4.12 A prototyped integrator mounted on copper plate.

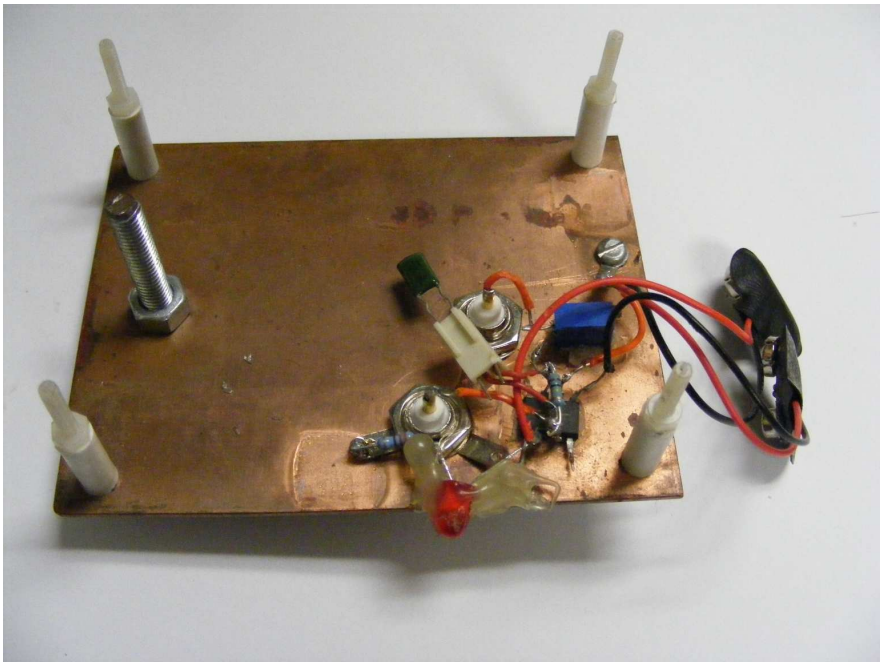

Figure 4.13 A prototyped integrator mounted on copper plate.

length of 6mm diameter wire connected over the secondary terminals. The wire was then rolled together to make a 20 loop turn which the RwC measured over. This gave the RwC a current of 4000A to measure at 50Hz. The coil/integrator gave a voltage output peak of 25mV giving a gain of 6.25×10^{-7}.

As the transformer testing gave acceptable results from the coil/intergrator combination the combination was then tested in the lab. The combination gave noisy results but usable for the 15kV to 12kV exploding wire tests but seemed to saturate at higher current levels. The integration unit was examined and several problems were discovered. The op-amp has a input voltage limit of 15V which would be surpassed by the coil input at higher current levels than the 15kV to 12kV test. The shielding was not completely enclosing the analog circuit allowing noise to enter the circuitry, there was a large amount of common mode noise being introduced through the shielded cable and the battery power supply voltage dropped during the test period.

Because of these problems it was decided that a new circuit should be built on a custom made printed circuit board (PCB). The new circuit included a common mode rejection circuit to remove noise. This was then housed in a fully enclosed steel case to help remove any noise inception. The common mode rejection circuit gives the advantage of having voltage division before the signal is received by the op-amp. This allows for the circuit to receive relatively high amplitude signals which are then reduced in their magnitude before the signal reaches the voltage sensitive op-amps. The circuit was initially modelled in p-spice to give component values.

A PCB circuit board was designed and produced for this purpose and the components were soldered into place. The board gave the option to turn the dual 9V batteries off with a switch and had the LED "power on" indicator light. A section of steel box tube was cut and a endplate wielded on. The endplate had a 10mm hole drilled in it to allow for a BNC connector to be fastened to it for the output connection. 3mm sheet steel was folded to form a tray that would slide inside the box for the mounting of electronics and batteries. The tray had a flat end to cover the opening of the box to shield the internals. A catch was mounted on the box so that the tray could be secured into place. The tray end then had the LED indicator, switch and a opening for the cabling to the RwC put in place. The PCB was mounted on foam to give the tracks insulation from the casing and glued in place. This new unit was then tested in the laboratory with a wire explosion. The unit is shown in Figure 4.5.2

To find the real gain and error of the new RwC the unit measured alongside the before mentioned Fluke 3000i Flexible AC current probe. A 3m long 0.2mm diameter wire was exploded at 15kV and current measured on both current probes. The wave forms measured on the produced equipment required. The differences between the waveforms

Figure 4.14 The integrator circuit and case

were noted as follows;

- There was noise on the RwC wave form particularly at the beginning of the current rise. This is suspected be induced from the flashover from the switch.
- There is a resistor-capacitor decay bias on the waveform from the "leaking integrator".

Whilst the output from the produced RwC and integration circuit gave a readable result to obtain better accuracy both of these differences need to be addressed in the computational analysis of the waveforms. The first difference maybe removed with the use of a low pass filter designed to an appropriate frequency. The second can be removed by finding the RwC decay constant and removing that from the active part of the waveform. For this analysis software was produced using on the MATLAB platform.

A optimised elliptical low-pass filter removes high frequency noise from the waveform. A elliptical filter was chosen as it requires a low order for a step cutoff slope to the stop-band. The digital filter was designed to be 1st order with a cut off of 30kHz. The filter was allowed 3dB of ripple in the pass-band and a 30dB reduction in the stop band. Using the "eplip" filter design tool in MATLAB the transfer function was found to be as in Equation 4.7

$$H = \frac{0.0364 + 0.0364(2)z^{-1}}{1 - 0.9271(2)z^{-1}} \tag{4.7}$$

The initial starting voltage of the RWC decay (Vo) is unknown as it is included with the waveform itself. To find the RWC decay The program samples points near the end of the waveform. As the conduction period has finished at these points the only remaining signal is the RWC decay. Several points are sampled and averaged (removing noise). Using the standard RWC decay equation (given in Equation 4.8) the first sampled point is taken as time zero and voltage Vo. Knowing the voltage and time difference relative to the first for other sampled points the program solves for τ. Using the found decay it is extended backwards from the samples and found over the period of the waveform. This decay is then removed from the waveform. This process is shown graphically in Figure 4.15.

$$V = V_o \times e^{\frac{-t}{\tau}} \tag{4.8}$$

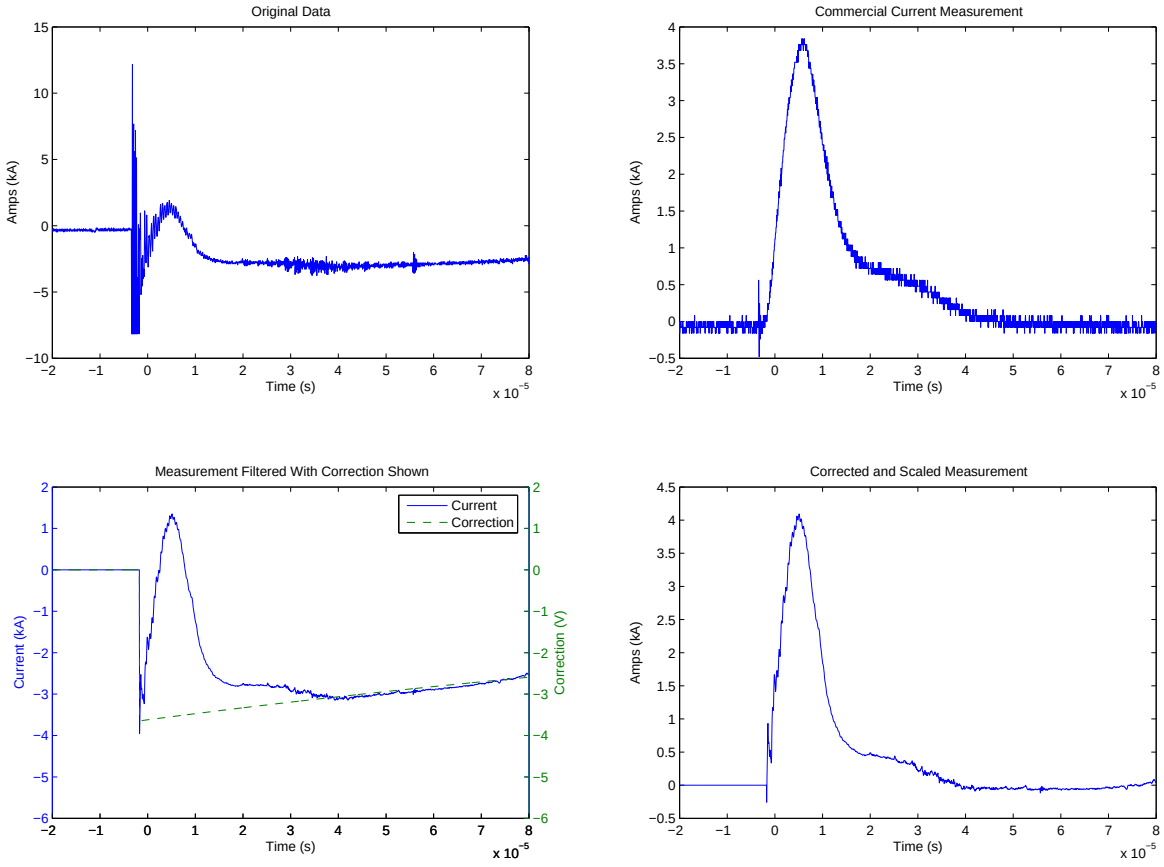

Figure 4.15 A step by step example of the processes the analysis software conducts to give a correct current waveform.

Using this process the input waveform is filtered, de-biased and scaled using the software created.

Chapter 5

TESTING

5.1 INTRODUCTION

This chapter describes a set of formal testing conducted to find the nature of exploding wires on the built equipment. Various procedures were made to ensure that the results were reliable and that the operators were not at risk. Results of each test where recorded with observations. From the testing the waveforms and energy, dissipation are compared over different voltage levels and different wire sizes and lengths.

5.2 TESTING PROCEDURE

Testing procedures were developed for use during the testing conducted. The principal reason for such procedures is to ensure that testing is conducted in a manner which will minimise hazards to the operators and equipment. The secondary purpose of these procedures is to ensure that the experimental results are found under consistent conditions so that they are directly comparable for analysis.

Initially before testing several tasks must be completed. A "Laboratory Class Safety Sheet" is filled out by the operators. This sheet describes the known hazards in the laboratory and gives controls to avoid, reduce, or minimise these hazards. The sheet is filled with all those in the laboratory during the period of testing present so that they understand the known hazards and all sign off onto the sheet. All present then put on the appropriate safety equipment. For the operators a set of flame proof overalls, ear muffs or plugs, and safety eye wear is a minimum. For those further back from the equipment the overalls are not required. The purpose of the safety equipment is to reduced the impacts of any explosion or failure. Finally the supply circuits via a isolating transformer are turned on so that the equipment may be livened when required.

The procedure for charging is as follows;

1. The water resistor, used for discharge, is filled and left cycling water to avoid overheating.

2. The high voltage high current switch is loaded.

3. Any measurement equipment is turned on and triggers are set.

4. The load wire is measured and strung out between the switch and earth return.

5. Earth sticks and discharge probes are removed for the high voltage equipment. These are placed on a table close to the capacitor stacks.

6. The operators move into the Faraday Cage and begin charging with the VariAC.

7. Ear muffs are removed so that the operators can hear any “ticking” or corona coming from equipment.

8. During charging the voltage is checked to ensure even charging over the layers of capacitors. This may need to be done by binoculars if the layers are to be charged to such a voltage where the measurement equipment is isolated at a high potential.

9. Once charging is complete the VariAC is turned down, off, and isolated.

10. A countdown is begun and the switch is fired by releasing the sliding electrode from the electromagnet in the switching mechanism.

The procedure for post-explosion is as follows;

1. The operators assess how much charge is remaining on the capacitors by checking the voltage measurement equipment.
2. A operator leaves the Faraday cage and makes his/her way to the discharge probes, being mindful of the fact the explosion may have left stray conductors in the area.
3. The operator uses the discharge probe on the top of the capacitor stack to discharge the remaining energy via the water resistor.
4. The operator still inside the Faraday cage will announce when the capacitors are less than 200V per layer and that earthing may begin.
5. The operator attaches the earth sticks to each layer starting from the bottom of the capacitor layers towards the top.
6. Once all layers of capacitors are earthed then equipment such as the step-up transformer and capacitive voltage transducer are earthed with sticks.
7. Once all equipment is earthed then operators will save measurements and make observations of the remanence of the exploded wire.

5.3 PURPOSE

The purpose of this formal testing is to make observations of the explosion of wire of various diameters over lengths of 1m to 9m at voltages of 15kV to 60kV on the built equipment. The purpose of these observations is to gain empirical data of the explosion's electrical characteristics under certain conditions and determine what conditions are required for the creation of long distance directional plasma. To ensure these observations are of use, the experiments were completed in a consistent controlled environment.

5.4 TESTING CONDITIONS

To ensure the integrity of the test results all things should remain the same apart from the testing variables. The testing that was done utilised only one of the capacitor stacks for simplicity. The capacitor stack was to be left in its initial location and connections not changed for the period of test so as not to change the electrical properties. The

high voltage switch's spheres had to be adjusted for different voltage levels, this would only have a small effect on the overall circuits characteristics. The wire explosion was situated 1m above the laboratory earth plane and the wire is exploded in a straight line. The current return path was placed 1m bellow the exploding wire so that its electromagnetic effects on the explosion remain constant.

The voltage remaining on the capacitors after explosion is noted so that the energy discharged may be known. The voltage and current over the test piece is also measured for the duration of the explosion. A simple four grouping system is used to describe the visible explosion;

- Wire remains.
- Visible sparks from wire.
- Beads of plasma present and after the explosion there are short lengths of wire remaining.
- Full plasma over length of wire with no lengths of wire remaining.

The variables in the testing is the initial voltage, length, and diameter of wire. The initial voltages used are 15kV, 30kV, 45kV, and 60kV. The wire diameters used are 0.20mm, 0.27mm, 0.3mm, 0.45mm, 0.63mm. The lengths used are 1m, 3m, 5m, 7m, 9m. This gives a total of 100 tests to be conducted. Each test took around 30 minutes to conduct requiring an extended period of testing.

5.5 RESULTS OF TESTING

5.5.1 Energy Dissipation

From the results of testing, energy calculations were conducted to find the energy dissipated over each test. These results are found by using the initial voltage and the voltage remaining after the test is completed. Using the Equation 5.1 the energy is calculated with these two results.

$$\omega_{dis} = n_{cap}\frac{1}{2} \times C \times V_{intial}^2 - n_{cap}\frac{1}{2} \times C \times V_{final}^2 \tag{5.1}$$

Where ω_{dis} is energy dissipated, n_{cap} is the number of capacitors, C is the capacitance of each capacitor, V_{intial} is the charge voltage of each capacitor, V_{final} is the voltage remaining for each capacitor. This energy calculation is that which is removed from

the capacitors. This is not only the energy dissipated in the exploding wire but that dissipated in the associated circuitry (losses).

In practice the voltage for each layer is noted after a test. As the layer capacitors are in parallel all of their voltage are considered equal.

During testing the voltage is noted before and after a test for each layer. From the testing results and using Equation5.1, three dimensional graphs can be created showing the energy dissipation over various wire lengths and diameters for a initial charge voltage. These graphs are shown in Figure 5.1 and Figure 5.2.

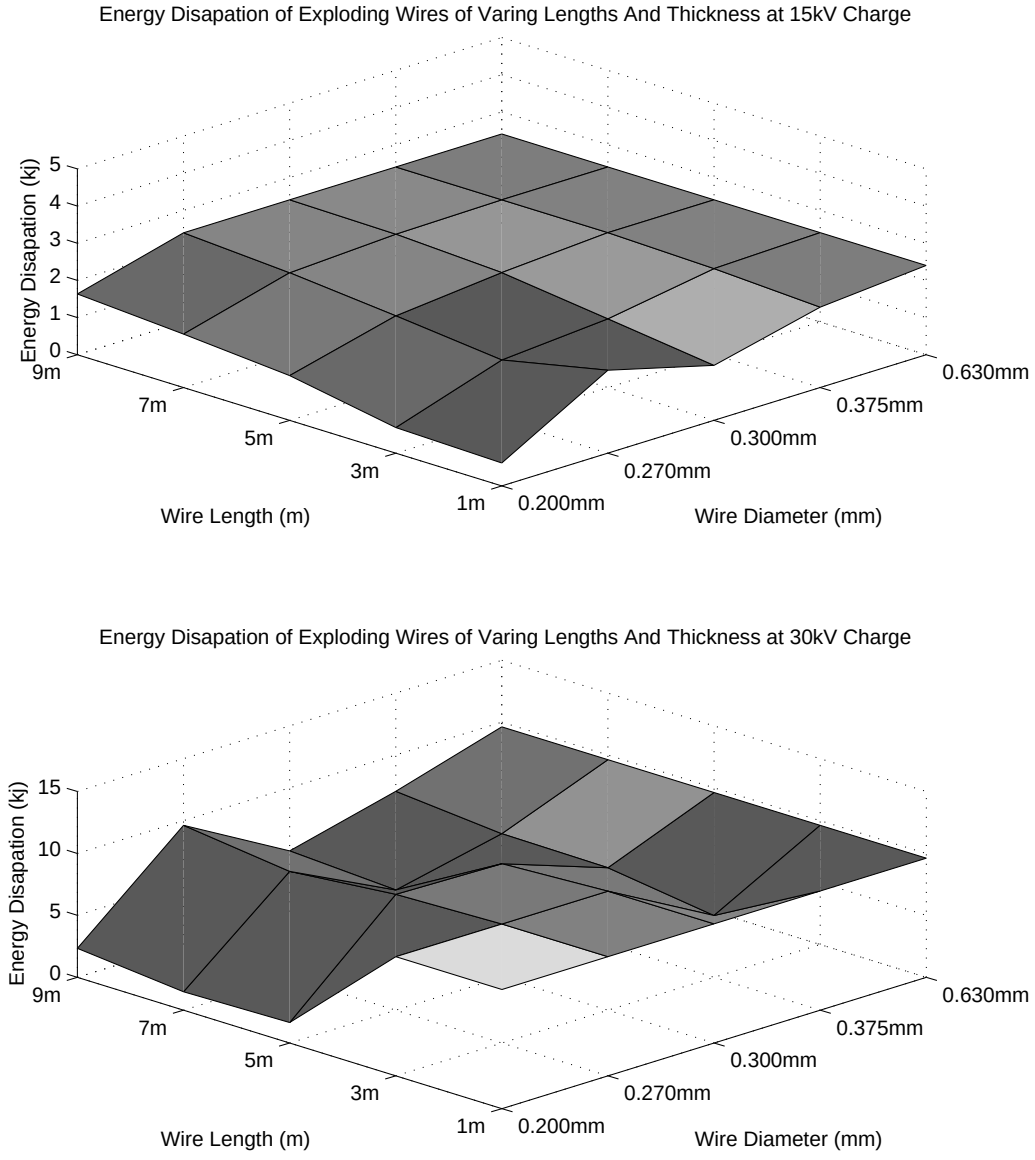

Figure 5.1 Energy Dissipation for the 15 and 30kV tests for all wire diameters and lengths.

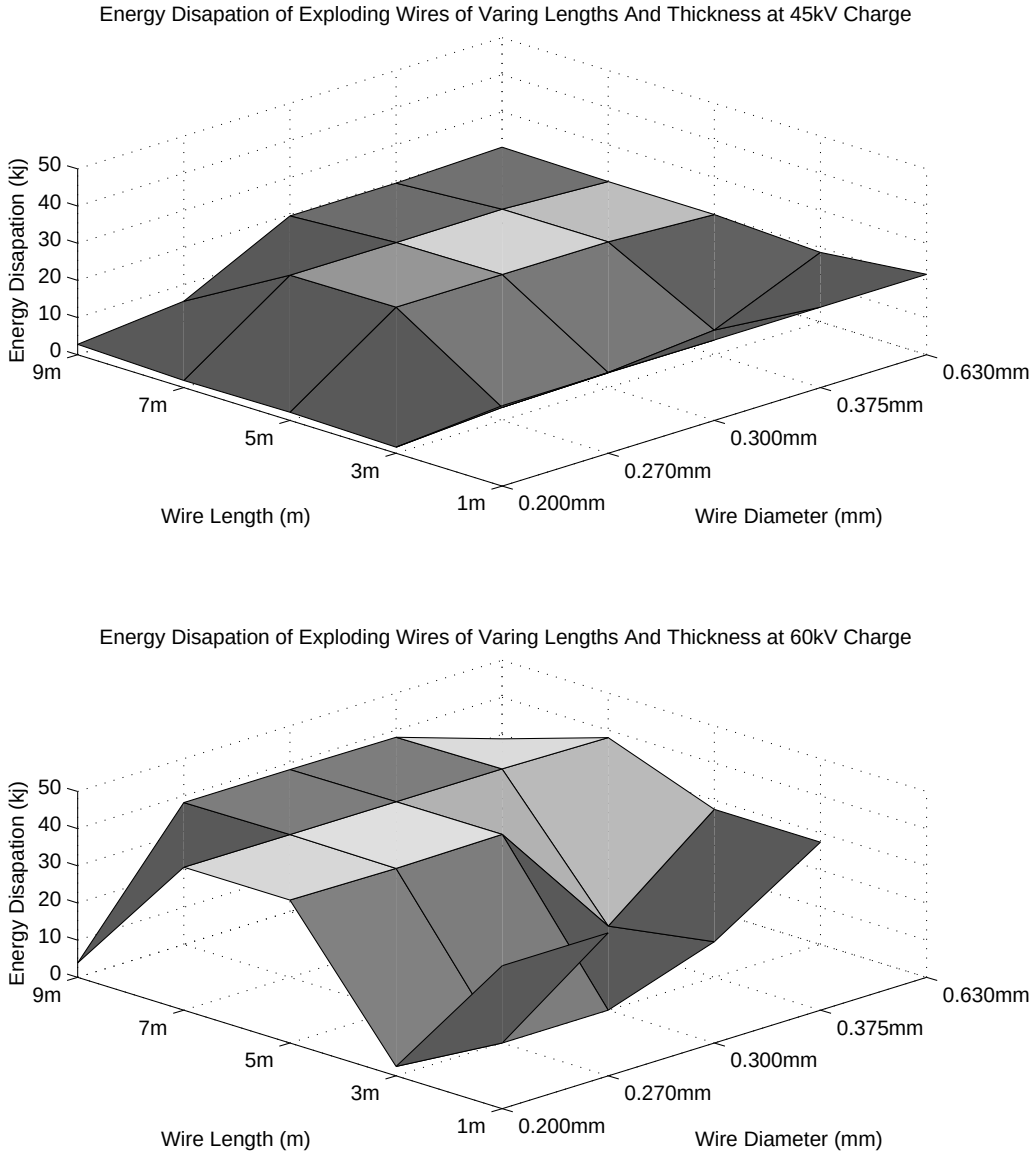

Figure 5.2 Energy Dissipation for the 45 and 60kV tests for all wire diameters and lengths

5.5.1.1 Energy Dissipation at 15kV

The 15kV three dimensional graph in Figure 5.1 shows a distinct area of full discharge. The energy dissipation begins to reduce as the wire lengths get shorter and the wire sizes reduce. From this the 15kV results for energy dissipation can dissected into three main areas;

- "Area A": That of full discharge
- "Area B": That of partial discharge of capacitor energy
- "Area C": An abnormality.

Individual tests can be split into these areas as shown in Table 5.5.1.1 from Figure 5.1

At this voltage level the "Area A" section is that of full discharge. The waveforms of these full discharges could be considered simple resistor-inductor-capacitor damped oscillations. In "Area A", the large wire size of 0.630mm gave the most pronounced oscillations as shown in Figure 5.3. Less obviously, the smaller wire sizes only give half or one oscillation. Similar to a circuit breaker's characteristics it is expected that the exploding wire will extinguish as the voltage across it falls to a zero crossing. If there is not enough voltage remaining on the capacitors at a zero crossing the plasma will not reignite for another half cycle leaving a sinusoid truncated at a zero crossing.

By counting the number of cycles the sinusoidal ring takes to complete Table 5.5.1.1 can be produced which gives a interesting result. It appears that as the conditions of wire size and diameter approach that of a incomplete discharge, the number of complete cycles is reduced. This can be taken that the resistor-capacitor-inductor model is less relevant as the initial conditions approach that of wire explosion.

The "Area A" section resistor-inductor-capacitor damped sinusoids relate well to the observations made during testing. For the wire size of 0.63mm the wire remained intact after testing for all lengths. For the wire size of 0.375mm the wire remained intact for all

Wire Diameter (mm) \ Wire Length (m)	1	3	5	7	9
.630	A	A	A	A	A
.375	A	A	A	A	A
.300	B	B	A	A	A
.270	C	B	B	A	A
.200	B	B	B	B	B

Table 5.1 The distinct areas of the 3d energy discharge graph for 15kV.

Wire Diameter (mm) \ Wire Length (m)	1	3	5	7	9
.630	1/2	1 + 1/2	1 + 1/2	1 + 1/2	1 + 1/2
.375	1	1/2	1/2	1/2	1/2
.300	1	1/2	1/2	NA	NA
.270	1	1/2	NA	NA	NA
.200	NA	NA	NA	NA	NA

Table 5.2 The number of full oscillations of the voltage waveform for the 15kV tests

but the 1m and 3m length. Kinks are noticeable along the wire which maybe the result of vibrations noted in Chapter 2. With more energy available (higher charge voltage) to the wire these vibrations would be expected to rip the wire at points causing the wire explosion.

For the 0.370mm at 1m and 3m the wire the wire explodes in a shower of sparks but without the presence of a plasma path (as shown in Figure 5.4). This is the same observation for the remaining "Area A" tests. Here the wire is seen to explode but it is suspected without the remaining voltage to force a plasma path through the breaks in the wire. The bright streaks in the photograph relate to the paths taken by globs of molten copper thrown from the wire due to the long photograph exposure time. Also visible in the photo is the presence of some arcing at the wire ends and within the switch. The arcing around the wire ends is due to the fine wire conductor joining to a larger conductor the connection point. As the electric field in this region will be considerably high power arcing will occur from the connector to the wire. As this plasma path may give less resistance than the wire path (due to its diameter) the arcing will be of high current. Due to the high current these plasma paths will appear to be bright [29].

For the "Area B" of Figure 5.1 the discharge was incomplete. In this region all waveforms are of similar shape. A example of this shape is given in Figure 5.5. The shape is odd in the fact that it is quite similar to that of the "Area A" except with a added "hump" towards the end of the wave shape. This "hump" is not noted in any of the short wire explosion literature to date. Whilst the wave-shape is similar for all of these "Area B" tests the period of the wave form is different. The period of conduction is related to the wire length and wire size. As shown Figure 5.6 the period of the explosion is extended as the wire gets longer or smaller in diameter. As increasing the length or decreasing the diameter of the wire both have the effect of increasing the resistance, the period may be related to the resistance of the test piece.

The observations of the "Area B" section of Figure 5.1 were of total wire explosion. After testing all wires had exploded in that no long fragments could be found. There

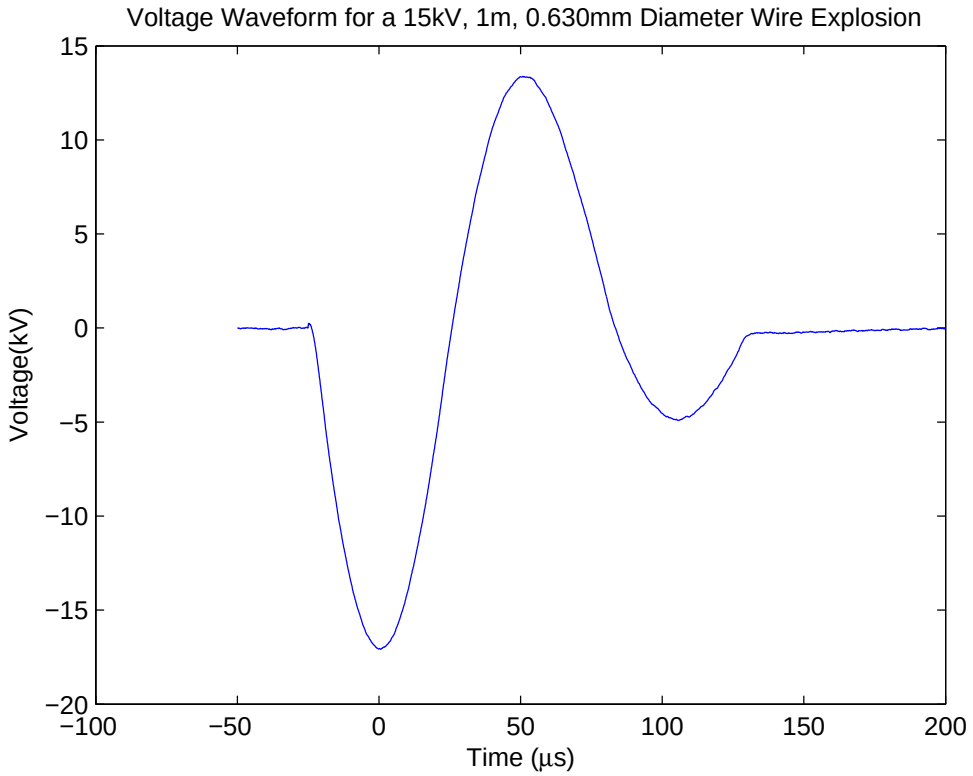

Figure 5.3 The voltage measurements for a 15kV, 1m, 0.630mm diameter wire explosion

were two observations made during the explosion. Some wires gave a full plasma trail as they exploded (as shown in Figure 5.8). Other wires (the majority) gave a beaded plasma trail as shown in Figure 5.7. The 0.200mm at 1m and 3m gave a plasma trail as did the 0.270mm at 1m. The remaining tests in "Area B" are all of the beaded type.

The abnormality at "Area C" is curious. The current and voltage waveforms for this test were very similar to that of that of the"Area B" waveforms with the distinction of a greater magnitude of current. During testing the observation was that the of a full plasma trail.

At these energy levels the separation between wire explosion and no wire explosion can be observed. Theoretical calculations find the energy available to the wire from the capacitors (excluding losses) is able to boil the mass of the copper for all sizes and lengths. The temperature of the wire for the theoretical case can be calculated using the wire's mass.

$$V = \frac{\pi(\frac{1}{2}d_{cm}}{2}))^2 l_{cm} \tag{5.2}$$

Figure 5.4 A "sparky" wire explosion at 15kV

Where V is Volume, d_{cm} is diameter in cm, l is length in cm

$$m = \rho \times V \tag{5.3}$$

Where m is mass in grams, ρ is density in grams per cm^2, V is volume. For copper ρ is taken as 8.96 [13].

$$q = m \times C_g \times (T_f - T_i) \tag{5.4}$$

Where q is the energy input, m is the mass, C_g is the specific heat capacity [13], T_f is the final temperature, T_i is the initial temperature taken to be $18 \deg C$.

Rearranging Equation 5.4 we find the final temperature.

$$T_f = \frac{q}{m \times C_g} + T_i \tag{5.5}$$

By doing this calculation for all 15kV tests the Figure 5.9 is created. From this we can see that all wires should have boiled away yet some did not. The first observation to be made is that the efficiency of delivering the energy to the wire will not be 100% as

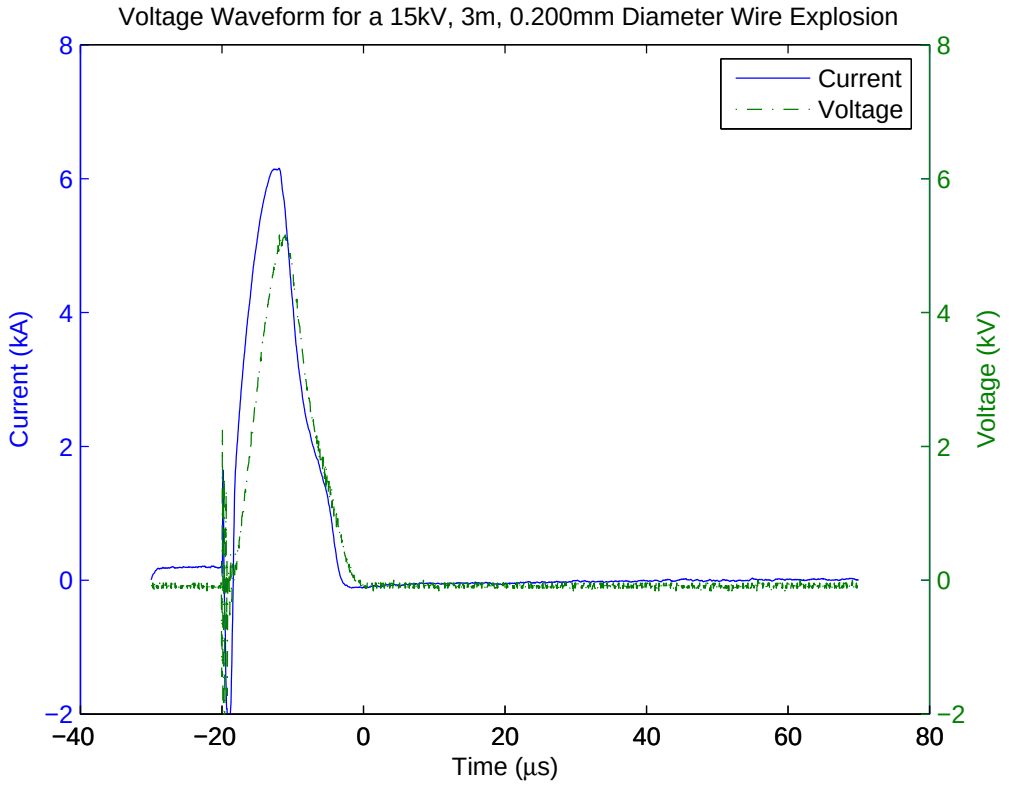

Figure 5.5 The current and voltage measurements for a 15kV, 3m, 0.200mm diameter wire explosion

is assumed in calculation. Losses due to the connections and the switch will cause a reduced energy input into the wire despite efforts taken to reduce these. Secondly the tests done that are contained in "Area B" had energies remaining in the capacitors, so the full energy was not used. And finally this calculation ignores all thermal losses of the copper reducing the ability to heat the wire. It is suspected that the radiative losses of the wire are significant.

In the case of those tests that lie in "Area B" it is interesting that the wire exploded before all the capacitors' charge could be deposited in to it. As the aim of this project is to find the physical requirements to make a long distance directional discharge efficiently it is undesirable that the capacitors' energy not be completely utilised. By choosing the correct wire parameters for the equipment, or vice versa, one should be able to use almost all of the capacitors energy in the explosion itself. This will reduce the requirements of equipment or make best use of what is available to the operators. The goal is in essence to tune the circuit for maximum energy output via explosion. In the case of the partial discharges, this is not achieved.

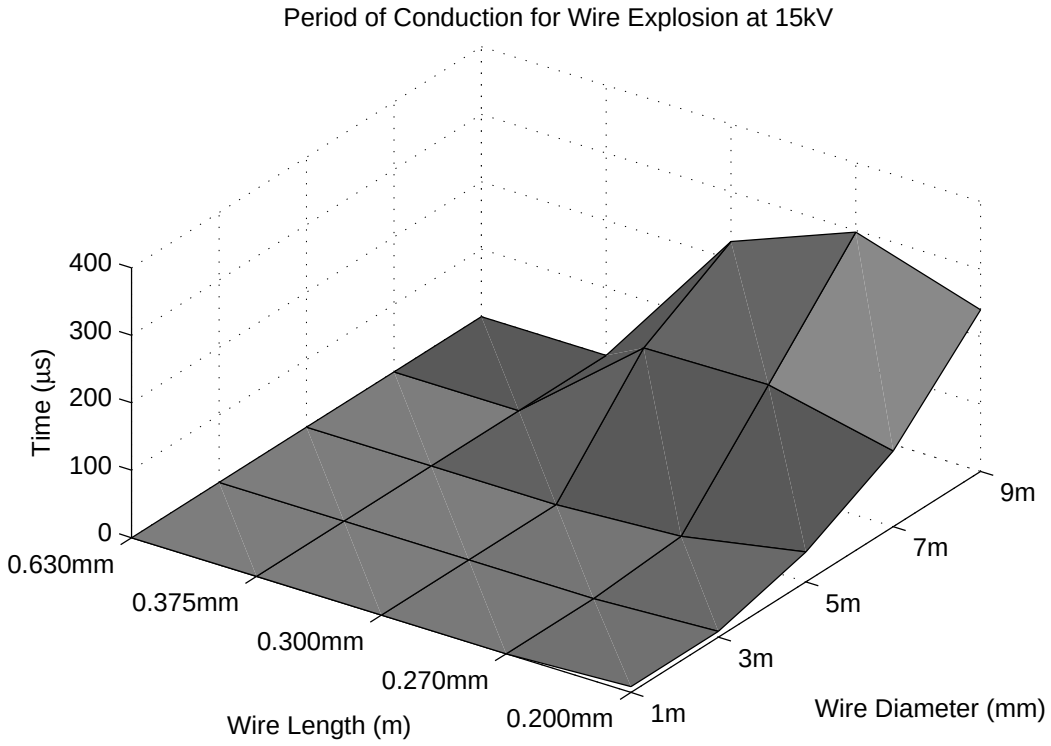

Figure 5.6 The period of conduction for 15kV wire explosions excluding those of full discharge

5.5.1.2 Energy Dissipation at 30kV

The 30kV three dimensional graph as shown in Figure 5.1 is notably different from the 15kV dissipation graph, but it is important to note that the Z axis is 10 times greater than the 15kV case. Energy dissipation for each wire size and length combination is greater when compared to that of the similar combination 15kV cases. In shape the graph differs to the 15kV in that there is a distinct area of full energy dissipation at the shorter thinner wire lengths rather than the opposite for the 15kV case. The vast difference can be attributed to all wires exploding at 30kV rather than only some at 15kV. The effect of having a resistive wire remaining over the duration of the test is removed. Splitting into three separate regions we have;

- "Area A": That of full discharge with presence of substantial plasma production
- "Area B": That of partial discharge of capacitor energy
- "Area C": That of full discharge without the presence of a plasma path

These are outlined in Table 5.5.1.2;

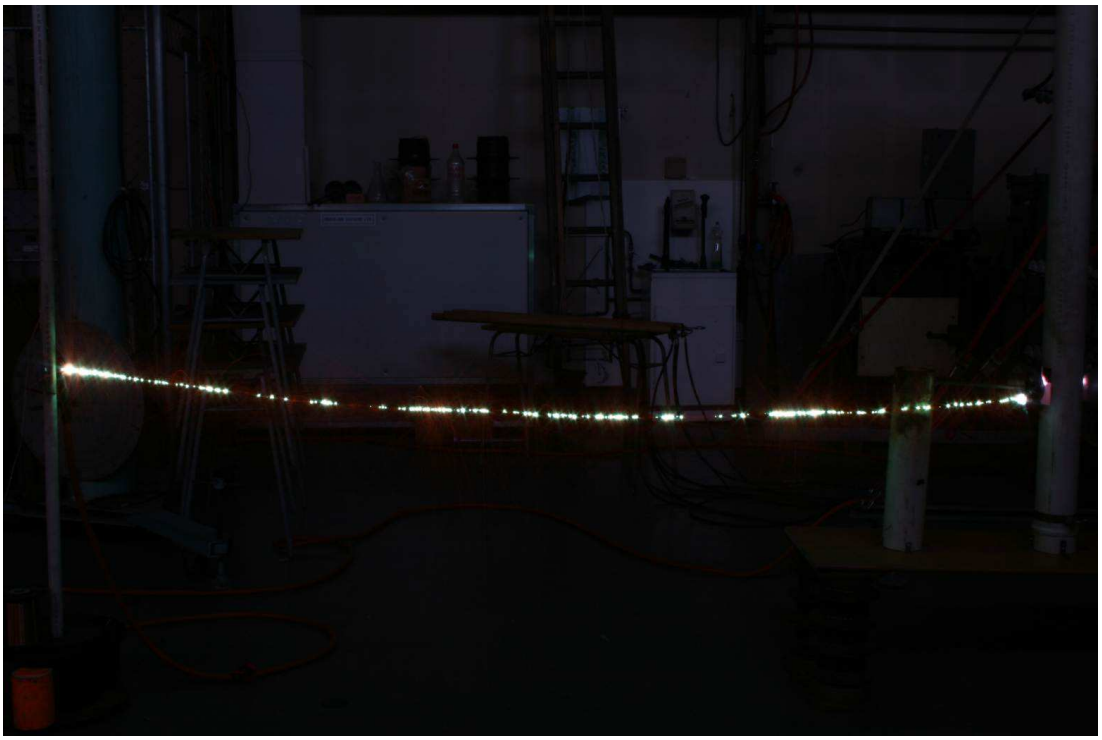

Figure 5.7 A "beaded" discharge

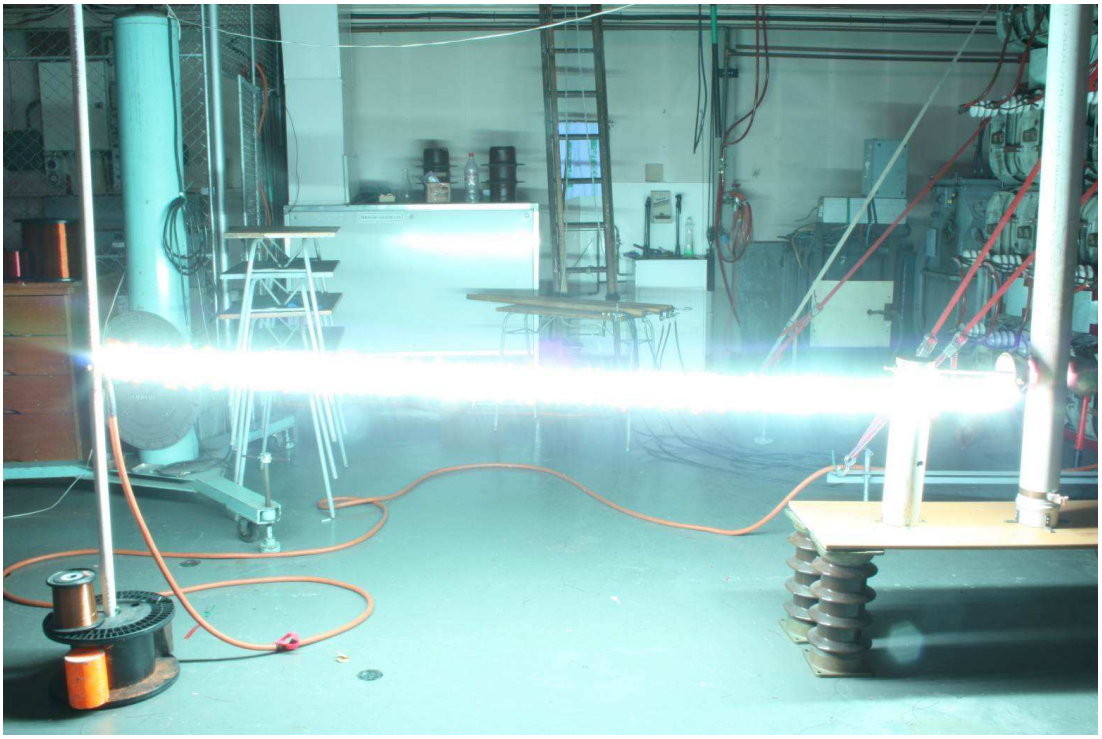

Figure 5.8 A full plasma path as result of wire explosion

All those combinations contained within the "Area A" region resulted in full plasma creation. An examination of the "Area A" region wave shapes gives a curious result. The wave-shapes of similar lengths are related but there is little relation between similar wire diameters and the wave-shape. For the 1 metre tests the wave shapes for 0.200mm, 0.270mm, and 0.300mm diameter wires are of similar shape as Figure 5.10. Of interest in this waveform is the long period of reduced current flow. In the 30kV, 1m, 0.300mm diameter case for example, the period lasts 30μs, 34% of the total period of the waveform. Also of interest: after this reduced current region the voltage linearly collapses for a relatively long period. For the similar wave-shape waveforms of 1m of 0.200mm and 0.270mm diameter the period of reduced current flow is longer as the wire size is reduced.

The remaining "Area A" 1m tests (0.630mm and 0.375mm) have a oscillating waveform similar to that of the resistor-capacitor-inductor wave-shapes of the 15kV tests. The difference between these being that the 15kV wave-shape related to little damage to the wire whereas the 30kV tests lead to the total destruction of the wire and a plasma path. The 3m and 5m tests in "Area A" both have a similar wave-shape. Similar to that of the 1m tests in "Area A", they also feature a no-current region which is related

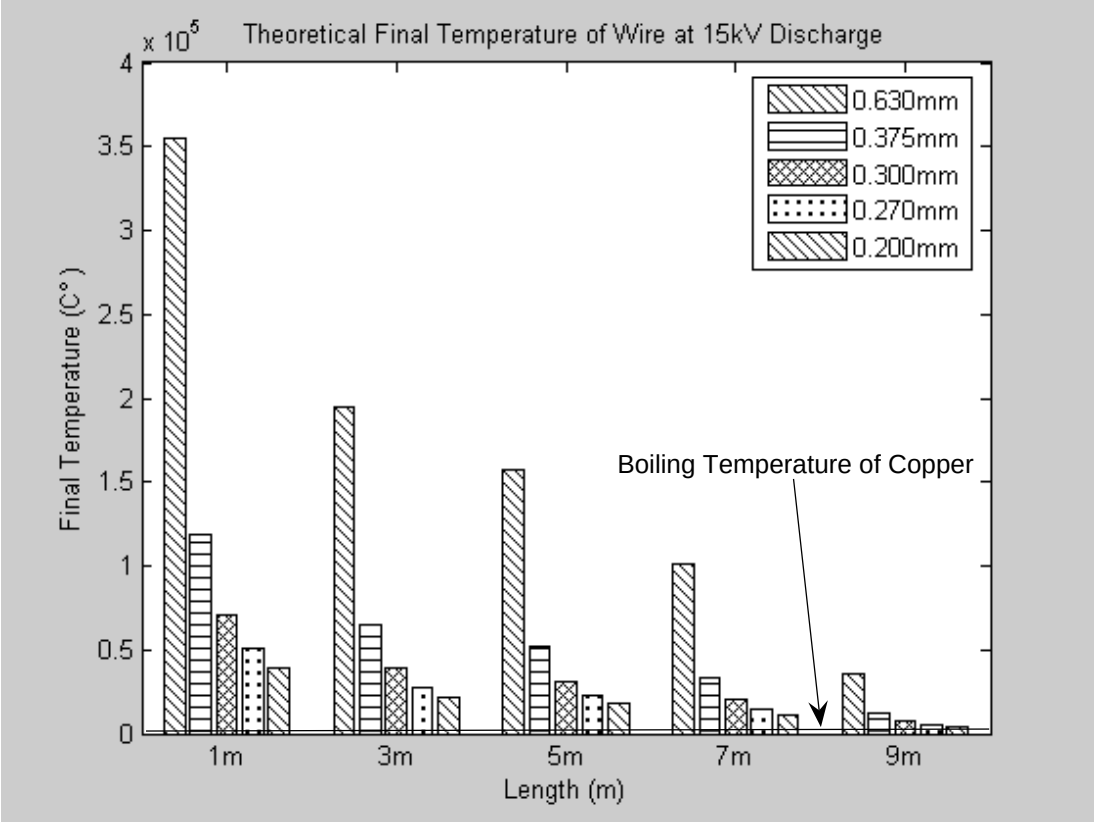

Figure 5.9 The calculated final wire temperature for the 15kV tests.

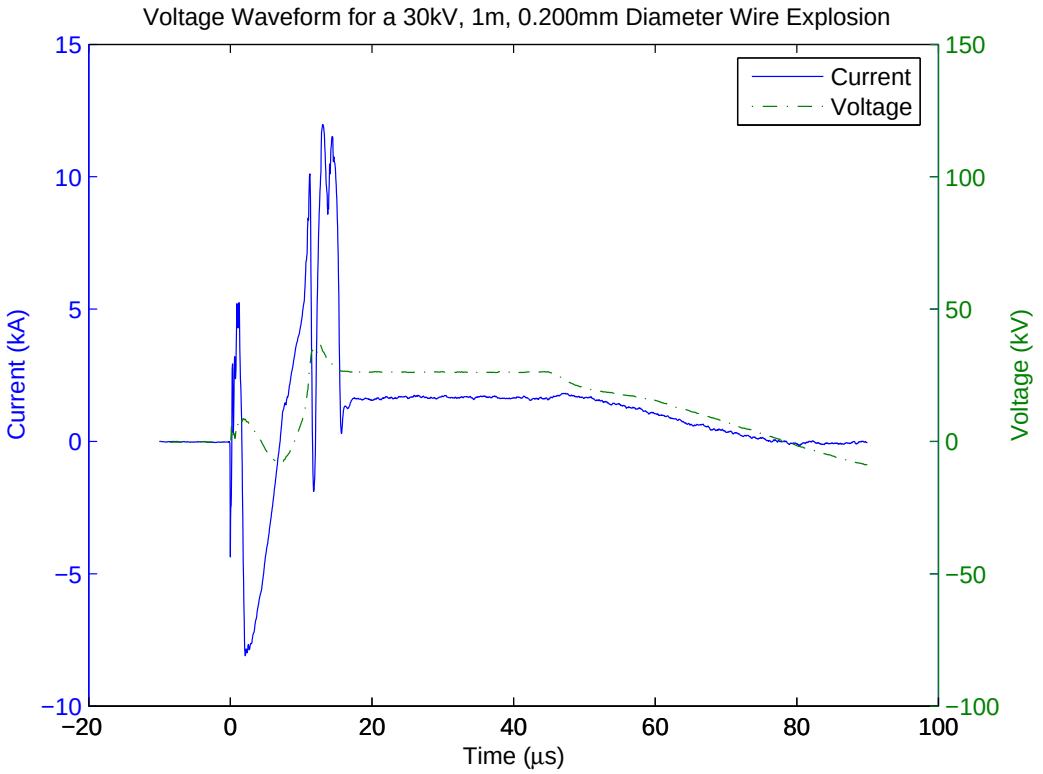

Figure 5.10 The voltage and current waveform of a 1m, 0.300mm diameter wire explosion at 30kV initial charge. The wave-shape is similar to that of the .200mm and .270mm diameter 1m explosions also.

to wire size, but a vastly different wave-shape. An example of the wave shape is shown in Figure 5.11. The 0.300mm wire has the shortest no current period of 400μs and the 0.200mm having a no current period of 0.21μs. This waveform may be related to the current "hump" described in the previous section. In this case it is possible the physical mechanism causing the "hump" has been delayed beyond the initial current flow. From the literature it is this reduced current region called "dwell time" has been noted. It is unknown why the current reduces and then re-strikes but its occurrence is related to wire dimensions [10]. The 5m "Area A" tests have a similar wave-shape but with a extended no dwell time.

Wire Diameter (mm) \ Wire Length (m)	1	3	5	7	9
.630	A	C	C	C	C
.375	A	B	B	B	B
.300	A	A	A	B	B
.270	A	A	A	B	B
.200	A	A	B	B	B

Table 5.3 The distinct areas of the 3D energy discharge graph for 30kV.

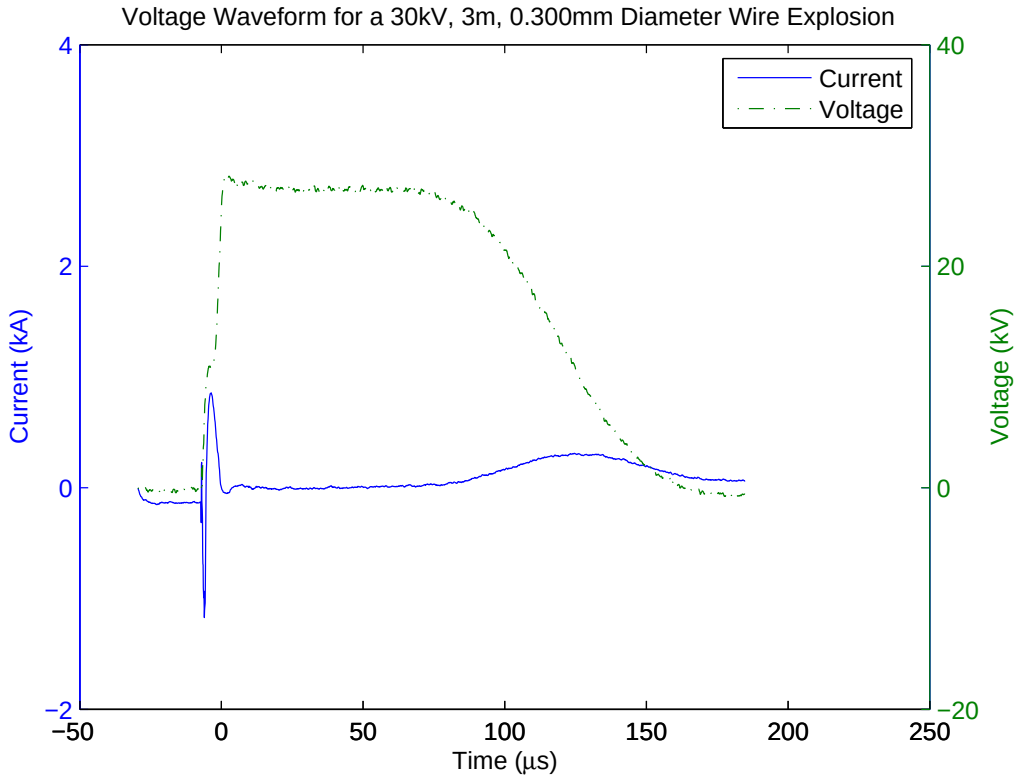

Figure 5.11 The voltage and current waveform of a 3m, 0.300mm diameter wire explosion at 30kV initial charge. The wave-shape is similar to that of the .200mm and .270mm diameter 3m explosions also.

The "Area B" of the 30kV tests given in Table 5.5.1.2 and Figure 5.1 all have a similar wave-shape, shown in Figure 5.12. The wave-shapes are all defined by a peak in current and a rise in voltage to that remaining. The current peak in this case is approximately 35kA. On closer inspection of the graph, a slight voltage "hump" can be seen after its initial rise. This slight rise and drop highlighted by the ellipse's in Figure 5.12 also aligns with a reduction in current decay and a short period of no current flow.

For "Area C", the waveforms consist of oscillating voltage and current wave shapes. Of interest is that the oscillations in voltage reach peak levels higher than that of the initial charge. The 5m, 0.63mm wire explosion reaches a voltage of -76kV at its first peak and 58kV at its second both higher than the 30kV initial charge (shown in Figure 5.13). In a classical unforced RLC circuit a gain above 1 would not be possible. it is unknown why this circuit has such a response.

The observations for "Area A" are that of full length plasma over the wire's path. The plasma in this area is seen to have a greater diameter to the user than the 15kV plasma discharges. The discharge is accompanied by a much louder audible "bang". The observations for that of Area B and C is similar to that of Figure 5.4, again with

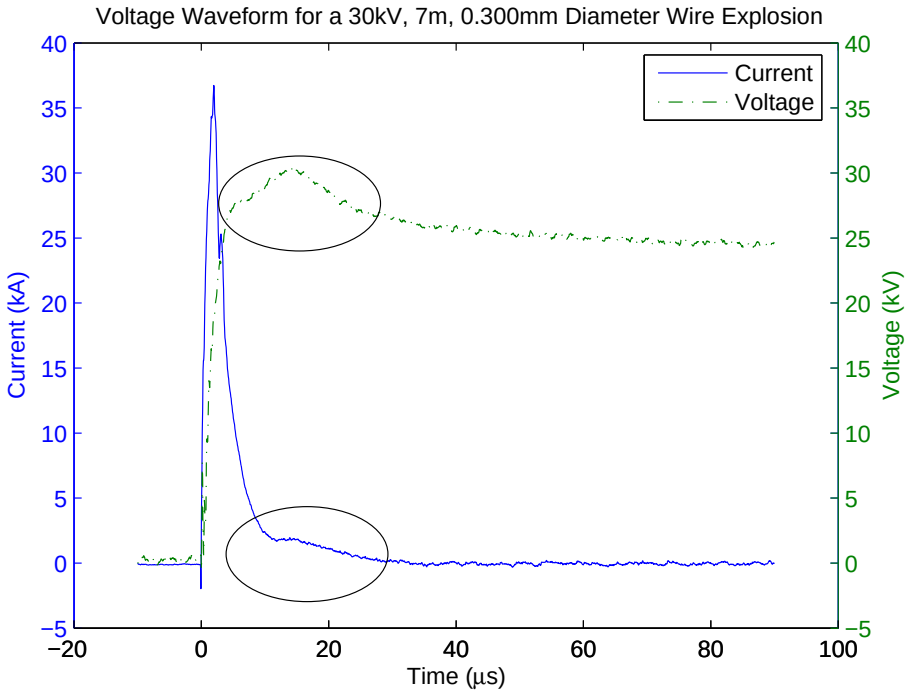

Figure 5.12 The voltage and current waveform of a 7m, 0.300mm diameter wire explosion at 30kV initial charge.

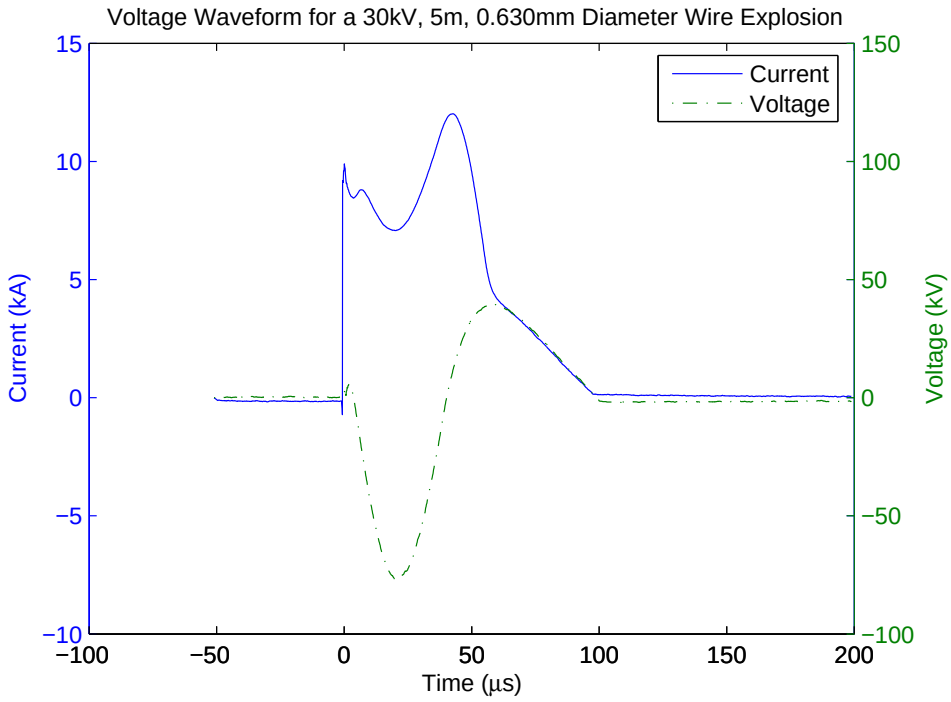

Figure 5.13 The voltage and current waveform of a 5m, 0.630mm diameter wire explosion at 30kV initial charge.

a louder bang than the 15kV tests. The copper fragments are thrown longer distances than that of the 15kV tests due to the much more energetic explosion.

5.5.1.3 Energy Dissipation at 45kV

For the 45kV case the energy dissipation results of Figure 5.2 can be split into three sections. Whilst all but a few combinations of wire diameter and length gave full plasma discharge, these do not seem related to the wave shapes captured. The results are therefore split into three sections as per their wave-shape as listed bellow;

- "Area A": A damped oscillating waveform, similar to that captured in lower voltage testing, resulting in a full discharge.
- "Area B": Contains a dwell time of reduced current flow.
- "Area C": That of full discharge with very little plasma production.

The "Area A" section contains wave shapes of a damped oscillating type. Contrary to that of the damped oscillating waveforms found in the 15kV testing, the wire no longer remains and a large plasma path is achieved. The wave-shape gives many more oscillations than the 15kV case. As the wire is destroyed it is expected that the oscillations are conducting in the plasma. An example of this wave-shape is given in Figure 5.14. The example gives 4 full cycles compared to a maximum of 2 in the 15kV cases. As all "Area A" cases are for 1m (with the exception of one) it is suspected that the energy input into such a short length is such that the plasma is hot enough and large enough in diameter to cause a good conduction path to be produced. This allows for continuous conduction over a long period.

The "Area B" contains both full capacitor discharges and some partial discharges. The wave shape of the full discharges is similar to the wave shapes in the 30kV with a dwell time of reduced or no current flow. In Figure 5.15 we can see a example of the reduced current flow period. Some wire diameter, length combinations did not achieve

Wire Diameter (mm) \ Wire Length (m)	1	3	5	7	9
.630	C	C	C	C	C
.375	A	B	B	B	B
.300	A	B	B	B	B
.270	A	B	B	B	B
.200	A	A	B	B	B

Table 5.4 The distinct areas of the 3D energy discharge graph for 45kV.

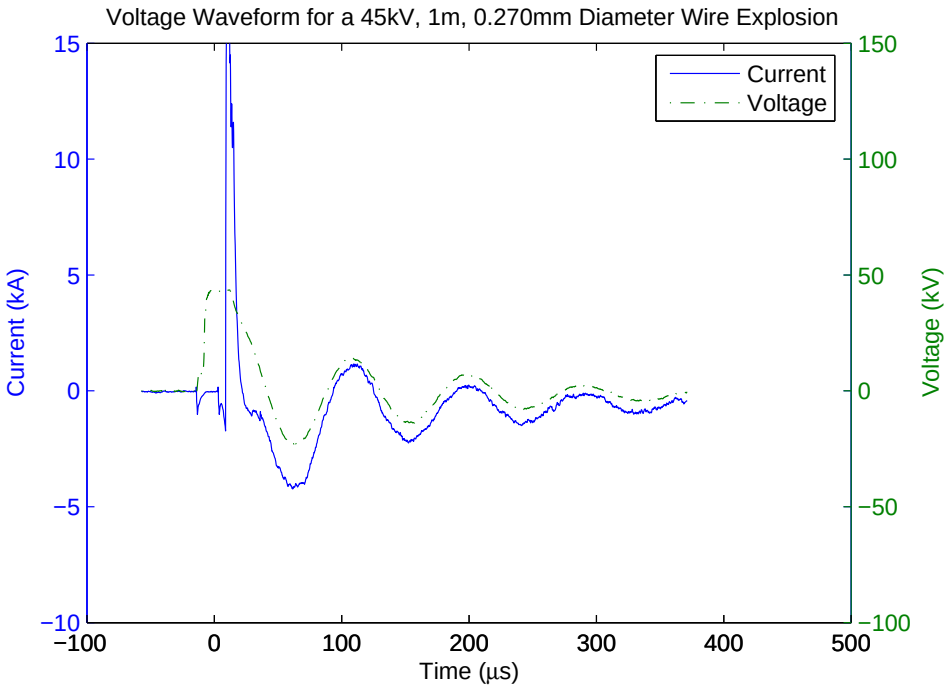

Figure 5.14 The voltage and current waveform of a 1m, 0.270mm diameter wire explosion at 45kV initial charge.

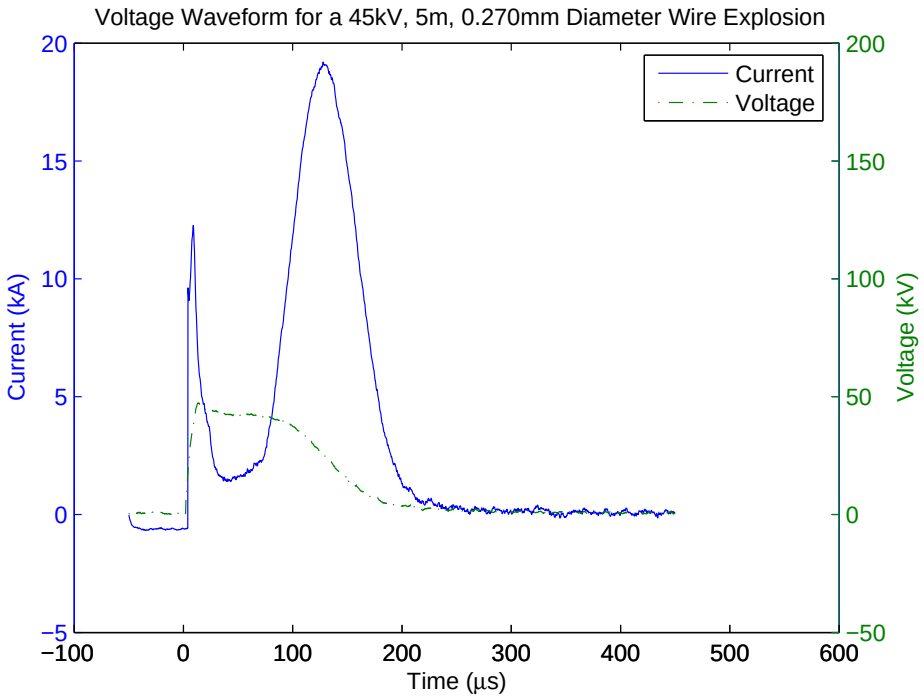

Figure 5.15 The voltage and current waveform of a 5m, 0.270mm diameter wire explosion at 45kV initial charge.

full discharge of the capacitors. The wave shapes for these partial discharges do not have the second section of current flow after the no current flow period as with the full discharge case. It is thought that the re-strike causing this second peak of current flow is not occurring. All of the cases in "Area B" which do not fully discharge are 3m long.

The "Area C" section of the 45kV tests occurred with the 0.630mm diameter wire at all lengths. Whilst all of these wires exploded they did so in a shower of sparks with very little plasma trail (similar to that shown in Figure 5.4). The explosion was more aggressive than the lower power levels with a louder report and the molten copper thrown further hitting objects 5 metres away.

5.5.1.4 Energy Dissipation at 60kV

Using the results from the 60kV tests, Figure 5.2 was produced. This graph shows a island of full discharge surrounded by partial discharge. The testing can be split into two distinct areas;

- "Area A": Full discharge.
- "Area B": Partial discharge.

The "Area A" section all have similar wave shapes. As before the wave-shape is that of a double current peak with a period of reduced or no current flow between peaks. An example of this is given in Figure 5.16. The Figure 5.16 is odd as the first current peak gives a hump as it reduces (seen before in the likes of Figure 5.5) with the addition of a second current peak after a time of no current flow. This may show that if there where more energy/voltage in the Figure 5.16 the second peak may have been achieved by forcing the re-strike. In all of the "Area A" cases there was a very loud report from the explosion. The operators had to wear ear plugs under grade 5 ear muffs so not to hurt their ears. The report could be heard in a separate building 200 metres away. The plasma produced was large in diameter and very bright. The operators could not look directly at the blast to protect their eyes.

Wire Diameter (mm) \ Wire Length (m)	1	3	5	7	9
.630	-	B	B	A	A
.375	-	B	B	A	A
.300	-	B	A	A	A
.270	A	B	A	A	A
.200	A	B	A	A	B

Table 5.5 The distinct areas of the 3d energy discharge graph for 30kV.

The “Area B” wave shapes were similar to that given in Figure 5.17. The observations of these explosions were that they were much less energetic than those in “Area A”. Whilst plasma trails were still produced the report and visuals were less intense.

It should be noted that some of the 1m test results are missing (0.300mm, 0.375mm, 0.630mm). This is due to the destruction of the measurement equipment after the 0.270mm 1m explosion. The 1m explosions where enormous in their report and visual effects. Unfortunately the voltage output from the rogowski coil was such that it destroyed the electronic integration circuit.

5.5.1.5 Conclusions From Testing

The initial conditions of wire length, diameter and charge voltage decide the result wire explosion. It is thought that there is a distinct series of distinct wire explosions dependant upon the energy input into the wire. The list below gives these types in the order of energy released;

- The wire is left unaffected by the discharge.
- The wires insulation is burnt showing that wire heating has occurred.
- The wire fractures into a shower of sparks. This usually removes all energy from the capacitors and is a relatively slow process compared to a wire explosion resulting in a plasma path.
- The wire fractures with sparks and distinct nodal beads of plasma or arcing.
- The wire explodes leaving a remaining trail of plasma in its position. The wire probably boils to gas in this case whilst being shrouded by the plasma.

The purpose of this work is to find the conditions for a wire to explode leaving a plasma path in its wake. From the list above this is the last item and hence requires the greatest energy input into the wire. In order to do this efficiently there should not be energy left on the capacitors at the end of a test hence placing as much energy is available from the capacitors into the wire explosion.

Consistently the final result is achieved at all voltages tested with short wires (1m). Whilst many of these 1m tests did not discharge the capacitors completely, the amount of energy required to explode the wire is small in comparison to the longer lengths. So the 1m tests meet the requirement of creating a plasma path but not the efficiency requirement.

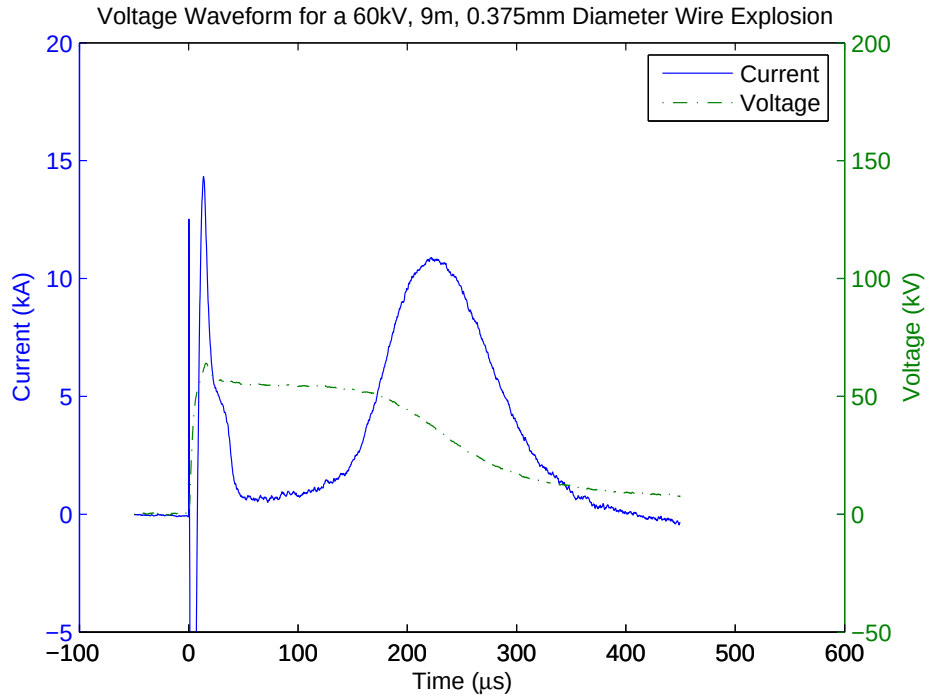

Figure 5.16 The voltage and current waveform of a 9m, 0.375mm diameter wire explosion at 60kV initial charge.

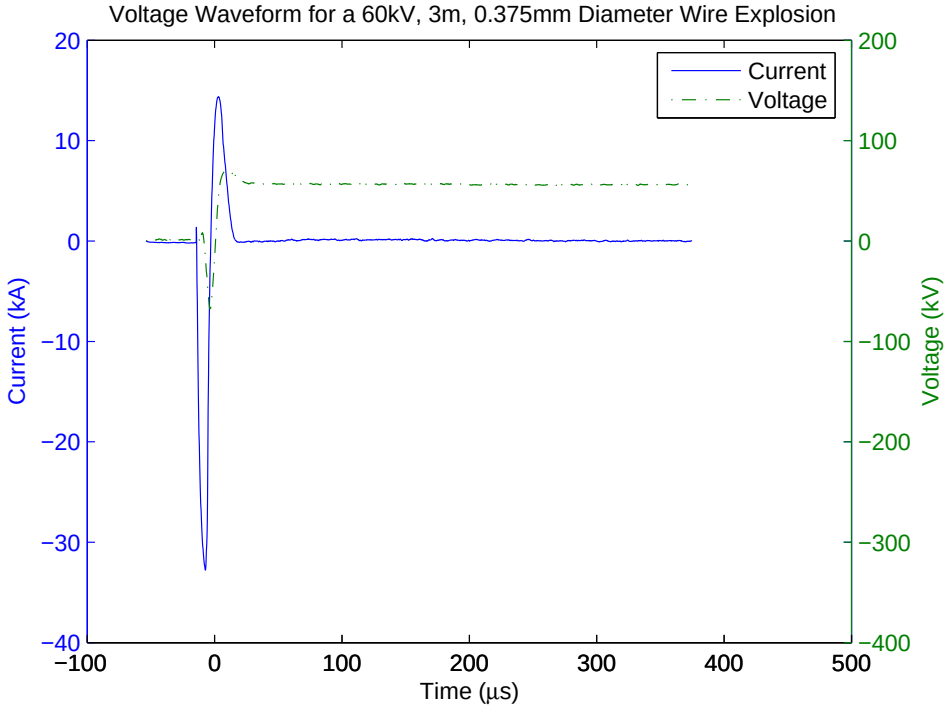

Figure 5.17 The voltage and current waveform of a 9m, 0.375mm diameter wire explosion at 60kV initial charge.

The thick wire of 0.630mm was consistently good at discharging the full energy from the capacitors at all voltages. As this wire has a much greater mass than the smaller diameter wires of the same length, considerably more energy is required to cause the wire to evaporate. As expected the 0.630mm wire did not give the loudest and brightest explosions due to the greater energy being used in its resistive heating and hence the presence of a plasma trail was rare. Whilst this wire size meets the requirement of full discharge it does not always result in a plasma path. At the opposite end of the scale, the 0.200mm wire was easily exploded. It was unable to withstand any voltage/length combination but was poor at producing a plasma trail. It was suspected that because the wire was so thin the current density was easily able to break the wire quickly. As this breaking occurs quickly the wire will break before all the energy had left the capacitors. The best wire diameter to give a plasma trail is therefore not thick, but not too thin and entirely dependent on the required length and voltage.

Increasing the voltage consistently gave a better plasma trail. As the voltage is increased three things occur within the exploding wire circuit;

- The energy available is increased by the squared difference in voltage.
- The higher voltage is able to force higher current levels within a wire.
- The higher voltage allows for a greater breakdown distance between the fragments of the exploding wire themselves.

The increased energy levels allow processes to occur which may not at the lower levels. A fine example of this is the current wave shapes with a double peak at 45kV and 60kV (as shown in Figure 5.15). It is believed that these were not observed at the lower voltage levels because there was simply not enough energy/voltage remaining to force the re-strike to occur. Treating the wire as a simple resistor, the higher voltage allows for a much greater current through the wire. This results in faster heating of the wire/plasma and will reduce losses of heat energy. As the plasma produced is hotter it will in turn be of lesser resistance allowing higher current levels to be achieved. The end result of this rapid heating is that the plasma will have higher currents and is therefore brighter, louder and bigger in diameter. As the wire breaks it uses energy from the capacitors, at the higher voltage levels there will be a higher amounts of energy/voltage remaining on the capacitors. As the exploded wire breaks this higher voltage is able to bridge the gap between the fragments better than if the voltage where lower at that point. Increasing the initial voltage is therefore a certain way to produce a plasma trail.

From the wave-shapes the loudest and brightest explosions generally were the double hump type. The period of dwell between the humps appears to be proportional to the intensity of the explosion. If the duration of this dwell was short the explosion was generally louder and brighter.

At the length of 1m in the 60kV and 45kV cases, the wires had a ringing wave-shape. As the wire was totally destroyed it is expected that the plasma trial was conducting this ring over its duration and that the energy was deposited in the plasma in the form of heat. The effect of this is that the explosions where very loud and bright. It may be possible to force this ringing wave-shape and resulting energetic explosion by increasing the voltage/energy level of the supply equipment.

For a operator to get the largest plasma trail possible, some initial conditions need to be decided upon. For the initial voltage, the more voltage the better. The operator will be limited by the equipment they have available for voltage. For the wire length, it is up to the operator's discretion. Shorter wire lengths give large explosions but longer wire lengths give a more spectacular observation. Once the wire length and voltage is decided the operator should consult the tables of Figures 5.1 and 5.2. From these the operator should follow the wire diameter axis increasing in size until the first full discharge is found. This will ensure that the wire diameter the operator is using is not wasting energy, forcing the wire to explode and putting the maximum amount of energy into the plasma itself.

5.5.2 Observations of Insulation Remnants

After a wire has exploded there are remnants of insulation remaining. The insulation is shed from the copper wire during the process of the explosion leaving empty "tubes" of insulation. The tubes seem to have resisted thermal damage of the exploding wire. The insulation on the wire consists of polyester amide which has a failure temperature of 180 °C. As the insulation resists burning it is thought that the speed of the explosion does not allow for the insulation to be heated to this point. The insulation tubes final length seems to rely on the exploding wire initial conditions of the voltage and wire diameter used.

Using a microscope the remnants of insulation were examined closely. This produced images such as that of Figure 5.18. These images show that the insulation is charred at its ends and had a clean cut down the length of the tube. The end charring is due to that point of the wire having broke and forcing a arc between segments. This point will have the longest duration of existence of hot plasma and hence the longest amount of time to transfer heat the insulation. The slit down the insulation is a little

puzzling as it implies that the copper leaves the insulation through one point where as the explosion appears to be consistently even radially. A explanation for this may be that as the copper removes itself from the insulation the insulation folds open from the slit allowing for the copper to escape radially.

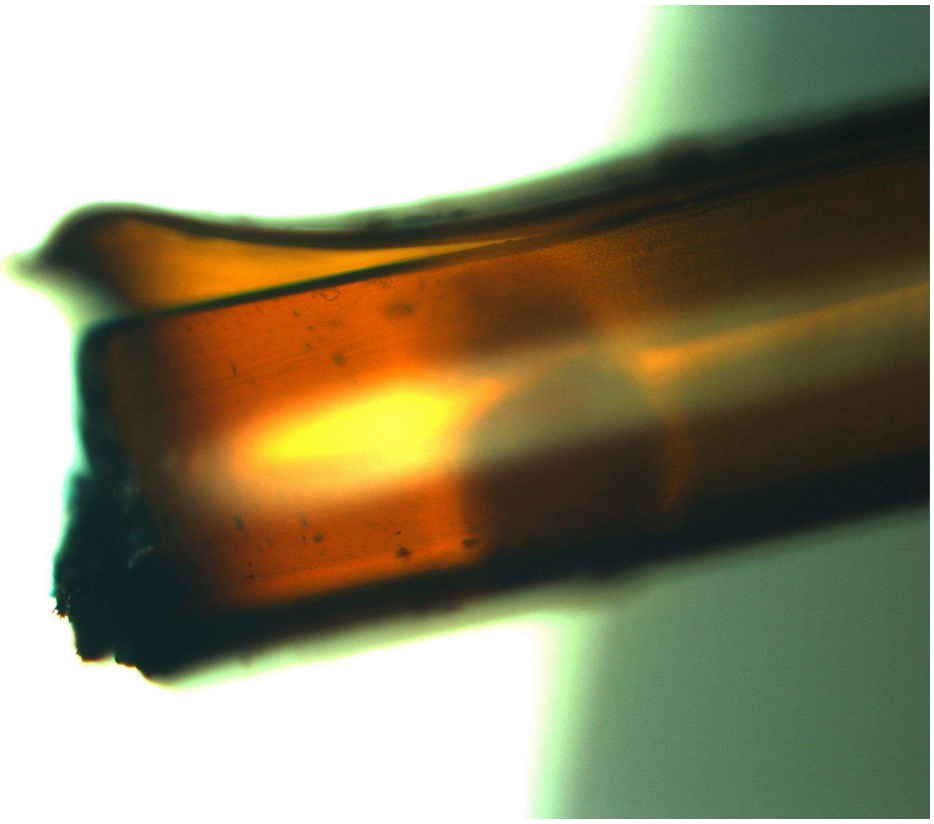

Figure 5.18 A microscopic photograph of the remaining insulation skin. Note the cut down the length of the insulation.

5.5.3 Equipment Damage

The equipment built for the purpose of testing withstood the testing environment with only one failure. A capacitor failed during the 60kV testing presumably due to the large current forced through it. As the capacitors are old and their life-cycle is a unknown, it is hard to presume why a single capacitor out of the twenty failed.

The failure was noticed during charging as the capacitor was brought up to voltage "ticking" was audible from the capacitor stack. Charging was stopped and the stack discharged through the water resistor. To find the capacitor at fault each layer of capacitors was slowly brought up to voltage and the operators listened for the "ticking". Once only one layer was found to make the noise each individual capacitor was brought up to voltage and it was found that only one capacitor was responsible for the noise.

This capacitor was then replaced. As the capacitor did not spill oil or catch fire the failure was not catastrophic.

The switch was found to have some high voltage breakdown in its electrode guide. This is a high stress area as while charging, the PVC pipe is in close proximity to a high voltage electrode on one side and a earth potential electrode on the other side. The treeing measured a length of 7mm next to the opening in the electrode guide as shown in Figure 5.19. As the treeing was not far advanced the guide is still useable, but care must be taken to check the guide periodically for before future use.

The switch's spheres and sliding electrode had also become pitted due to the high current arcing between them during switching. This pitting lowers the withstand strength of the switch as it allows for higher electric field strength on the sharp points. The sliding electrodes pits all were on the lower part of the electrode as expected. As soon as the electrode is exposed by the opening in the guide the spheres will arc to it. The pitting was removed with a rotary buffer to allow for future use. This pitting can be seen in Figure 5.20

5.5.4 Exploding Coils

In a extension of these studies an exploding coil arraignment was investigated. A plastic former was wound with turns of insulated copper wire and then exploded using the energy supply circuit. It was expected that the coil would explode creating a large toroid of plasma which would be of low resistance and allow for very high currents. A former was loosely wound with 5m of 0.300mm wire. 500mm of the 0.300mm wire was used at each end of the windings for connections to the switch and the earth return. The loosely wound coil exploded at 30kV with very little plasma production and a large amount of smoke from the charred insulation. The wire had been successfully destroyed but with little plasma production. The same former was then wound with 50 tightly packed windings of the same diameter and length in a uniform manner. The coil created a large plasma toroid and threw fragments of the wire around the room with great force.

Whilst the electromagnetic force can not be calculated as measurements were not taken the breaking stress of copper is known. Using a yield strength of $220N/mm^2$ and the diameter of .300mm the force applied to break the wire is 15.2N radially. This is therefore the minimum force applied to the windings.

The coil exploded with such force that wire fragments were lodged 2mm deep into a wooden set of draws 3m away. This fragment had to be removed with pliers. Fragments

were found as far away as 5m lodged in various objects. It was taken that a great force acted on the wire, much more than the minimum of 15.2N.

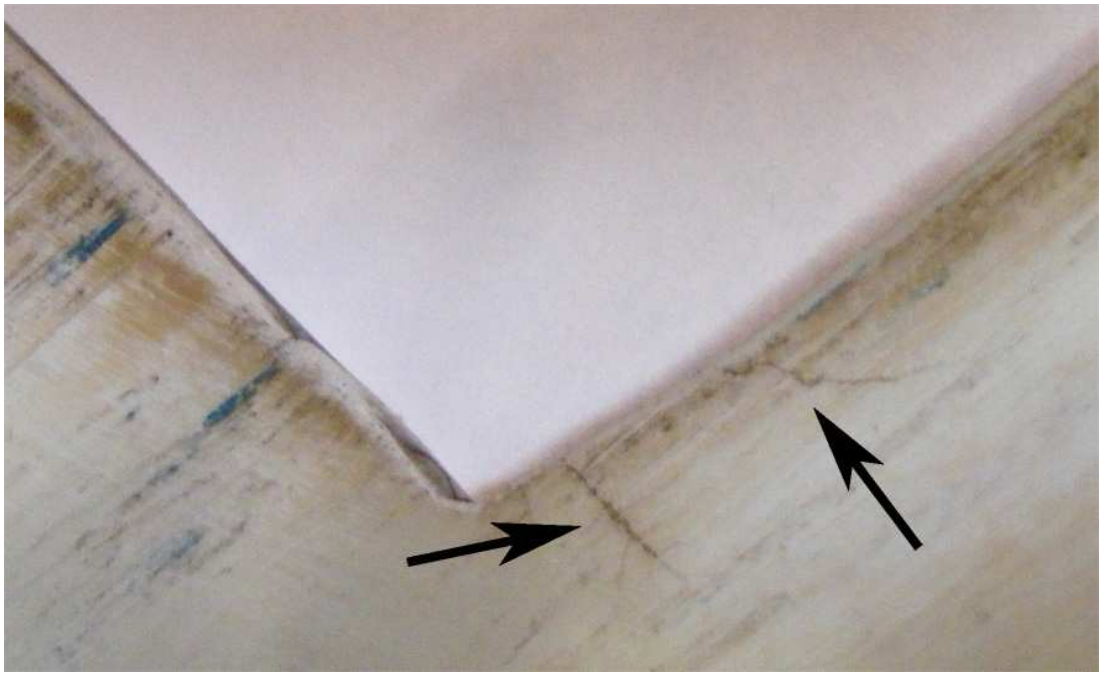

Figure 5.19 Treeing found on the interior of the electrode guide

Figure 5.20 Pitting from high current arcing on the 125mm spheres used on the switch

Chapter 6

CONCLUSIONS AND FUTURE WORKS

6.1 CONCLUSIONS

From the extensive literature review conducted it is clear that the process of exploding wires is not straight forward or well understood. Attempts to model a wire explosion from the starting conditions of voltage, capacitance, wire length and wire diameter from the information and models given in the literature appear to be exceptionally mathematically based. Many models have been put forward that only relate to a single situation. From this it was quickly found that attempts to design a theoretical model of the explosion over a large set of conditions would be pointless in the eight months allocated to this experimental research. In order to understand the exploding wire over a large set of conditions a experimental method could be conducted. In this experimental method many tests where conducted and analysed allowing for a understanding of what would happen if a test were repeated.

In order to gain wire explosion experience equipment had to be constructed for testing. A high voltage, high current test kit was designed and built to explode of wires. Within this test kit a bank of capacitors was required to store charge. The capacitor bank was designed with features to avoid runaway damage if a capacitor where to fail. This required that capacitors be appropriately spaced and sturdily connected to the rack. Cost effective insulation was built for the racks. The built capacitor banks are able to be charged up to 60kV each and variation of its properties is easy and quickly done. The banks as built withstood the testing of this work. A high voltage high current switch was designed to switch the exploding wire load to the charged capacitors. On a restricted budget the switch as built allows for range of voltages to be used. A charging circuit consisting of VariAC, step-up transformer, diode and associated cabling allows for the operator to charge the capacitors in a safe and controlled fashion. Earthing equipment built to International Standards was built. A set of hand earths and discharge probes was produced and tested.

As the research dealt with high energy explosions the safety of the operator needed to be assured. The operators conducted testing within a Faraday Cage with tight mesh allowing for electrical and mechanical protection. From the cage all aspects of the explosive testing could be completed, only having to leave the safety of the cage for discharge and reloading of the wire and switch. Operating procedures where used to ensure that the testing was done in a safe manner. Hazards where explained to those present during testing with the use of a "Laboratory Class Safety Sheet". Operators reduced hazards to themselves with the use of personal protection equipment: overalls, safety glasses and ear muffs.

In order to gain measurements from the explosions a set of measurement equipment was assembled. As each layer of capacitors voltages was needed to be known during charging a set of high voltage probes was obtained and used in conjunction with multimeters. The charging current was measured with a standard 20A ammeter. To measure the voltage waveform over the wire during explosion a 600kV capacitive voltage divider was used. In order to measure the current through the wire a rogowski coil was built. To gain meaningful results a integration circuit was designed and built to allow for current readings. As the results contained noise and nonstandard gain a computer algorithm was programmed to give calibrated results. These current measurements where verified against a commercial current measurement device.

A set of 100 tests was completed using different starting conditions for each. By using wires of various lengths, diameters, and different voltages a set of data was collected. From this testing a set of 3D graphs for various voltage have been presented giving the energy dissipation of the wire sizes and lengths. From these graphs a researcher is able to know what a explosion will be like from the initial conditions. Waveforms of current and voltage for all of the tests where recorded with the use of the measurement equipment. This allows a researcher to use these findings to know the result of a wire explosion with conditions similar to those tested. A empirical model has therefore been achieved.

From the testing completed a researcher is able to estimate the result of wire explosion before it has occurred. Wires of large diameters tended to use all energy within the capacitors but give a low intensity explosion if any at all. This is due to the relatively large amount of energy required to fracture and boil the wire. Smaller wires use little of the energy within the capacitors but explode easily with little intensity and generally without a plasma trail. The key to creating the largest intensity explosion at a given length and voltage is to optimise the wire diameter. The optimal diameter will only just be big enough to discharge all of the capacitor banks energy, no more. As a extension of the results it is thought that a wire of any length is able to be exploded

as long as the diameter allows. The intensity of the explosion is closely related to the energy/voltage available to it. Hence increasing the voltage supplied whilst keeping the capacitance the same will have a positive effect on the intensity of the explosion of any length. As a extension of the results this is particularly relevant to very long (50m+) wire explosions where the voltage will be needed to force a high current through the resistive wire. Whilst it maybe obvious that increasing the energy/voltage available to the wire explosion will increase its intensity less obviously the wire diameter needs to be optimised again with change in initial conditions.

6.2 SUMMARY OF CONTRIBUTIONS

1. The design and construction of a high voltage, high current test set for exploding wires was conducted and documented.
2. The design, construction and testing of a inexpensive, high voltage, high current switching system was conducted and documented.
3. The design, construction and testing of a Rogowski Coil, associated circuitry and software was conducted and documented.
4. A set of 3D graphs outlining the relationship between energy dissipation and wire diameter and length allows for a researcher to find the result of a test before it is conducted.
5. The method of producing the highest intensity plasma has been found to rely on optimisation of the wire diameter.

6.3 FUTURE WORKS

Whilst much work has been done exploring the properties of long exploding wires in this body of work, much more remains to be done. This work uses empirical methods to describe exploding wires with a set group of initial conditions. The initial conditions where set by the equipment available and time frame available to the Author. With further time and equipment the following could be explored further.

6.3.1 High Speed Image Capture

With the use of a high speed camera images of the exploding wire could be captured throughout the conduction period. With the ability to take images at high speed the

physical condition of the wire and or plasma could be compared the various stages of the wire explosion. The condition of the wire and or plasma during the no current region on the double peaked graphs would be of particular interest. If images where able to be captured during this region its physical process may be able to be explained and modelled.

6.3.2 Variation of Capacitance and Voltage

The equipment as built allows for the variation of capacitance. This was not done for the formal testing due the number of tests. With the variation of capacitance it would be of interest to compare testing of like energies but differing voltages. It is known from testing that the voltage of the supply circuit is of great importance to the size of the resulting wire explosion. But there may be a minimum limit of capacitance required to create an exploding wire. Using the equipment built one may be able to compare that of tests of varying capacitance and voltage with like energies to find the optimal capacitance/voltage level.

As two stacks where produced there is the ability to create a two stage Marx generator circuit. This circuit has the ability to double the energy input and voltage into an exploding wire over the single stack used. A study of the extended voltages and capacitance and its effects may be of interest.

6.3.3 Modelling of the Wire Explosion Mechanism

Using the data gained from testing it maybe able to produce a electrical model for the various sized exploding wires with reference to the initial conditions. By using the individual waveforms found during testing a relationship could be built for the current peak amplitude and no current period forming a standard waveforms for the intimal conditions.

6.3.4 Production of Very Long Wire Explosions

With the use of higher voltages it will be possible to produce very long plasma trails limited only by the supply circuitry. Testing could be conducted to produce the longest wire explosion for the test equipment already produced. This could be extended with the use of a higher capacity capacitor stack, or increasing the rating of the current capacitor stack.

6.3.5 Aspects of Exploding coils

Exploding coils have been shown to be possible to produce. With the current density provided by exploding wires it may be possible to produce high flux environments. Further studies could be conducted into the production of high flux and its uses. The use of exploding coils in a transformer configuration may also produce resulting high voltages on the secondary windings.

Appendix A

WAVEFORMS

This appendix gives the voltage and current waveforms for all 100 tests measured during the formal testing.

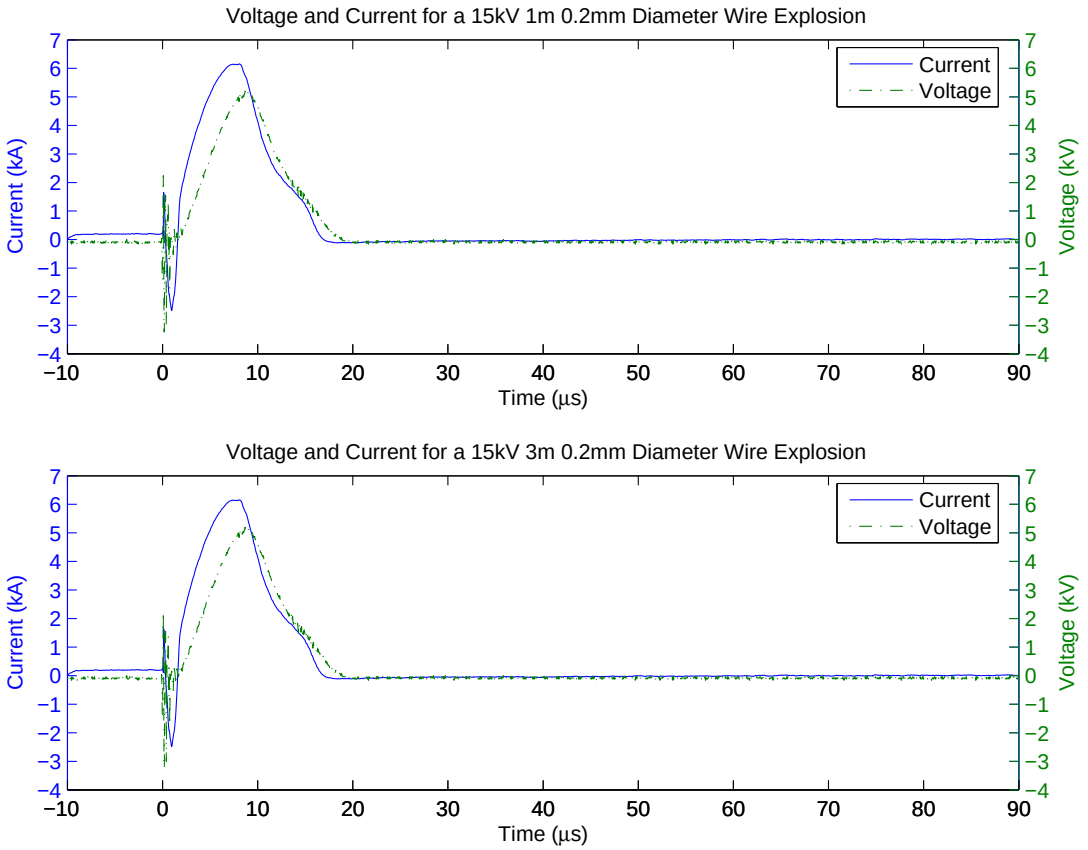
Voltage and Current for a 15kV 1m 0.2mm Diameter Wire Explosion
Current
Voltage
Current (kA)
Voltage (kV)
Time (µs)
Voltage and Current for a 15kV 3m 0.2mm Diameter Wire Explosion
Current
Voltage
Current (kA)
Voltage (kV)
Time (µs)

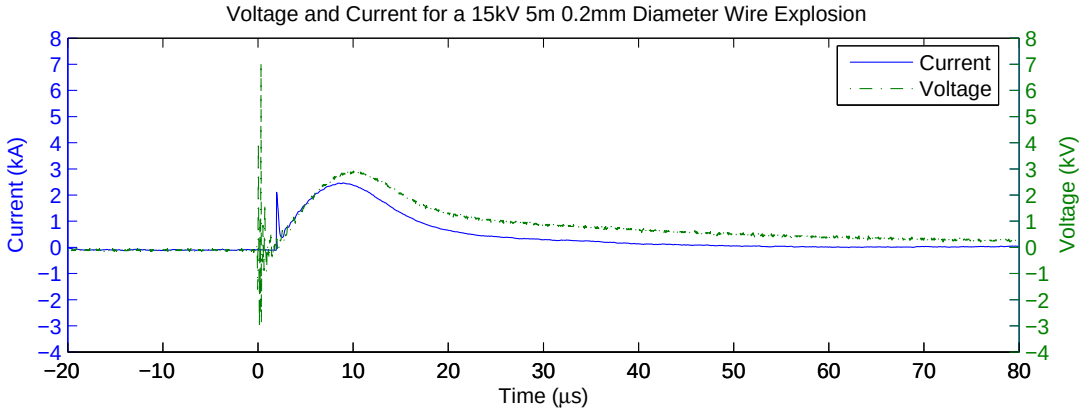
Voltage and Current for a 15kV 5m 0.2mm Diameter Wire Explosion
Current
Voltage
Current (kA)
Voltage (kV)
Time (μs)

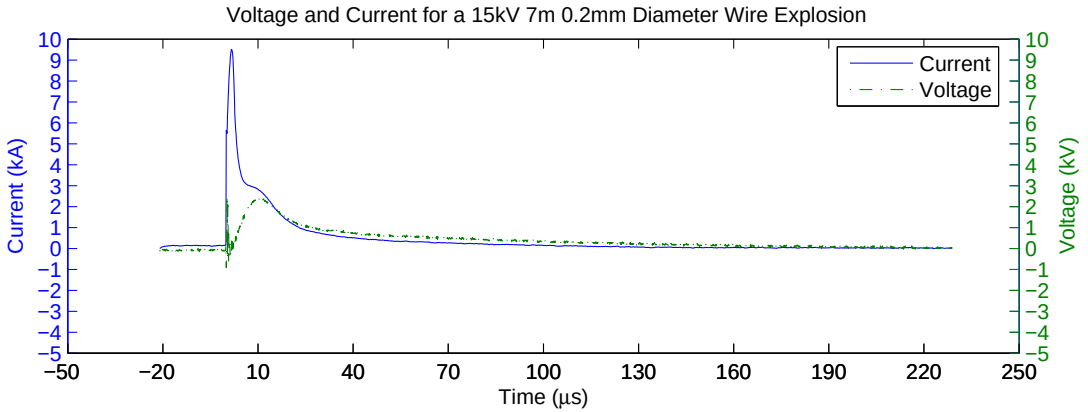
Voltage and Current for a 15kV 7m 0.2mm Diameter Wire Explosion
Current
Voltage
Current (kA)
Voltage (kV)
Time (μs)

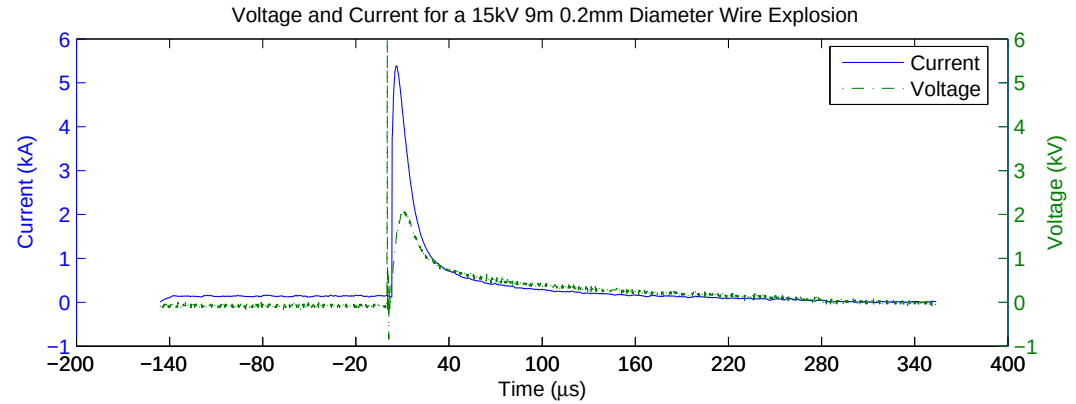
Voltage and Current for a 15kV 9m 0.2mm Diameter Wire Explosion
Current
Voltage
Current (kA)
Voltage (kV)
Time (µs)
6
5
4
3
2
1
0
−1
−200
−140
−80
−20
40
100
160
220
280
340
400

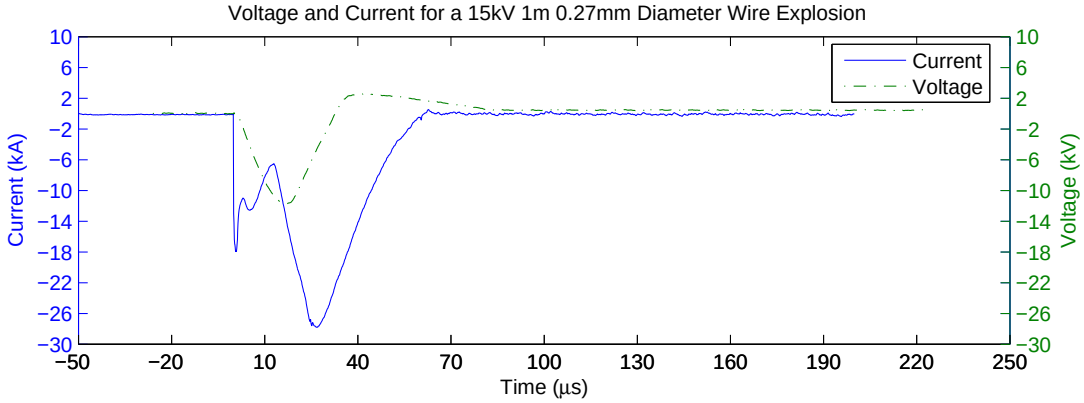
Voltage and Current for a 15kV 1m 0.27mm Diameter Wire Explosion
Current
Voltage
Current (kA)
Voltage (kV)
Time (µs)
10
6
2
−2
−6
−10
−14
−18
−22
−26
−30
−50
−20
10
40
70
100
130
160
190
220
250

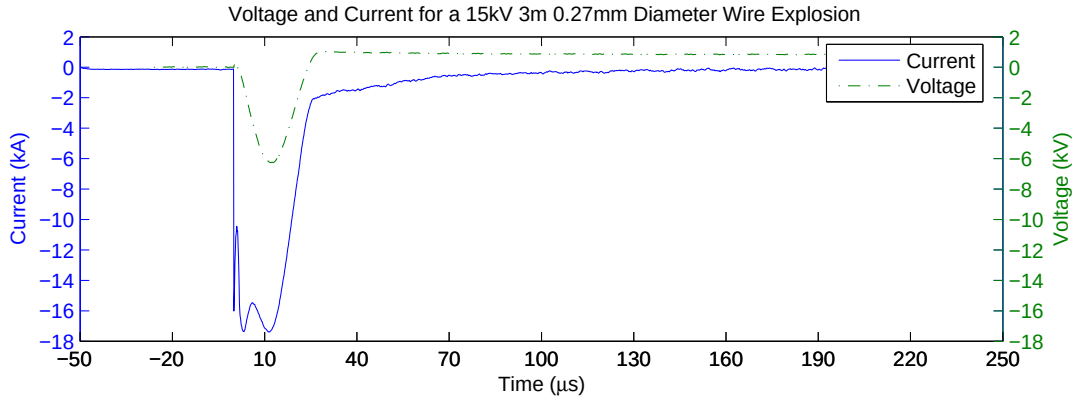
Voltage and Current for a 15kV 3m 0.27mm Diameter Wire Explosion
Current
Voltage
Current (kA)
Voltage (kV)
Time (μs)
2
0
−2
−4
−6
−8
−10
−12
−14
−16
−18
−50
−20
10
40
70
100
130
160
190
220
250

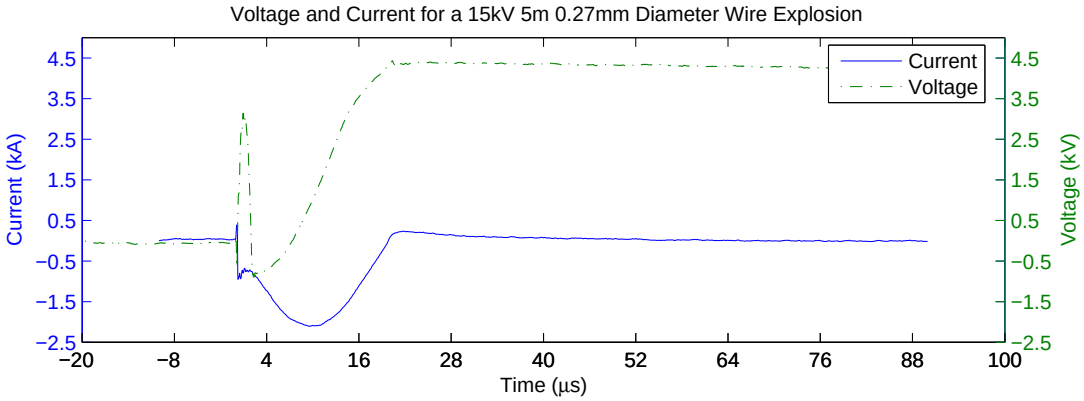
Voltage and Current for a 15kV 5m 0.27mm Diameter Wire Explosion
Current
Voltage
Current (kA)
Voltage (kV)
Time (μs)
4.5
3.5
2.5
1.5
0.5
−0.5
−1.5
−2.5
−20
−8
4
16
28
40
52
64
76
88
100

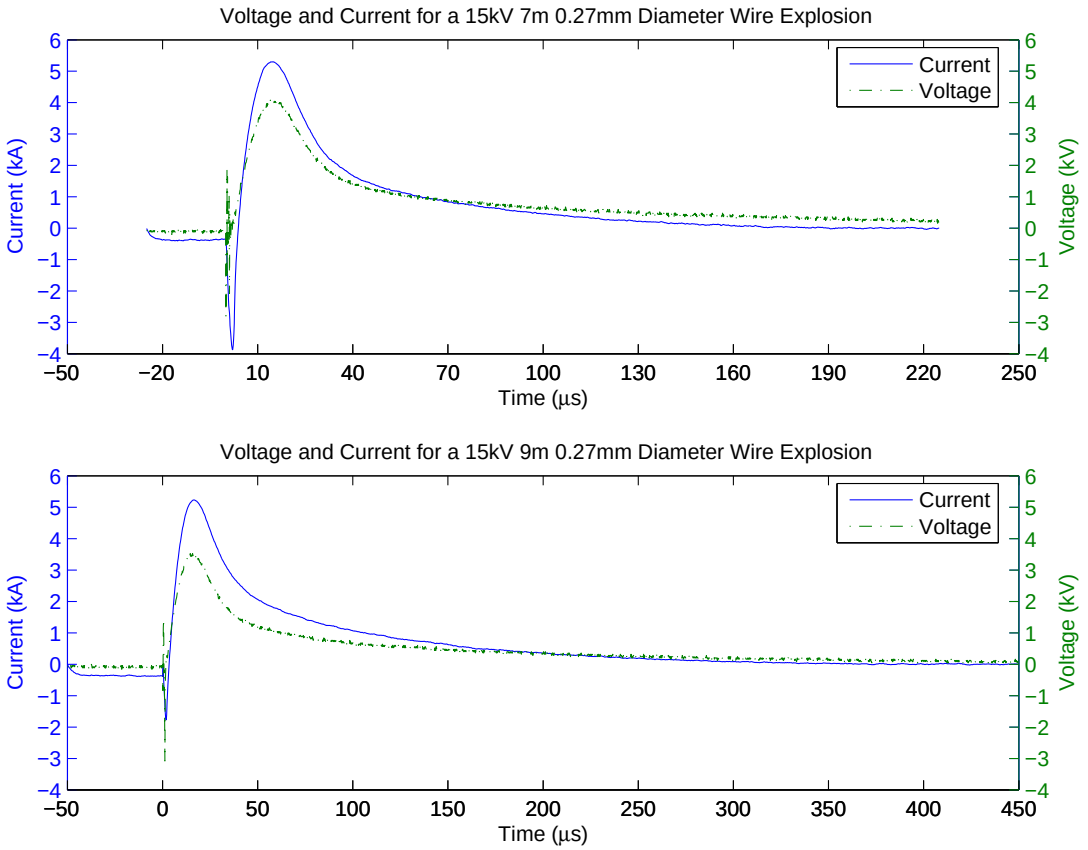
Voltage and Current for a 15kV 7m 0.27mm Diameter Wire Explosion
Current
Voltage
Current (kA)
Voltage (kV)
Time (µs)
Voltage and Current for a 15kV 9m 0.27mm Diameter Wire Explosion
Current
Voltage
Current (kA)
Voltage (kV)
Time (µs)

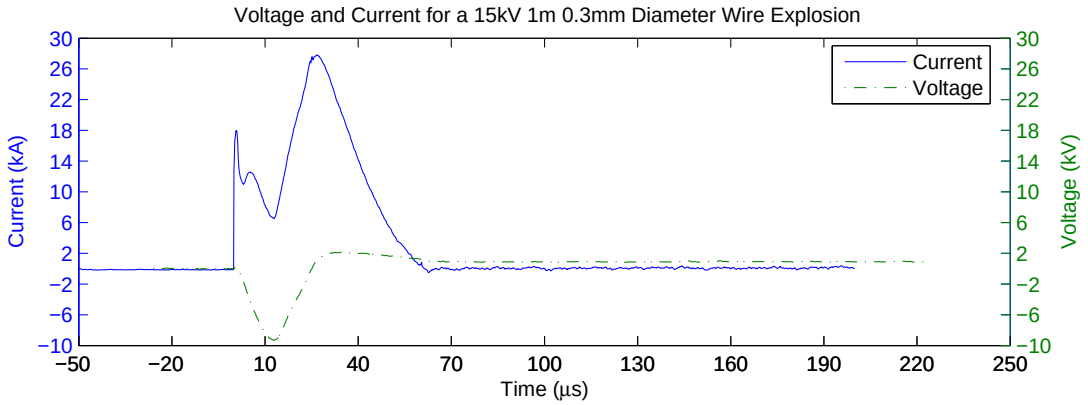
Voltage and Current for a 15kV 1m 0.3mm Diameter Wire Explosion
Current
Voltage
Current (kA)
Voltage (kV)
Time (µs)
30
26
22
18
14
10
6
2
−2
−6
−10
−50
−20
10
40
70
100
130
160
190
220
250

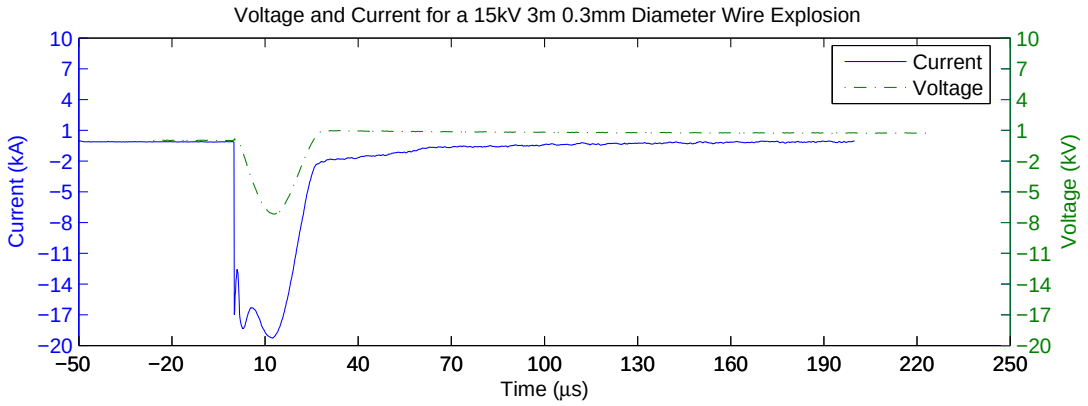
Voltage and Current for a 15kV 3m 0.3mm Diameter Wire Explosion
Current
Voltage
Current (kA)
Voltage (kV)
Time (µs)
10
7
4
1
−2
−5
−8
−11
−14
−17
−20
−50
−20
10
40
70
100
130
160
190
220
250

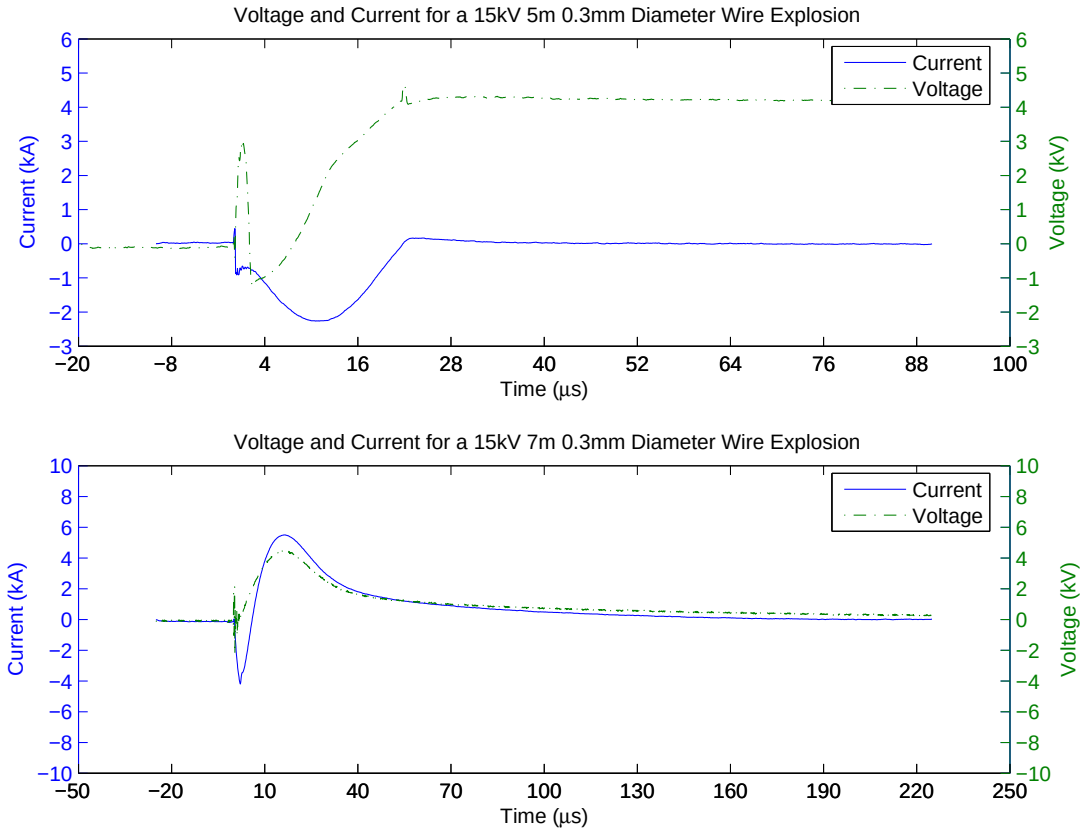
Voltage and Current for a 15kV 5m 0.3mm Diameter Wire Explosion
Current
Voltage
Current (kA)
Voltage (kV)
Time (μs)
Voltage and Current for a 15kV 7m 0.3mm Diameter Wire Explosion
Current
Voltage
Current (kA)
Voltage (kV)
Time (μs)

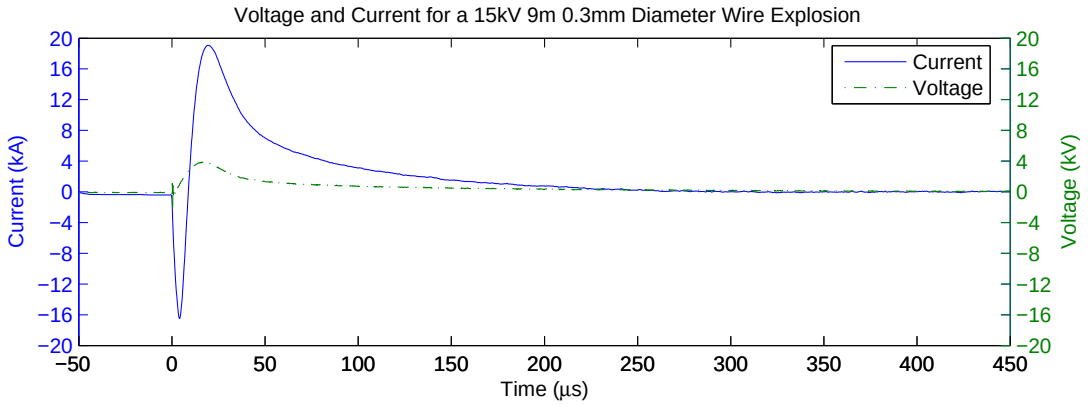
Voltage and Current for a 15kV 9m 0.3mm Diameter Wire Explosion
Current
Voltage
Current (kA)
Voltage (kV)
Time (µs)
20
16
12
8
4
0
−4
−8
−12
−16
−20
−50
0
50
100
150
200
250
300
350
400
450

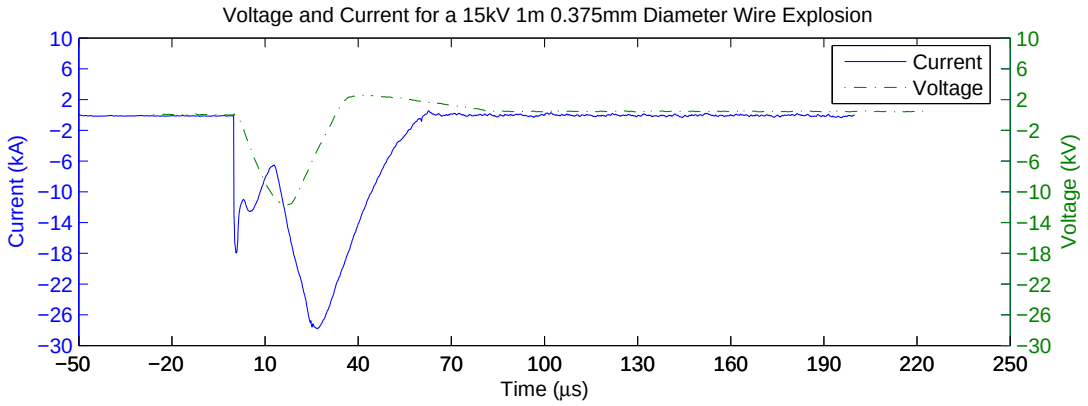
Voltage and Current for a 15kV 1m 0.375mm Diameter Wire Explosion
Current
Voltage
Current (kA)
Voltage (kV)
Time (µs)
10
6
2
−2
−6
−10
−14
−18
−22
−26
−30
−50
−20
10
40
70
100
130
160
190
220
250

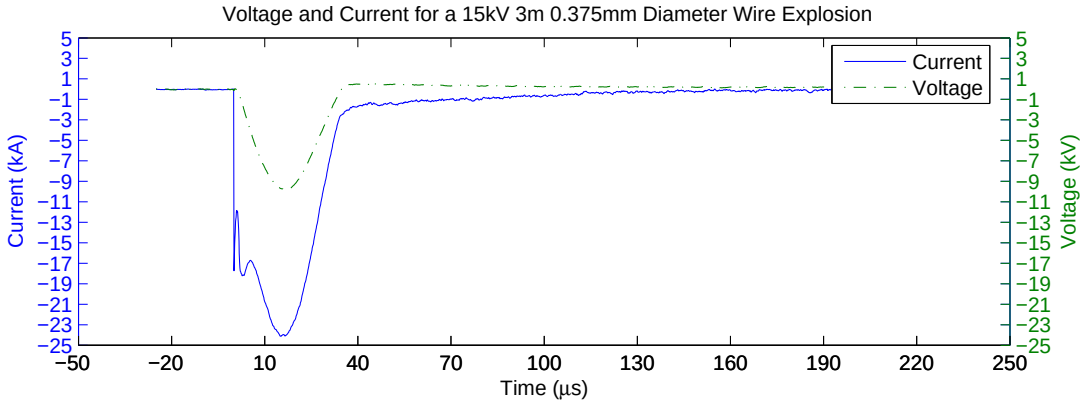
Voltage and Current for a 15kV 3m 0.375mm Diameter Wire Explosion
Current
Voltage
Current (kA)
Voltage (kV)
Time (μs)
5
3
1
−1
−3
−5
−7
−9
−11
−13
−15
−17
−19
−21
−23
−25
−50
−20
10
40
70
100
130
160
190
220
250

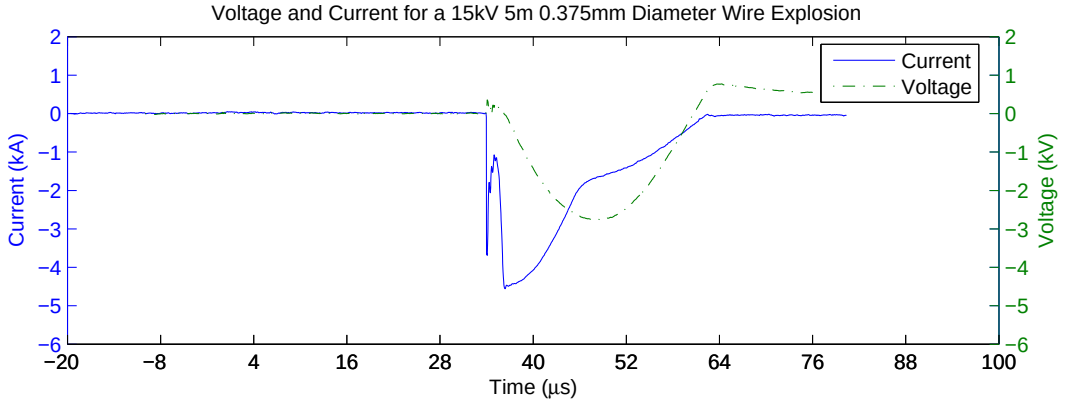
Voltage and Current for a 15kV 5m 0.375mm Diameter Wire Explosion
Current
Voltage
Current (kA)
Voltage (kV)
Time (μs)
2
1
0
−1
−2
−3
−4
−5
−6
−20
−8
4
16
28
40
52
64
76
88
100

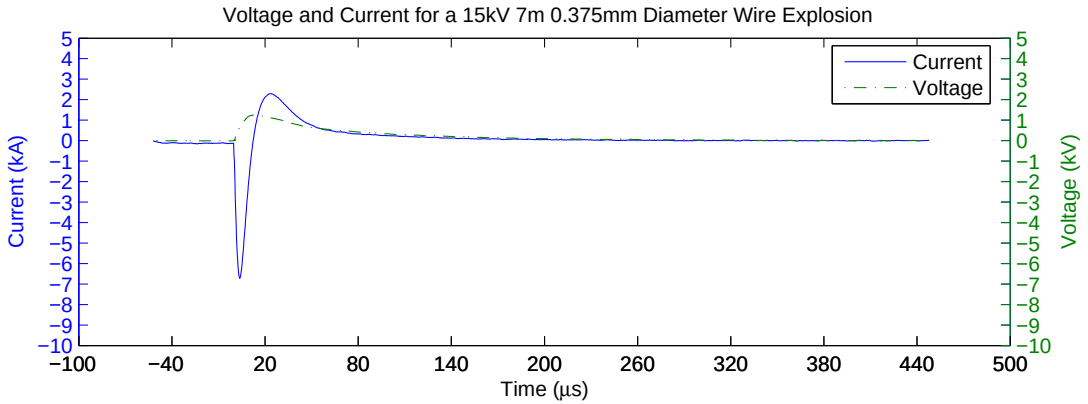
Voltage and Current for a 15kV 7m 0.375mm Diameter Wire Explosion
Current
Voltage
Current (kA)
Voltage (kV)
Time (µs)
5
4
3
2
1
0
−1
−2
−3
−4
−5
−6
−7
−8
−9
−10
−100
−40
20
80
140
200
260
320
380
440
500

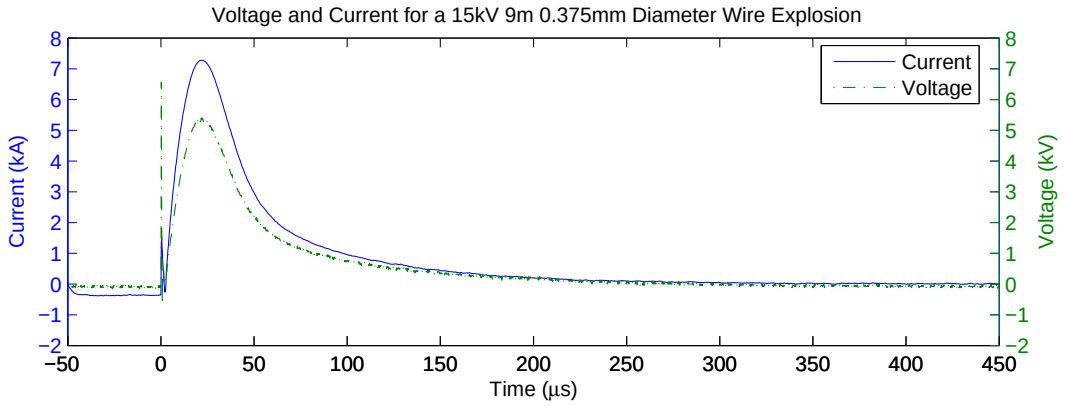
Voltage and Current for a 15kV 9m 0.375mm Diameter Wire Explosion
Current
Voltage
Current (kA)
Voltage (kV)
Time (µs)
8
7
6
5
4
3
2
1
0
−1
−2
−50
0
50
100
150
200
250
300
350
400
450

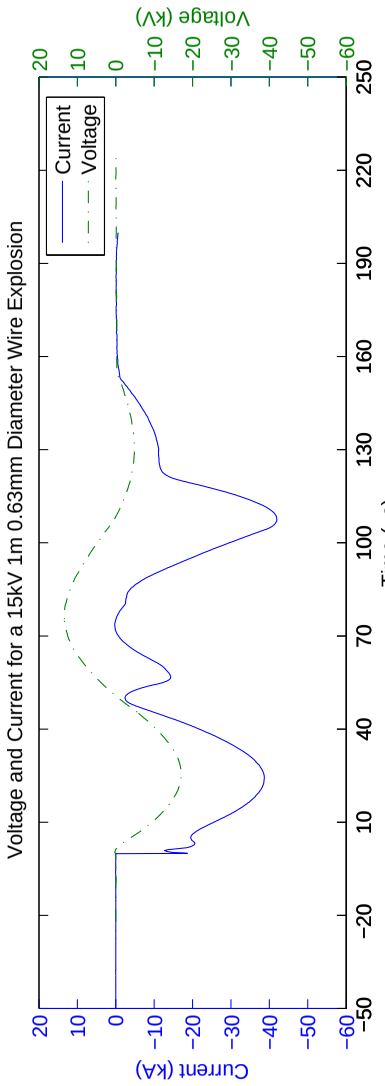
Voltage and Current for a 15kV 1m 0.63mm Diameter Wire Explosion
Current
Voltage
Current (kA)
Voltage (kV)
Time (µs)

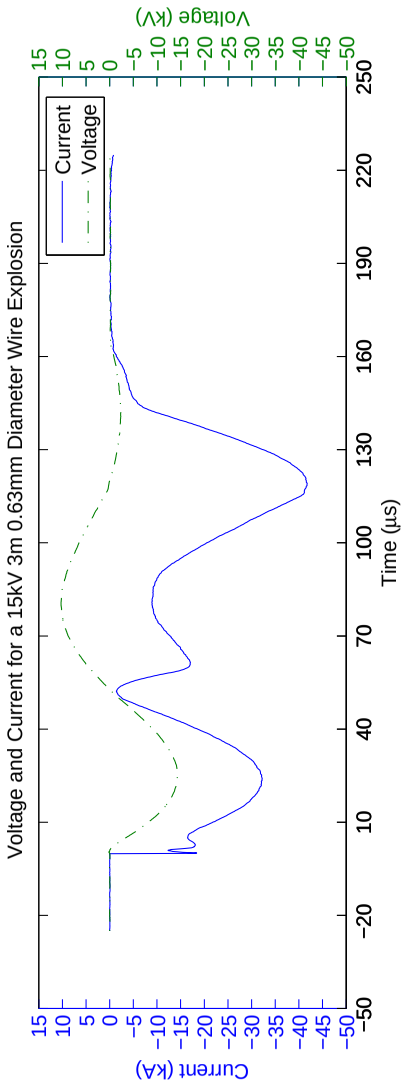
Voltage and Current for a 15kV 3m 0.63mm Diameter Wire Explosion
Current
Voltage
Current (kA)
Voltage (kV)
Time (µs)

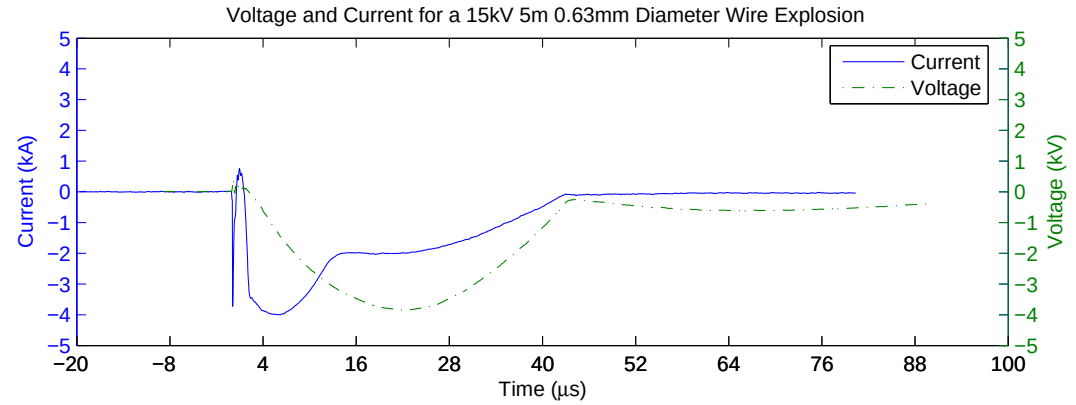
Voltage and Current for a 15kV 5m 0.63mm Diameter Wire Explosion
Current
Voltage
Current (kA)
Voltage (kV)
Time (μs)
5
4
3
2
1
0
−1
−2
−3
−4
−5
−20
−8
4
16
28
40
52
64
76
88
100

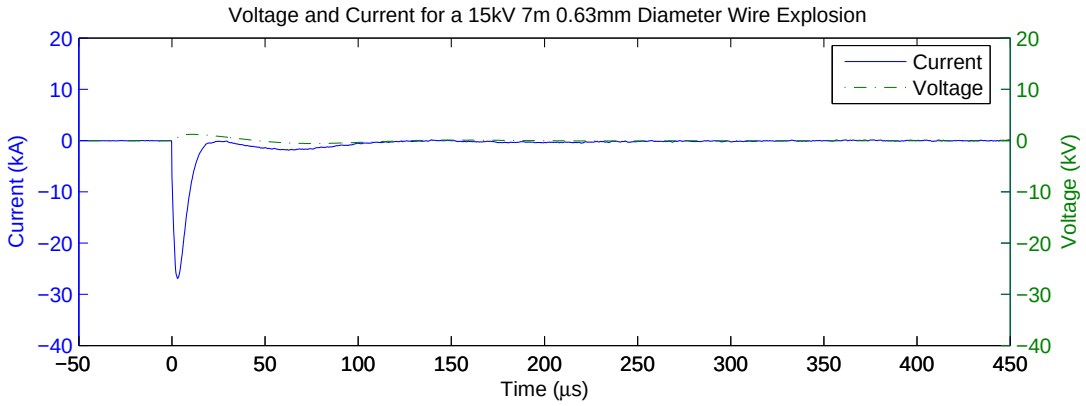
Voltage and Current for a 15kV 7m 0.63mm Diameter Wire Explosion
Current
Voltage
Current (kA)
Voltage (kV)
Time (μs)
20
10
0
−10
−20
−30
−40
−50
0
50
100
150
200
250
300
350
400
450

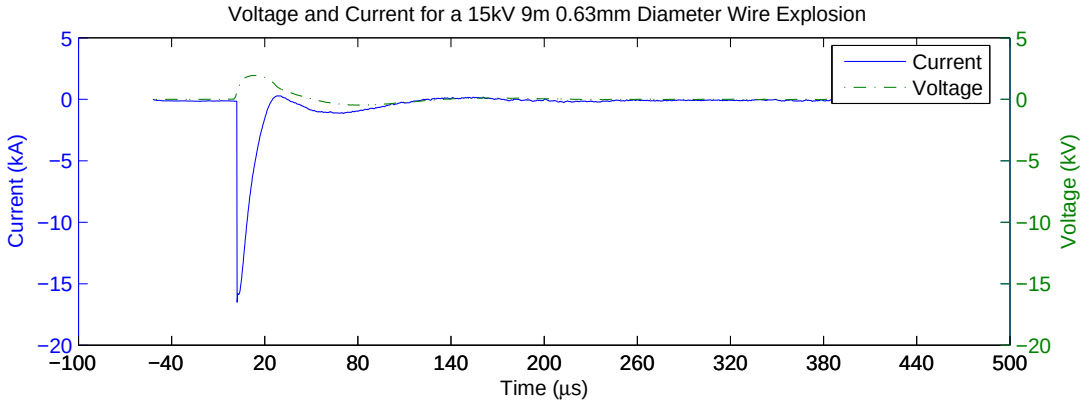
Voltage and Current for a 15kV 9m 0.63mm Diameter Wire Explosion
Current
Voltage
Current (kA)
Voltage (kV)
Time (μs)
5
0
−5
−10
−15
−20
−100
−40
20
80
140
200
260
320
380
440
500

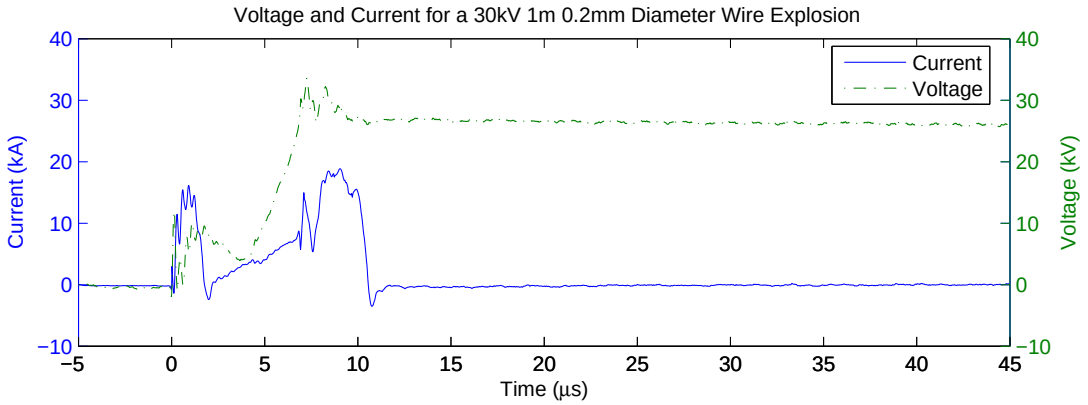
Voltage and Current for a 30kV 1m 0.2mm Diameter Wire Explosion
Current
Voltage
Current (kA)
Voltage (kV)
Time (μs)
40
30
20
10
0
−10
−5
0
5
10
15
20
25
30
35
40
45

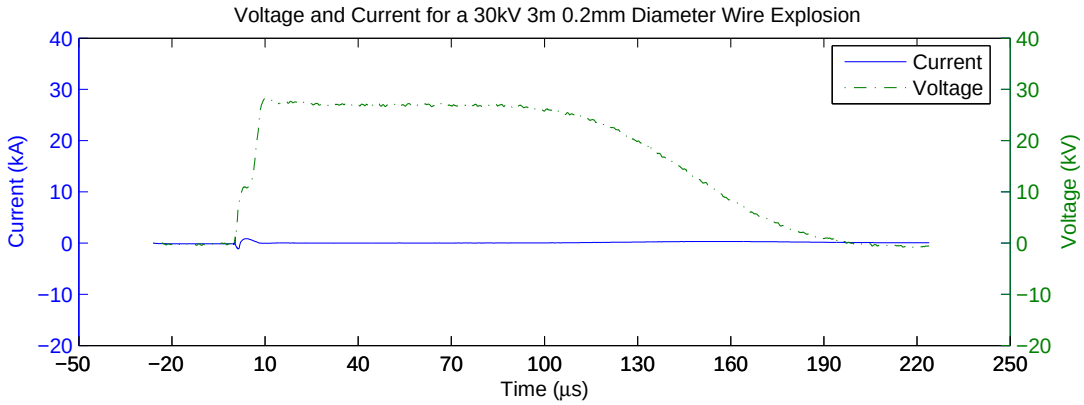
Voltage and Current for a 30kV 3m 0.2mm Diameter Wire Explosion
Current
Voltage
Current (kA)
Voltage (kV)
Time (µs)
40
30
20
10
0
−10
−20
−50
−20
10
40
70
100
130
160
190
220
250

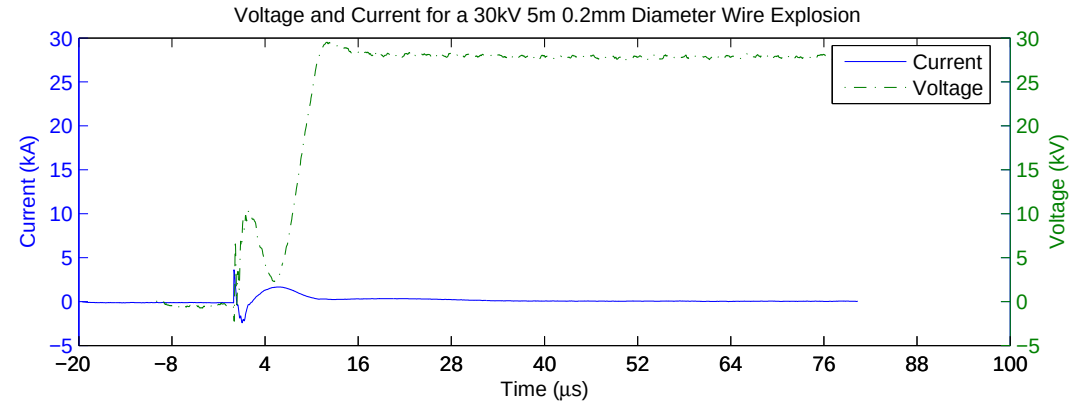
Voltage and Current for a 30kV 5m 0.2mm Diameter Wire Explosion
Current
Voltage
Current (kA)
Voltage (kV)
Time (µs)
30
25
20
15
10
5
0
−5
−20
−8
4
16
28
40
52
64
76
88
100

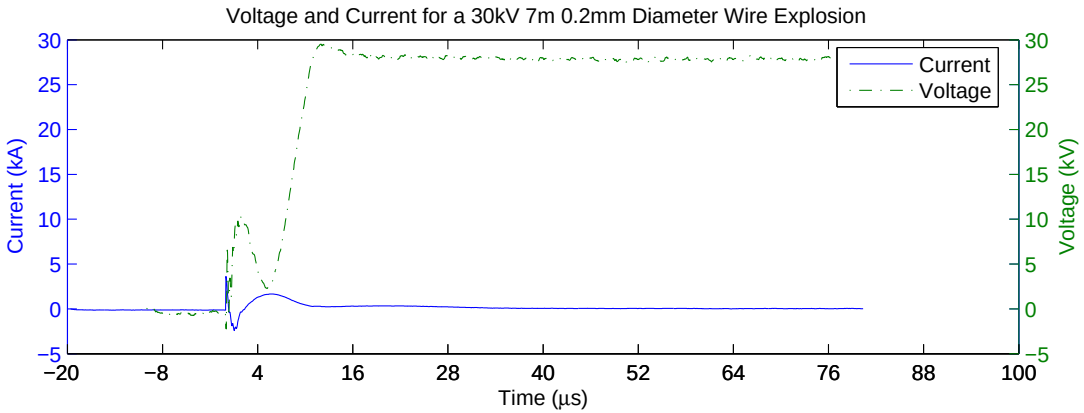
Voltage and Current for a 30kV 7m 0.2mm Diameter Wire Explosion
Current
Voltage
Current (kA)
Voltage (kV)
Time (µs)
30
25
20
15
10
5
0
−5
−20
−8
4
16
28
40
52
64
76
88
100

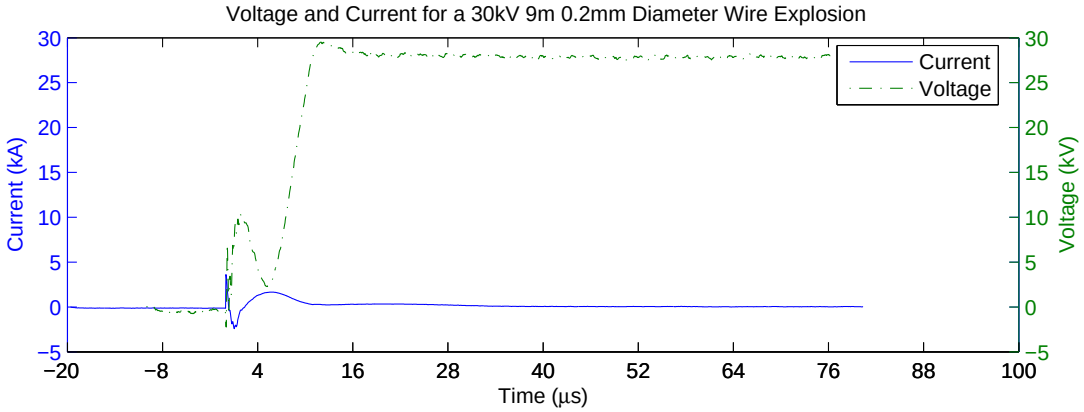
Voltage and Current for a 30kV 9m 0.2mm Diameter Wire Explosion
Current
Voltage
Current (kA)
Voltage (kV)
Time (µs)
30
25
20
15
10
5
0
−5
−20
−8
4
16
28
40
52
64
76
88
100

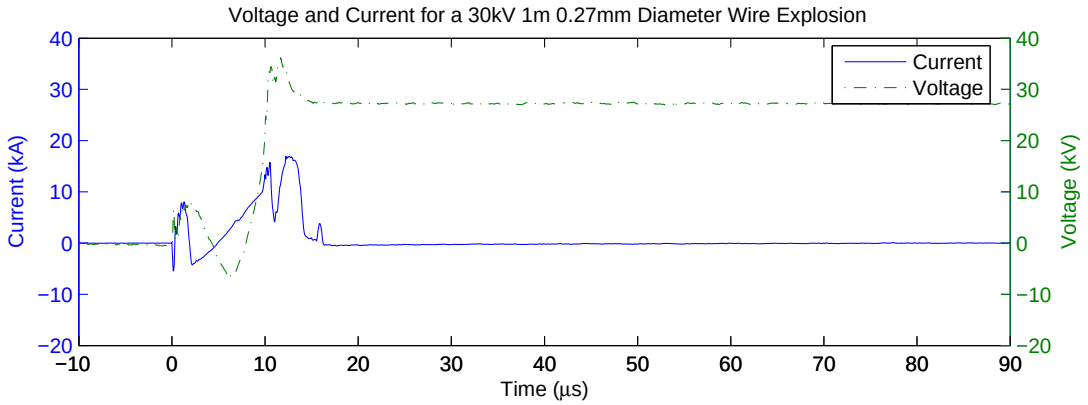
Voltage and Current for a 30kV 1m 0.27mm Diameter Wire Explosion
Current
Voltage
Current (kA)
Voltage (kV)
Time (μs)
40
30
20
10
0
−10
−20
−10
0
10
20
30
40
50
60
70
80
90

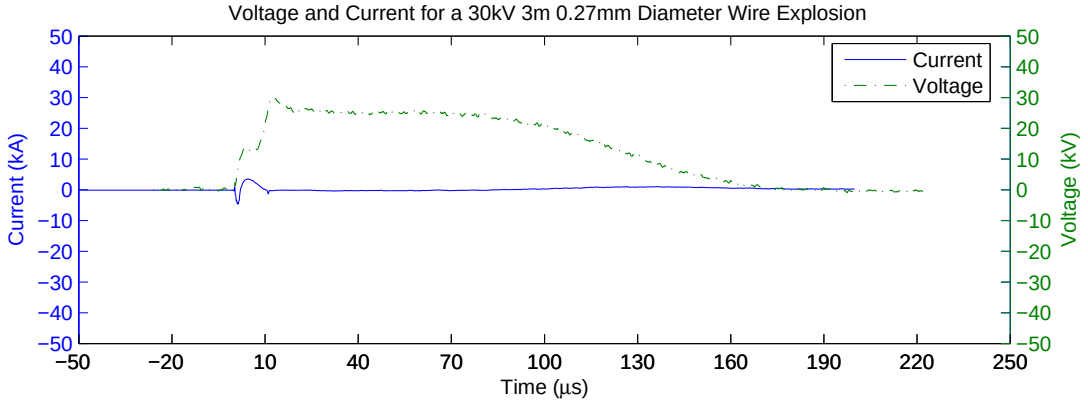
Voltage and Current for a 30kV 3m 0.27mm Diameter Wire Explosion
Current
Voltage
Current (kA)
Voltage (kV)
Time (μs)
50
40
30
20
10
0
−10
−20
−30
−40
−50
−50
−20
10
40
70
100
130
160
190
220
250

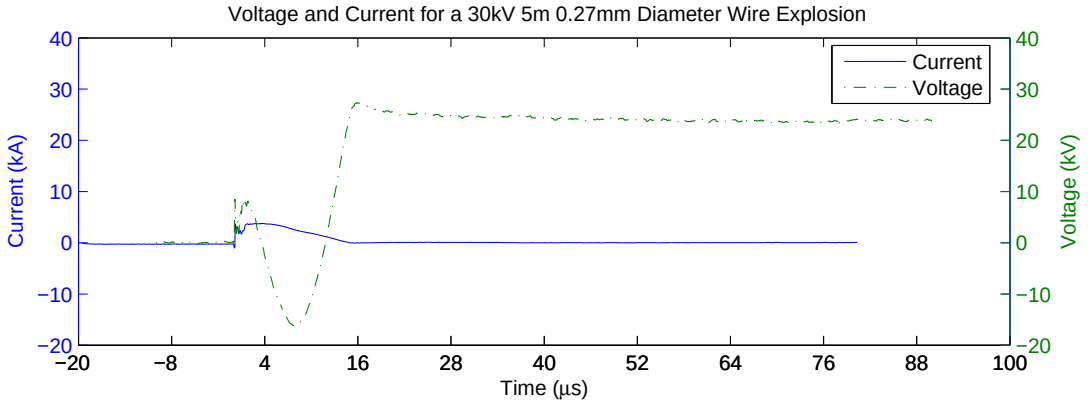
Voltage and Current for a 30kV 5m 0.27mm Diameter Wire Explosion
Current
Voltage
Current (kA)
Voltage (kV)
Time (µs)
40
30
20
10
0
−10
−20
−20
−8
4
16
28
40
52
64
76
88
100

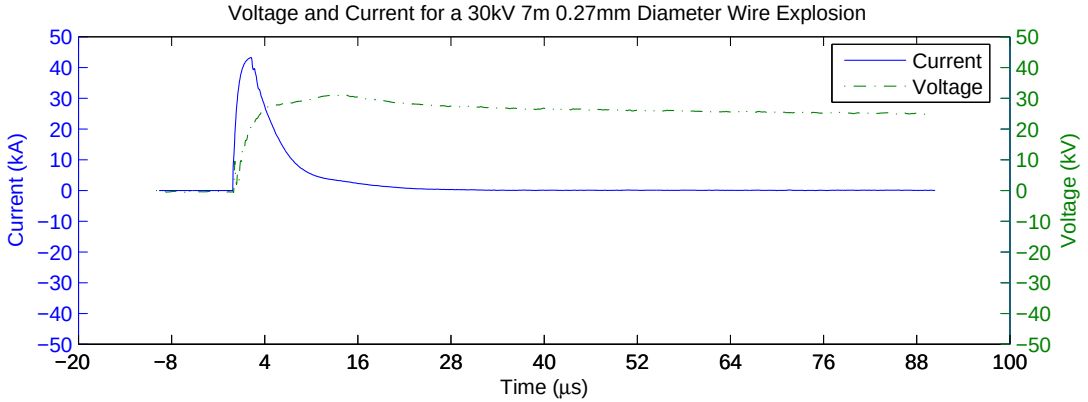
Voltage and Current for a 30kV 7m 0.27mm Diameter Wire Explosion
Current
Voltage
Current (kA)
Voltage (kV)
Time (µs)
50
40
30
20
10
0
−10
−20
−30
−40
−50
−20
−8
4
16
28
40
52
64
76
88
100

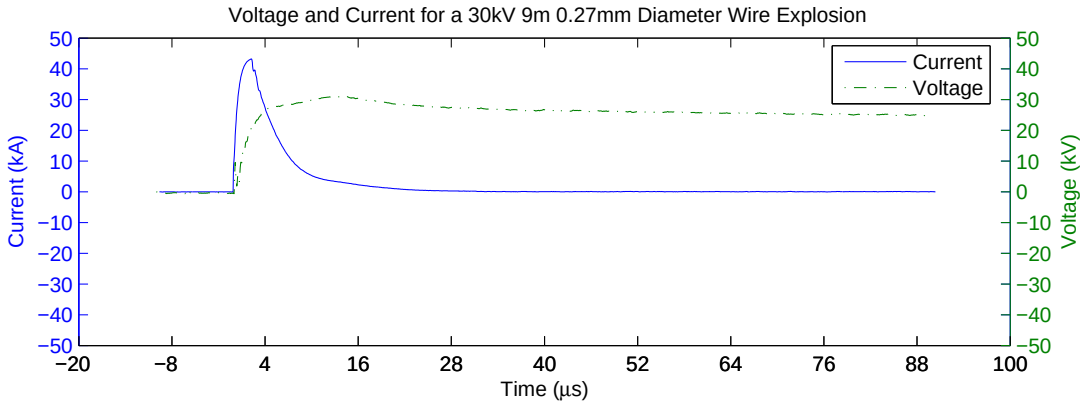
Voltage and Current for a 30kV 9m 0.27mm Diameter Wire Explosion
Current
Voltage
Current (kA)
Voltage (kV)
Time (µs)
50
40
30
20
10
0
−10
−20
−30
−40
−50
−20
−8
4
16
28
40
52
64
76
88
100

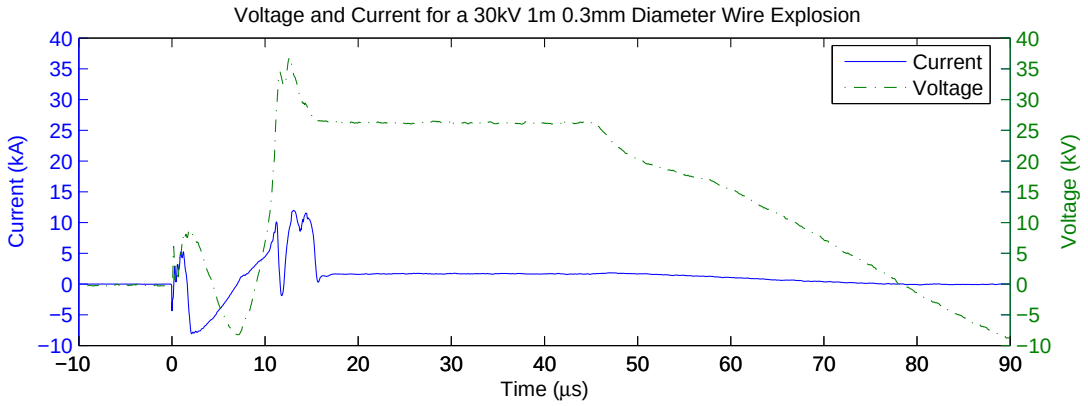
Voltage and Current for a 30kV 1m 0.3mm Diameter Wire Explosion
Current
Voltage
Current (kA)
Voltage (kV)
Time (µs)
40
35
30
25
20
15
10
5
0
−5
−10
−10
0
10
20
30
40
50
60
70
80
90

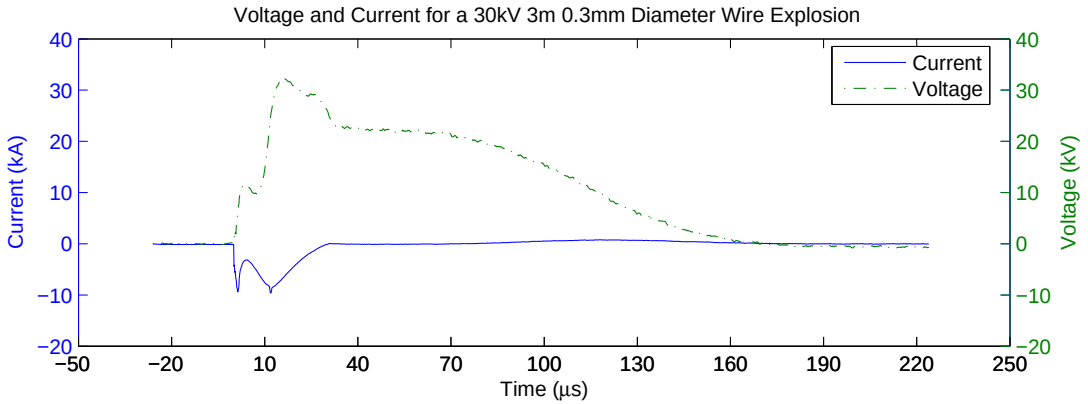
Voltage and Current for a 30kV 3m 0.3mm Diameter Wire Explosion
Current
Voltage
Current (kA)
Voltage (kV)
Time (µs)
40
30
20
10
0
−10
−20
−50
−20
10
40
70
100
130
160
190
220
250

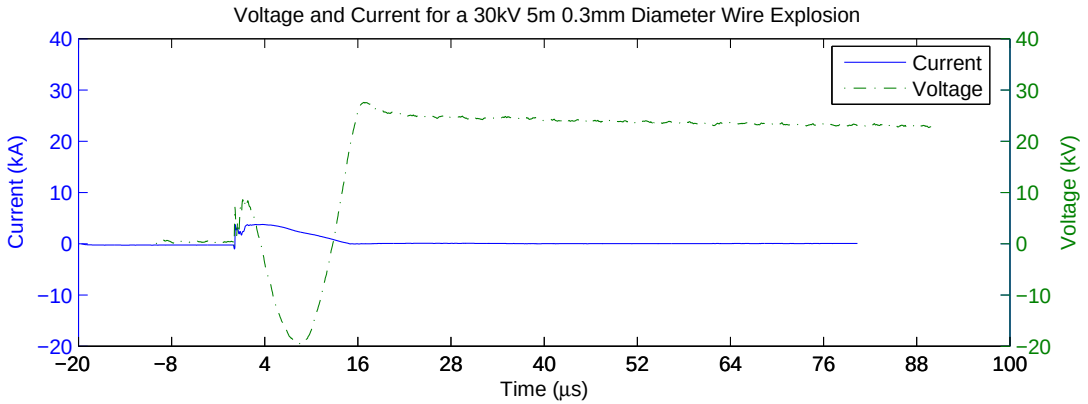
Voltage and Current for a 30kV 5m 0.3mm Diameter Wire Explosion
Current
Voltage
Current (kA)
Voltage (kV)
Time (µs)
40
30
20
10
0
−10
−20
−20
−8
4
16
28
40
52
64
76
88
100

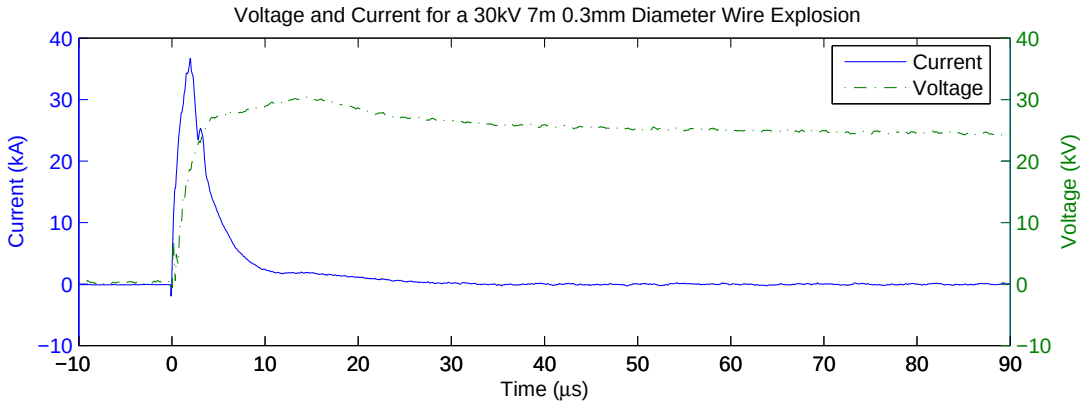
Voltage and Current for a 30kV 7m 0.3mm Diameter Wire Explosion
Current
Voltage
Current (kA)
Voltage (kV)
Time (μs)
40
30
20
10
0
−10
−10
0
10
20
30
40
50
60
70
80
90

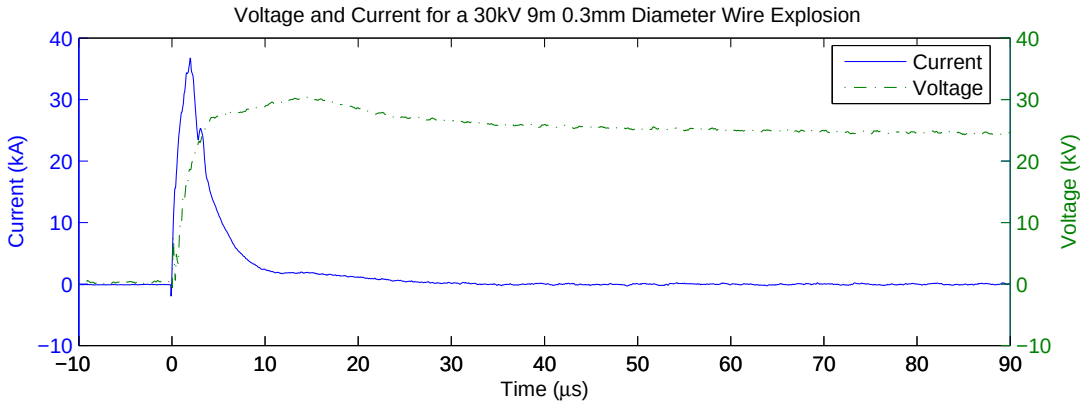
Voltage and Current for a 30kV 9m 0.3mm Diameter Wire Explosion
Current
Voltage
Current (kA)
Voltage (kV)
Time (μs)
40
30
20
10
0
−10
−10
0
10
20
30
40
50
60
70
80
90

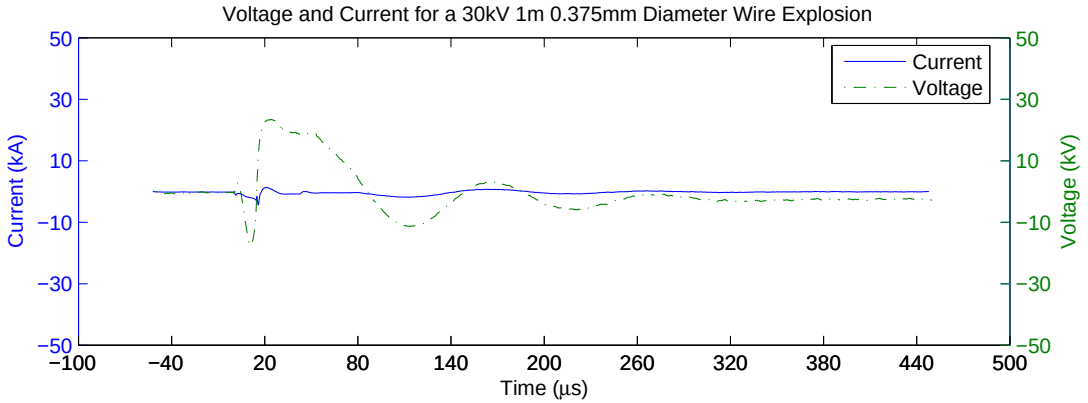
Voltage and Current for a 30kV 1m 0.375mm Diameter Wire Explosion
Current
Voltage
Current (kA)
Voltage (kV)
Time (μs)
50
30
10
−10
−30
−50
−100
−40
20
80
140
200
260
320
380
440
500

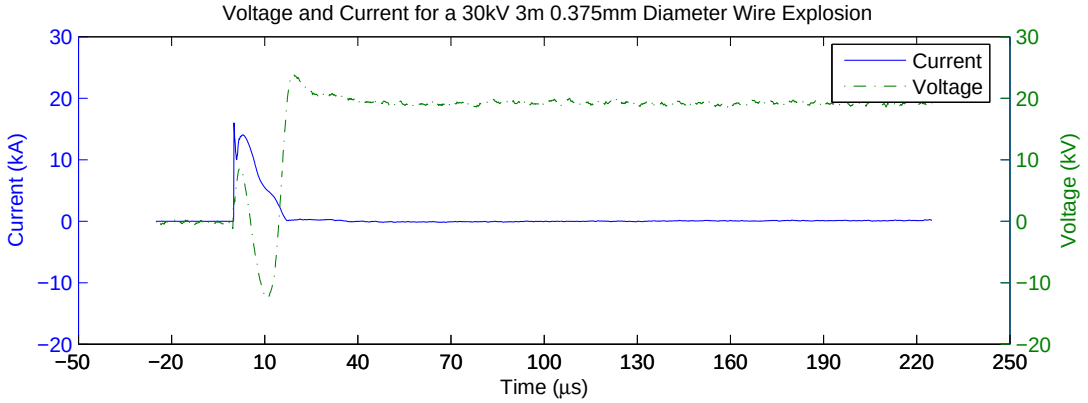
Voltage and Current for a 30kV 3m 0.375mm Diameter Wire Explosion
Current
Voltage
Current (kA)
Voltage (kV)
Time (μs)
30
20
10
0
−10
−20
−50
−20
10
40
70
100
130
160
190
220
250

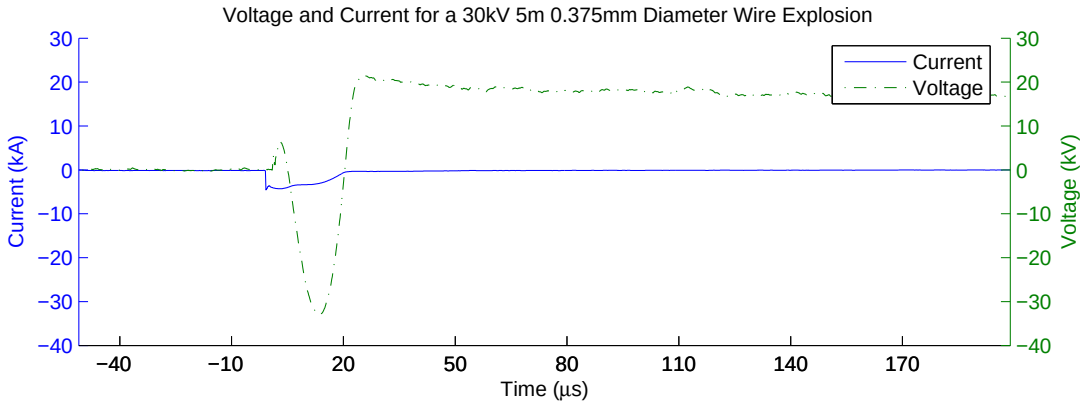
Voltage and Current for a 30kV 5m 0.375mm Diameter Wire Explosion
Current
Voltage
Current (kA)
Voltage (kV)
Time (µs)
30
20
10
0
−10
−20
−30
−40
−40
−10
20
50
80
110
140
170

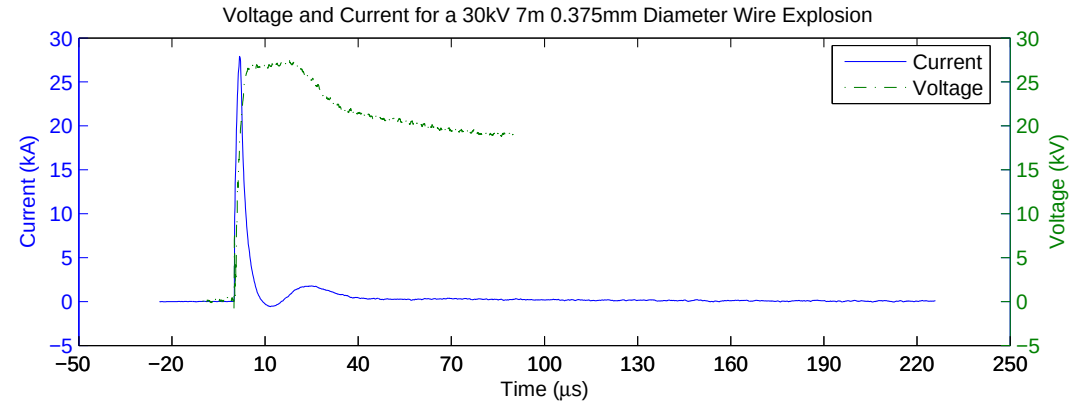
Voltage and Current for a 30kV 7m 0.375mm Diameter Wire Explosion
Current
Voltage
Current (kA)
Voltage (kV)
Time (µs)
30
25
20
15
10
5
0
−5
−50
−20
10
40
70
100
130
160
190
220
250

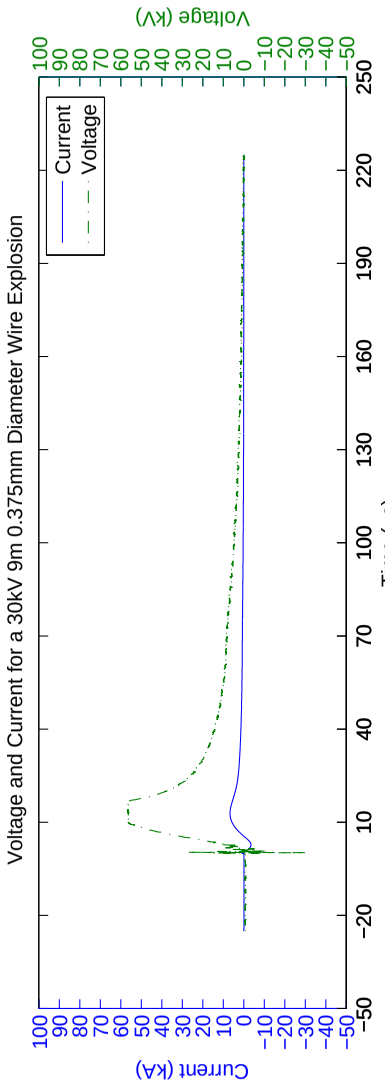
Voltage and Current for a 30kV 9m 0.375mm Diameter Wire Explosion
Current
Voltage
Current (kA)
Voltage (kV)
Time (µs)

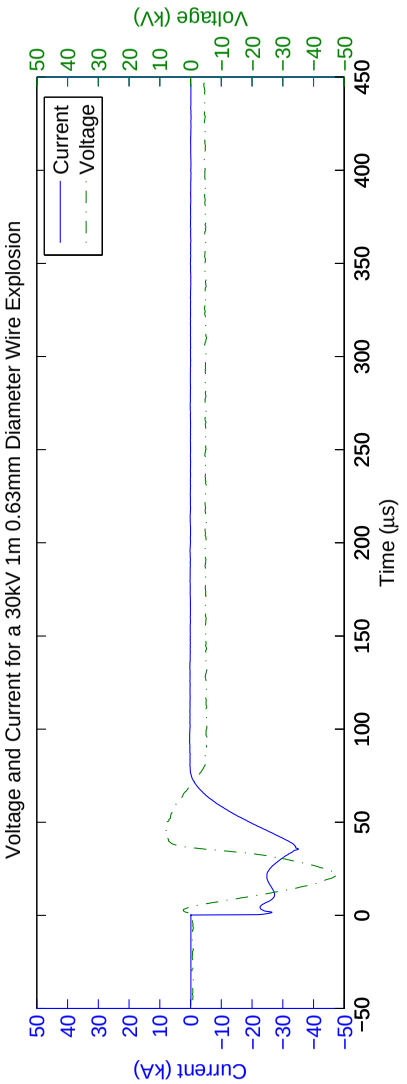
Voltage and Current for a 30kV 1m 0.63mm Diameter Wire Explosion
Current
Voltage
Current (kA)
Voltage (kV)
Time (µs)

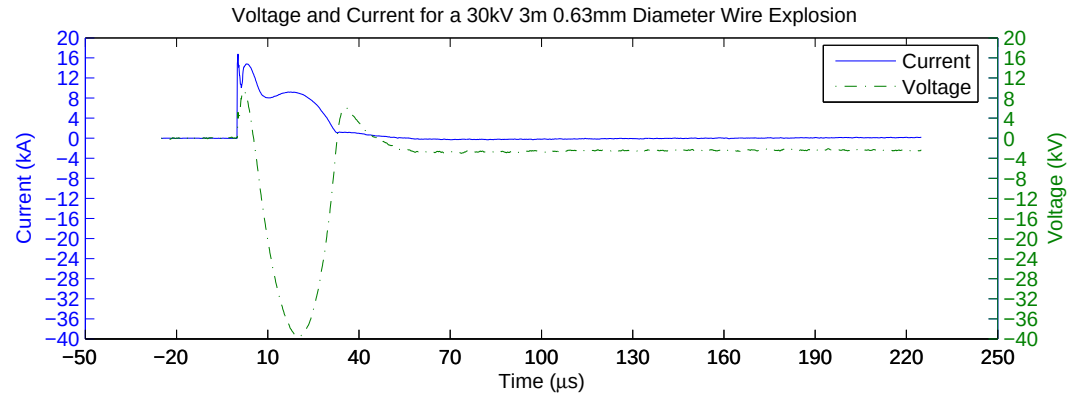
Voltage and Current for a 30kV 3m 0.63mm Diameter Wire Explosion
Current
Voltage
Current (kA)
Voltage (kV)
Time (μs)

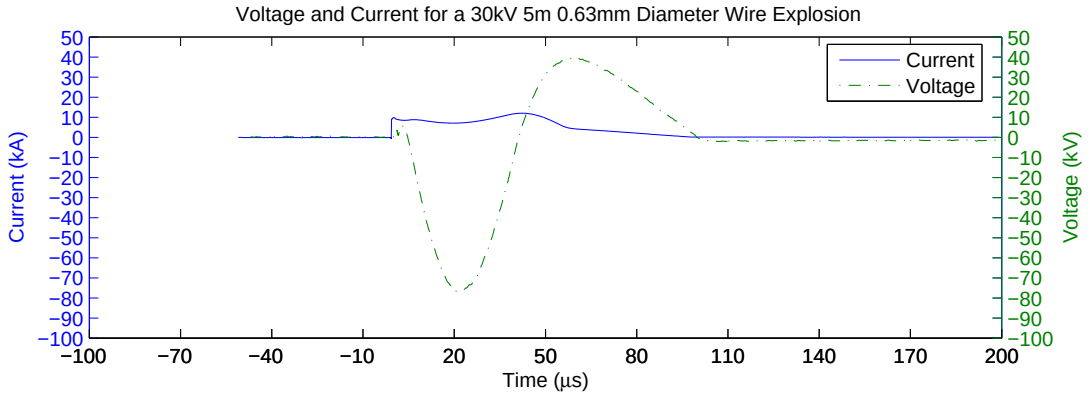
Voltage and Current for a 30kV 5m 0.63mm Diameter Wire Explosion
Current
Voltage
Current (kA)
Voltage (kV)
Time (μs)

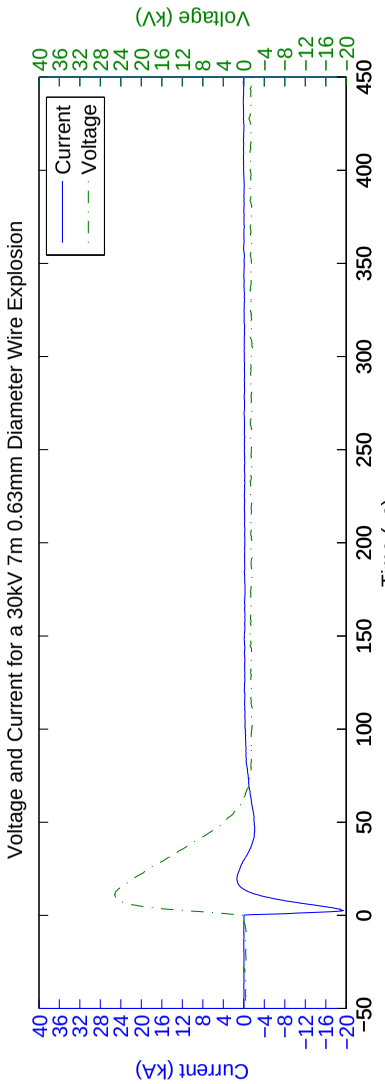
Voltage and Current for a 30kV 7m 0.63mm Diameter Wire Explosion
Current
Voltage
Current (kA)
Voltage (kV)
Time (µs)

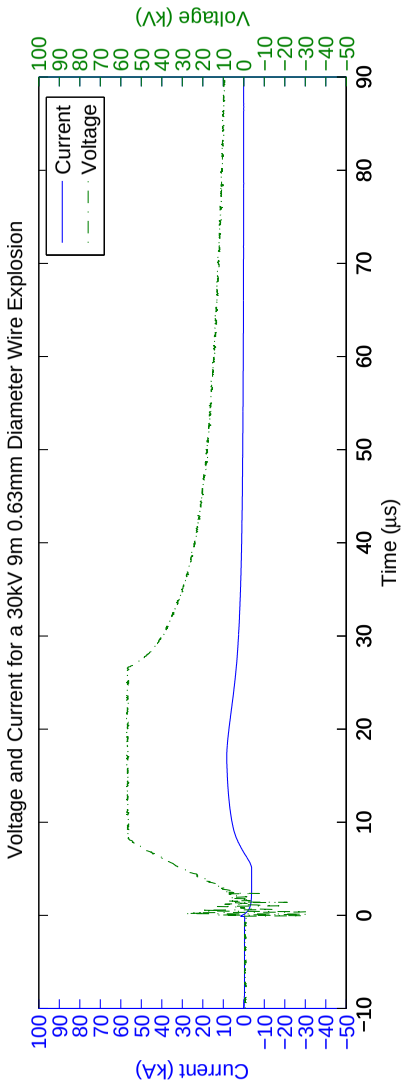
Voltage and Current for a 30kV 9m 0.63mm Diameter Wire Explosion
Current
Voltage
Current (kA)
Voltage (kV)
Time (µs)

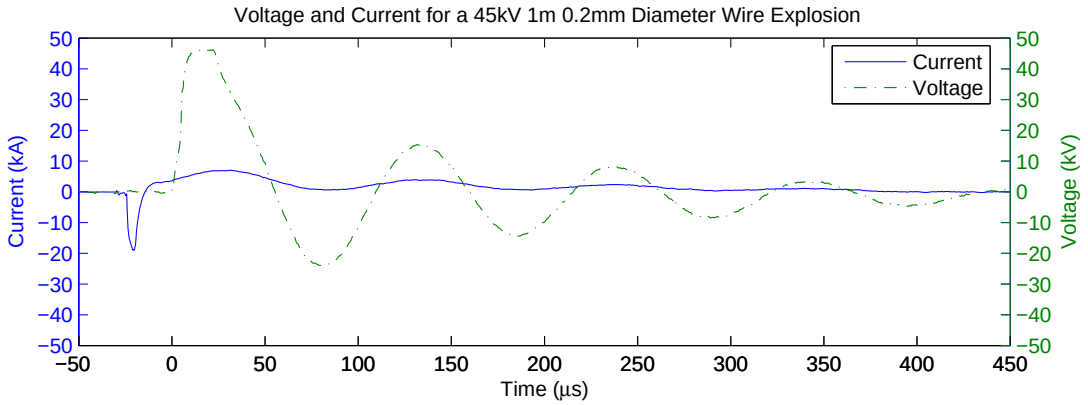
Voltage and Current for a 45kV 1m 0.2mm Diameter Wire Explosion
Current
Voltage
Current (kA)
Voltage (kV)
Time (μs)
50
40
30
20
10
0
−10
−20
−30
−40
−50
−50
0
50
100
150
200
250
300
350
400
450

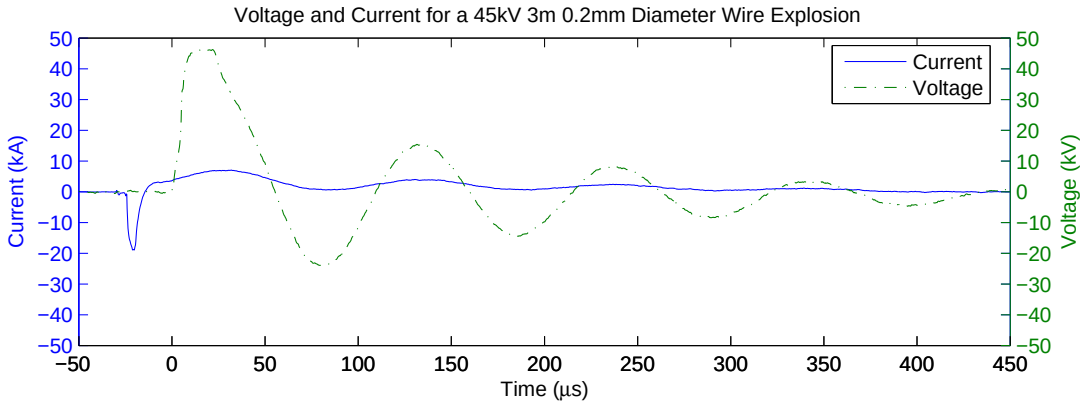
Voltage and Current for a 45kV 3m 0.2mm Diameter Wire Explosion
Current
Voltage
Current (kA)
Voltage (kV)
Time (μs)
50
40
30
20
10
0
−10
−20
−30
−40
−50
−50
0
50
100
150
200
250
300
350
400
450

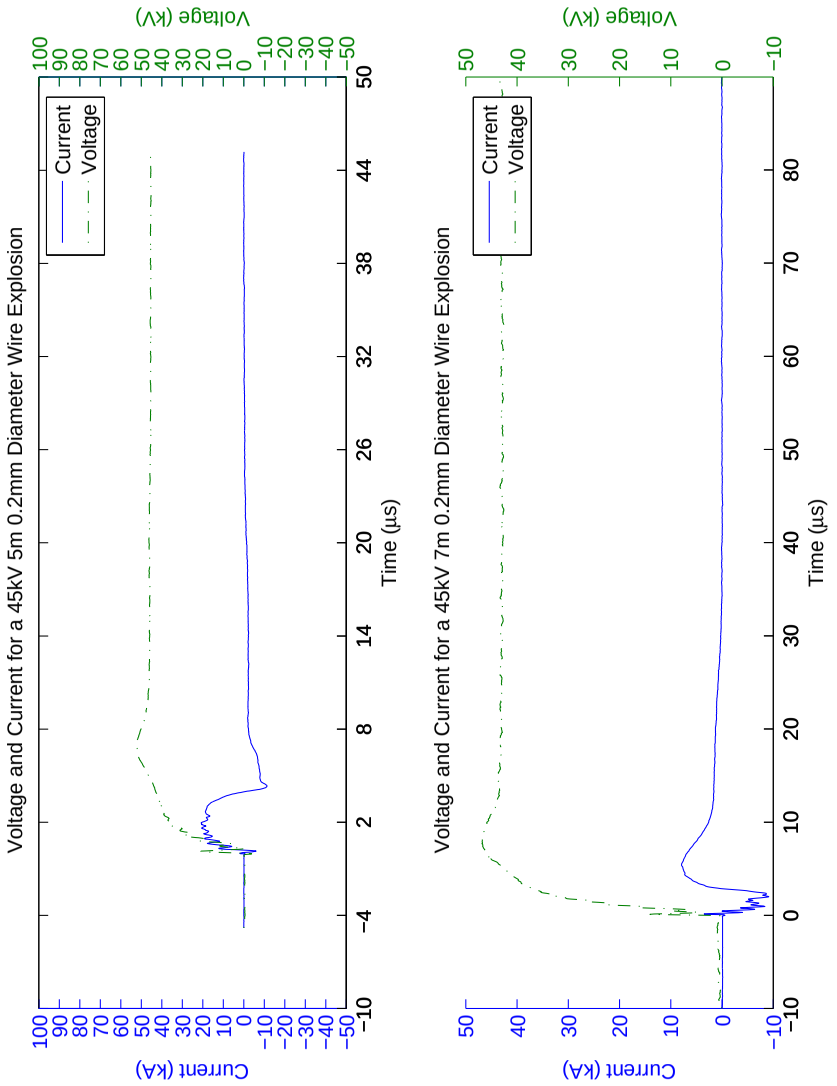
Voltage and Current for a 45kV 5m 0.2mm Diameter Wire Explosion
Current
Voltage
Current (kA)
Voltage (kV)
Time (µs)
Voltage and Current for a 45kV 7m 0.2mm Diameter Wire Explosion
Current
Voltage
Current (kA)
Voltage (kV)
Time (µs)

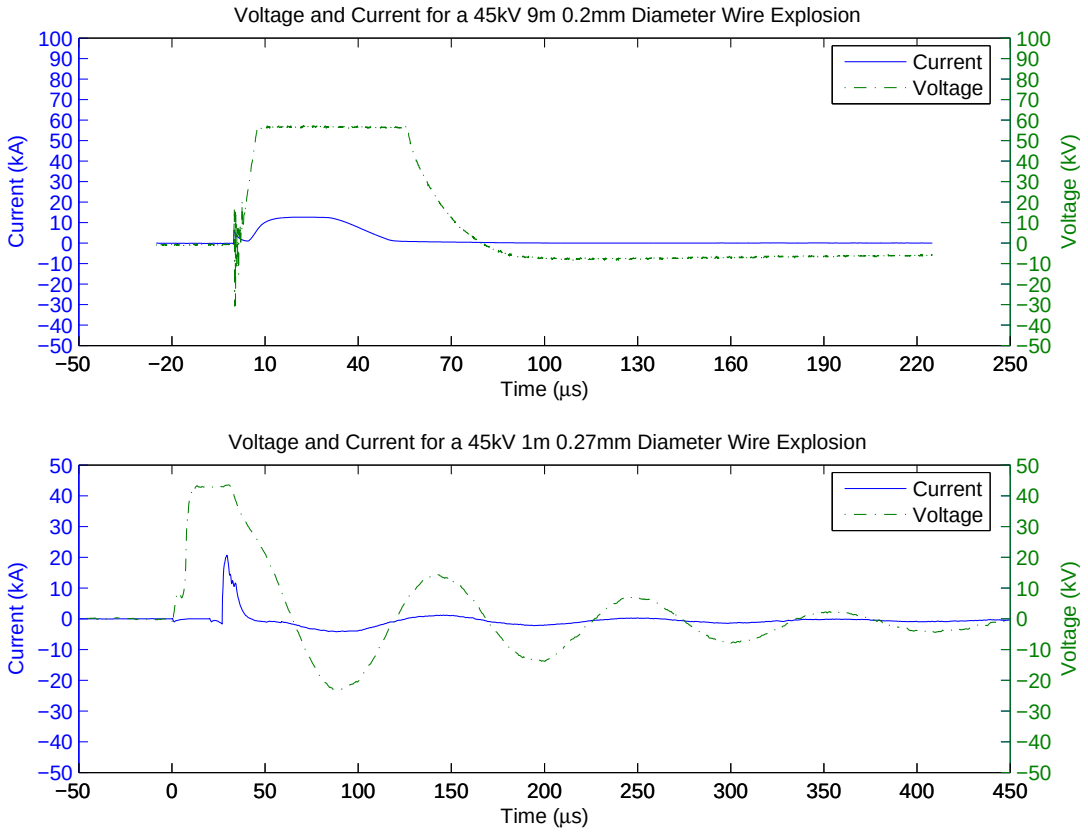
Voltage and Current for a 45kV 9m 0.2mm Diameter Wire Explosion
Current
Voltage
Current (kA)
Voltage (kV)
Time (μs)
Voltage and Current for a 45kV 1m 0.27mm Diameter Wire Explosion
Current
Voltage
Current (kA)
Voltage (kV)
Time (μs)

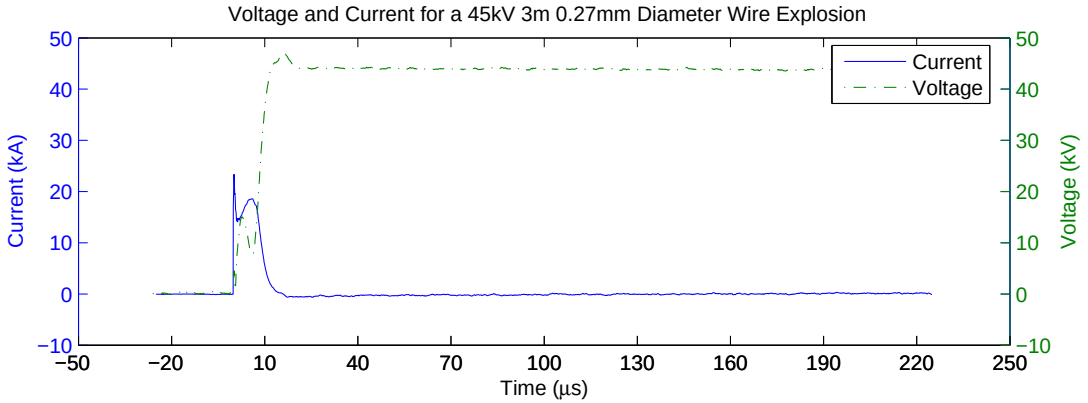
Voltage and Current for a 45kV 3m 0.27mm Diameter Wire Explosion
Current
Voltage
Current (kA)
Voltage (kV)
Time (μs)
50
40
30
20
10
0
−10
−50
−20
10
40
70
100
130
160
190
220
250

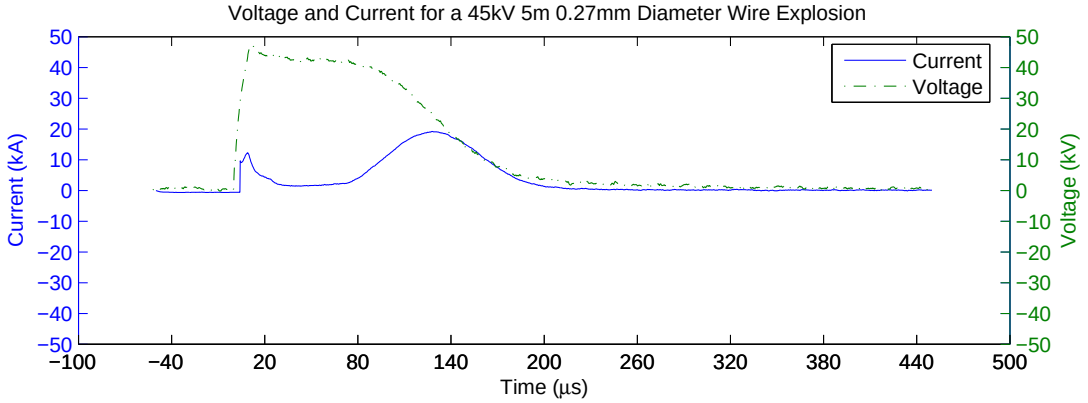
Voltage and Current for a 45kV 5m 0.27mm Diameter Wire Explosion
Current
Voltage
Current (kA)
Voltage (kV)
Time (μs)
50
40
30
20
10
0
−10
−20
−30
−40
−50
−100
−40
20
80
140
200
260
320
380
440
500

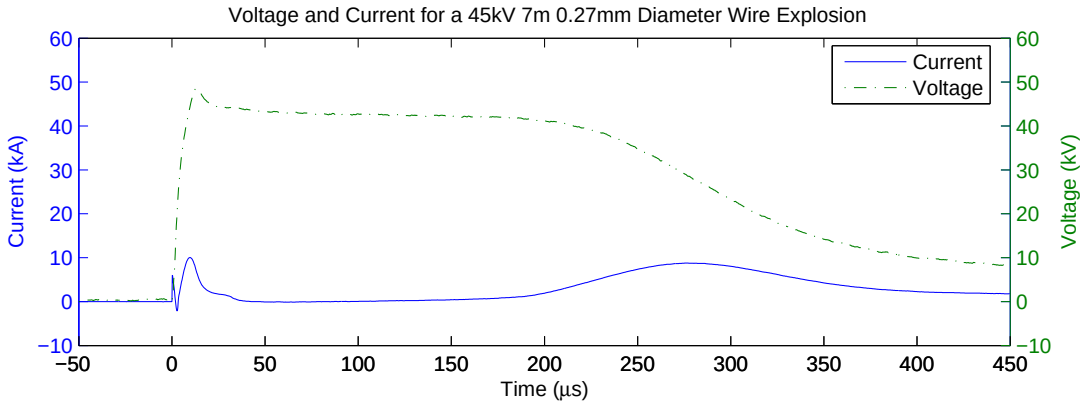
Voltage and Current for a 45kV 7m 0.27mm Diameter Wire Explosion
Current
Voltage
Current (kA)
Voltage (kV)
Time (μs)
60
50
40
30
20
10
0
−10
−50
0
50
100
150
200
250
300
350
400
450

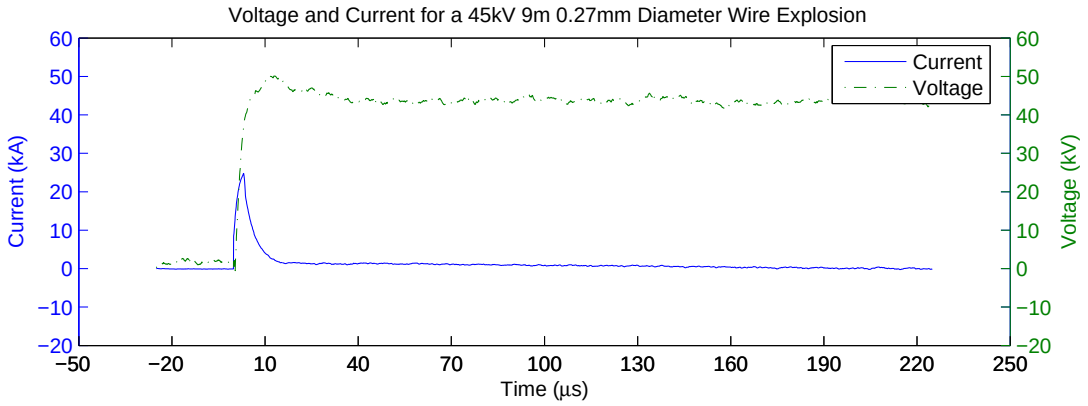
Voltage and Current for a 45kV 9m 0.27mm Diameter Wire Explosion
Current
Voltage
Current (kA)
Voltage (kV)
Time (μs)
60
50
40
30
20
10
0
−10
−20
−50
−20
10
40
70
100
130
160
190
220
250

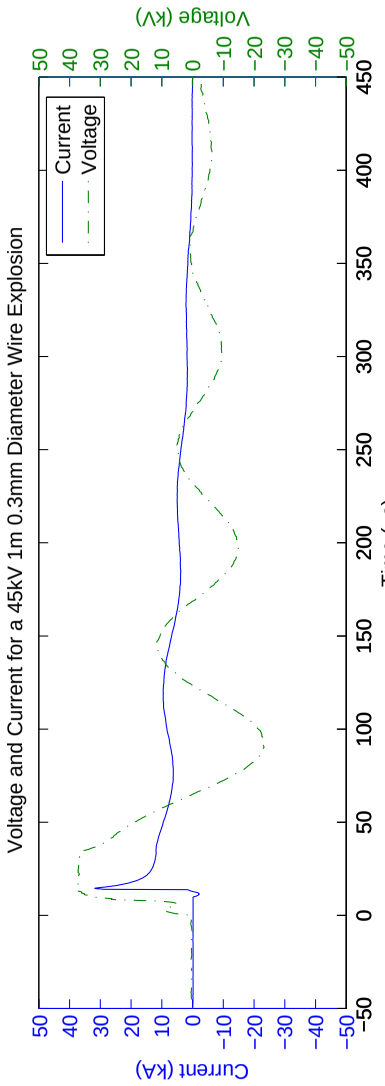
Voltage and Current for a 45kV 1m 0.3mm Diameter Wire Explosion
Current
Voltage
Current (kA)
Voltage (kV)
Time (µs)
50
40
30
20
10
0
−10
−20
−30
−40
−50
−50
0
50
100
150
200
250
300
350
400
450

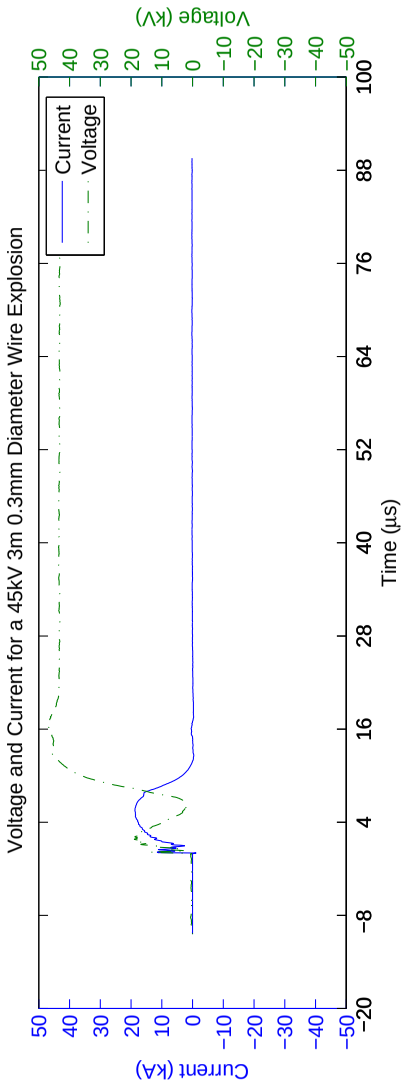
Voltage and Current for a 45kV 3m 0.3mm Diameter Wire Explosion
Current
Voltage
Current (kA)
Voltage (kV)
Time (µs)
50
40
30
20
10
0
−10
−20
−30
−40
−50
−20
−8
4
16
28
40
52
64
76
88
100

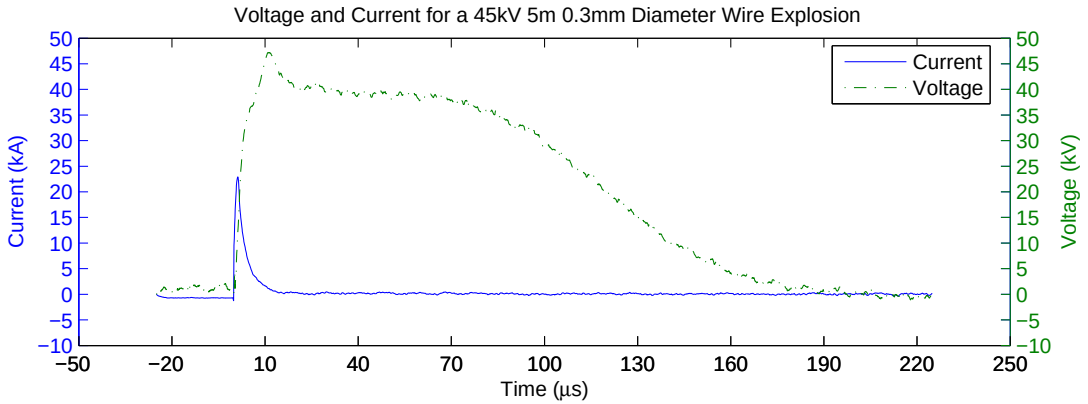
Voltage and Current for a 45kV 5m 0.3mm Diameter Wire Explosion
Current
Voltage
Current (kA)
Voltage (kV)
Time (µs)
50
45
40
35
30
25
20
15
10
5
0
−5
−10
−50
−20
10
40
70
100
130
160
190
220
250

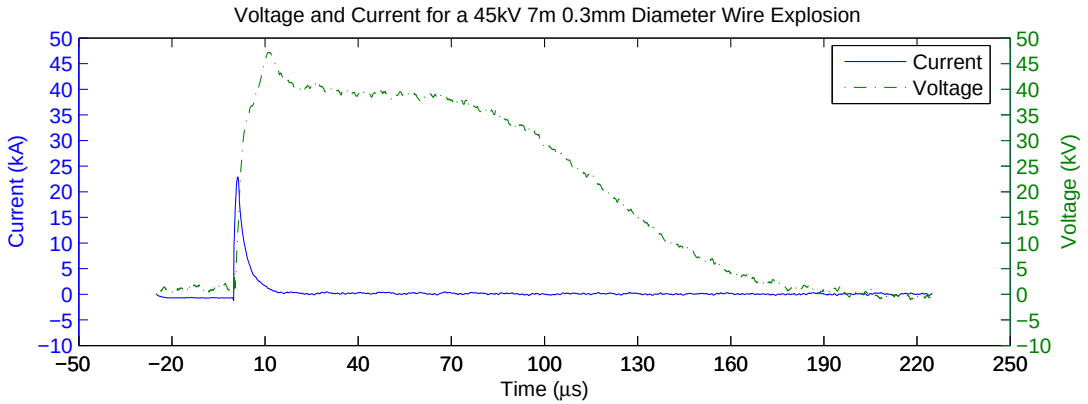
Voltage and Current for a 45kV 7m 0.3mm Diameter Wire Explosion
Current
Voltage
Current (kA)
Voltage (kV)
Time (µs)
50
45
40
35
30
25
20
15
10
5
0
−5
−10
−50
−20
10
40
70
100
130
160
190
220
250

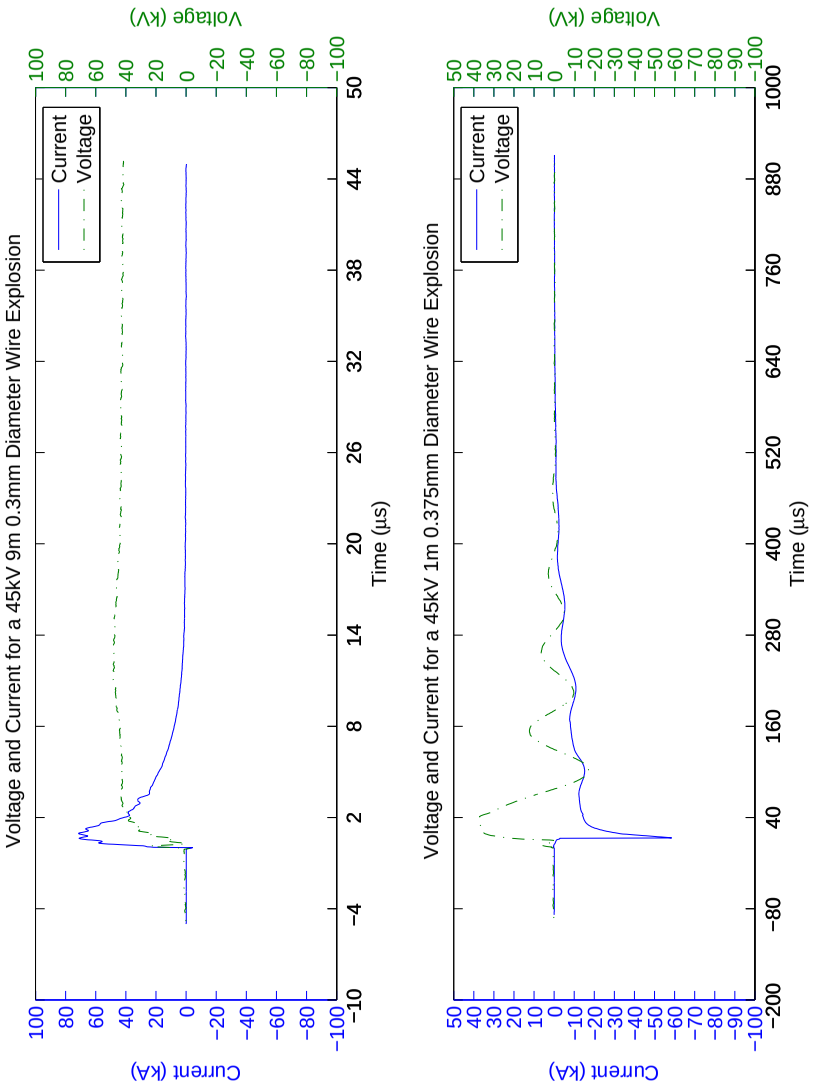
Voltage and Current for a 45kV 9m 0.3mm Diameter Wire Explosion
Current
Voltage
Current (kA)
Voltage (kV)
Time (µs)
Voltage and Current for a 45kV 1m 0.375mm Diameter Wire Explosion
Current
Voltage
Current (kA)
Voltage (kV)
Time (µs)

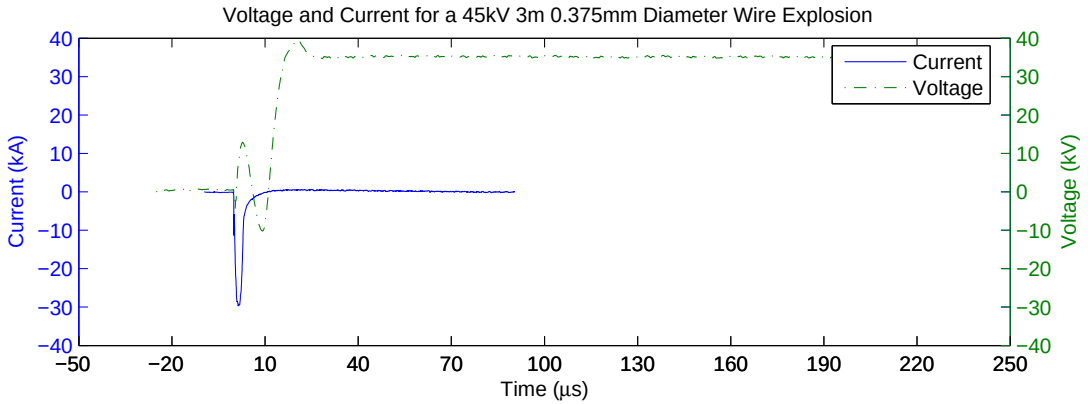
Voltage and Current for a 45kV 3m 0.375mm Diameter Wire Explosion
Current
Voltage
Current (kA)
Voltage (kV)
Time (μs)
40
30
20
10
0
−10
−20
−30
−40
−50
−20
10
40
70
100
130
160
190
220
250

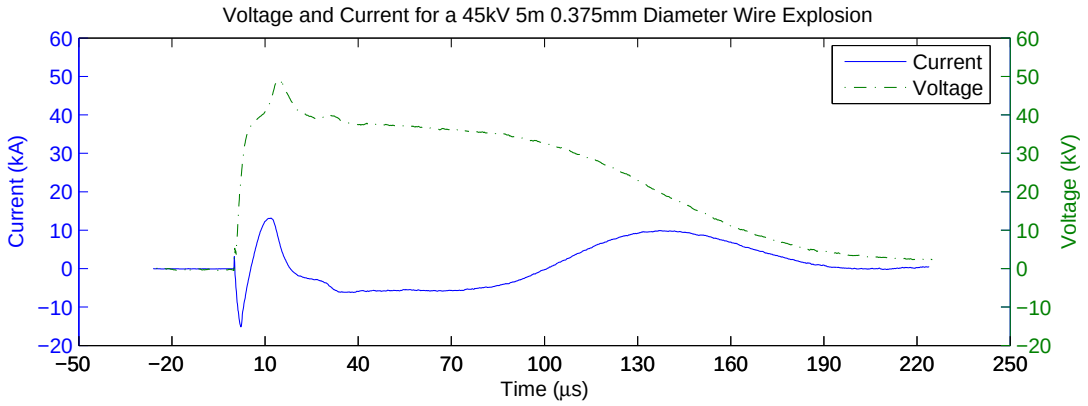
Voltage and Current for a 45kV 5m 0.375mm Diameter Wire Explosion
Current
Voltage
Current (kA)
Voltage (kV)
Time (μs)
60
50
40
30
20
10
0
−10
−20
−50
−20
10
40
70
100
130
160
190
220
250

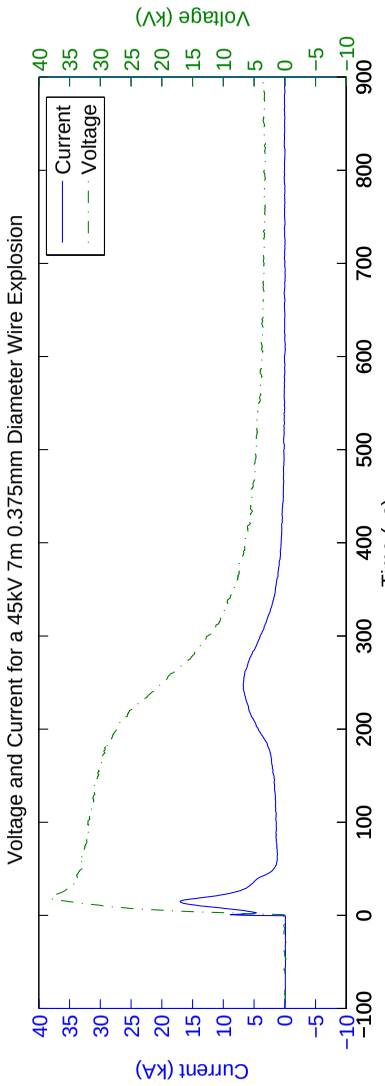
Voltage and Current for a 45kV 7m 0.375mm Diameter Wire Explosion
Current
Voltage
Current (kA)
Voltage (kV)
Time (µs)
40
35
30
25
20
15
10
5
0
−5
−10
−100
0
100
200
300
400
500
600
700
800
900

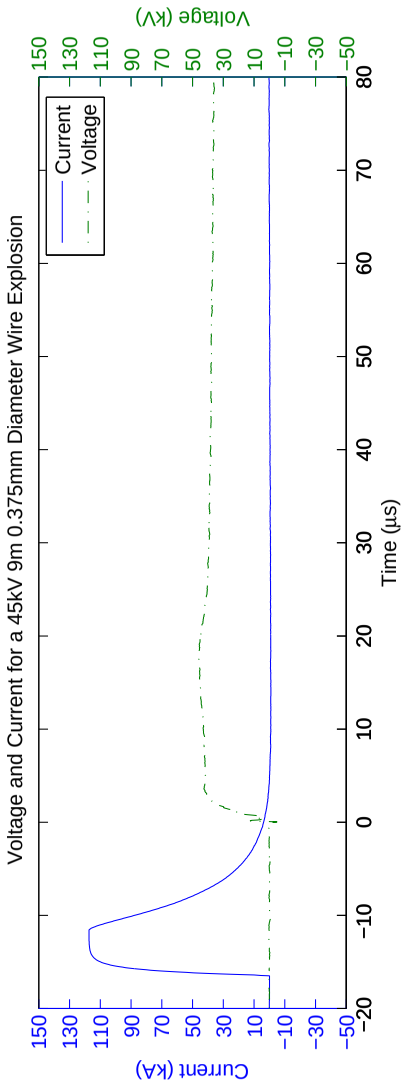
Voltage and Current for a 45kV 9m 0.375mm Diameter Wire Explosion
Current
Voltage
Current (kA)
Voltage (kV)
Time (µs)
150
130
110
90
70
50
30
10
−10
−30
−50
−20
−10
0
10
20
30
40
50
60
70
80

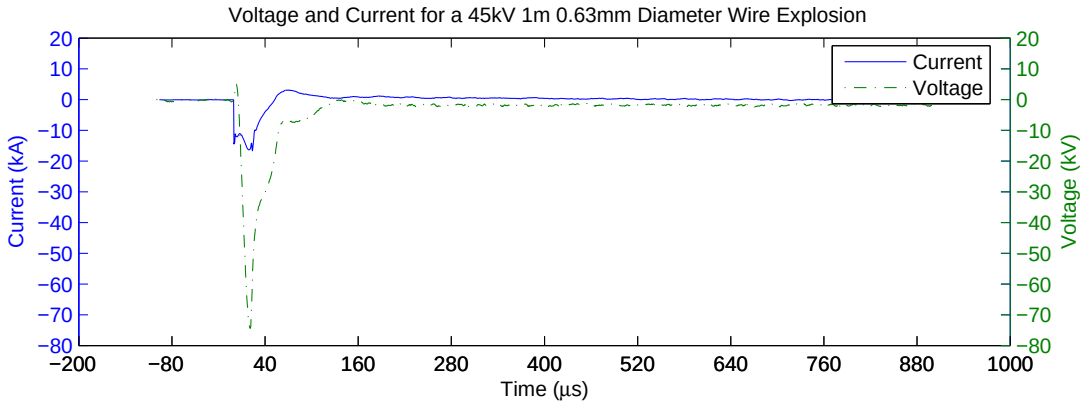
Voltage and Current for a 45kV 1m 0.63mm Diameter Wire Explosion
Current
Voltage
Current (kA)
Voltage (kV)
Time (µs)
20
10
0
−10
−20
−30
−40
−50
−60
−70
−80
−200
−80
40
160
280
400
520
640
760
880
1000

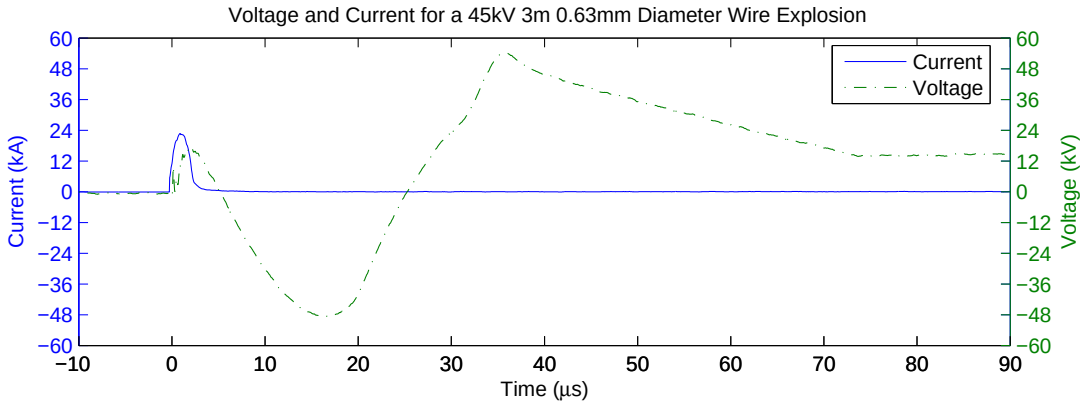
Voltage and Current for a 45kV 3m 0.63mm Diameter Wire Explosion
Current
Voltage
Current (kA)
Voltage (kV)
Time (µs)
60
48
36
24
12
0
−12
−24
−36
−48
−60
−10
0
10
20
30
40
50
60
70
80
90

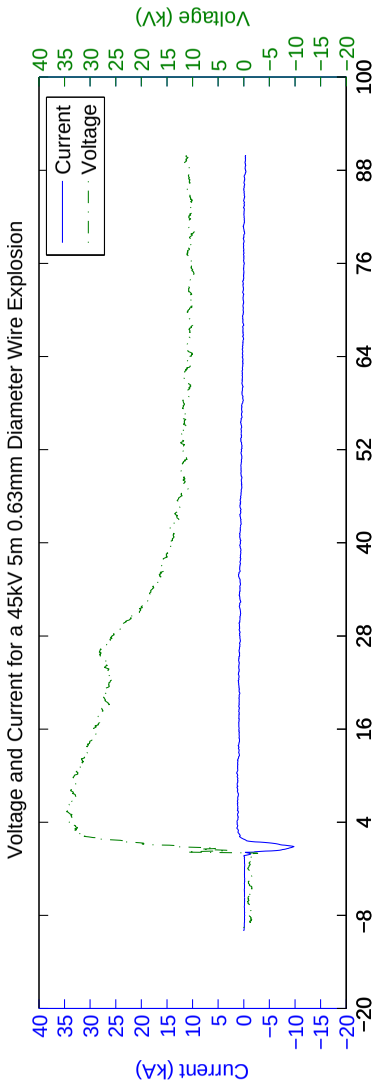
Voltage and Current for a 45kV 5m 0.63mm Diameter Wire Explosion
Current
Voltage
Current (kA)
Voltage (kV)
Time (µs)
40
35
30
25
20
15
10
5
0
−5
−10
−15
−20
−20
−8
4
16
28
40
52
64
76
88
100

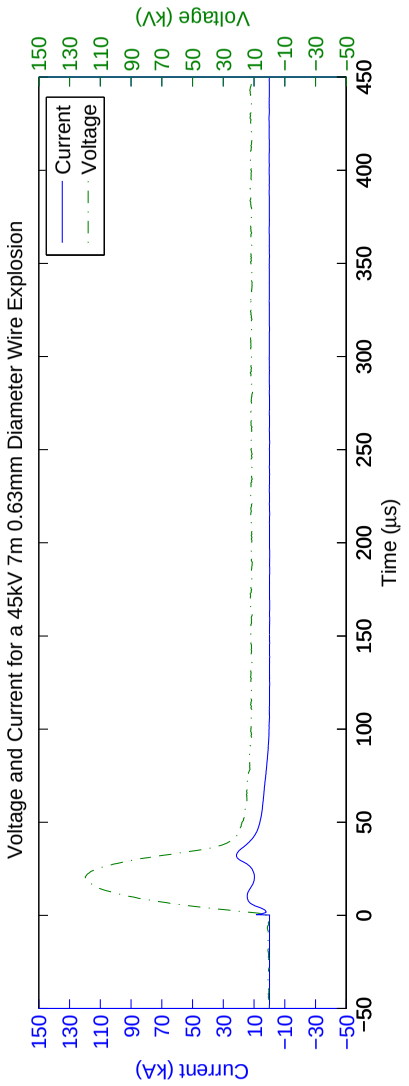
Voltage and Current for a 45kV 7m 0.63mm Diameter Wire Explosion
Current
Voltage
Current (kA)
Voltage (kV)
Time (µs)
150
130
110
90
70
50
30
10
−10
−30
−50
−50
0
50
100
150
200
250
300
350
400
450

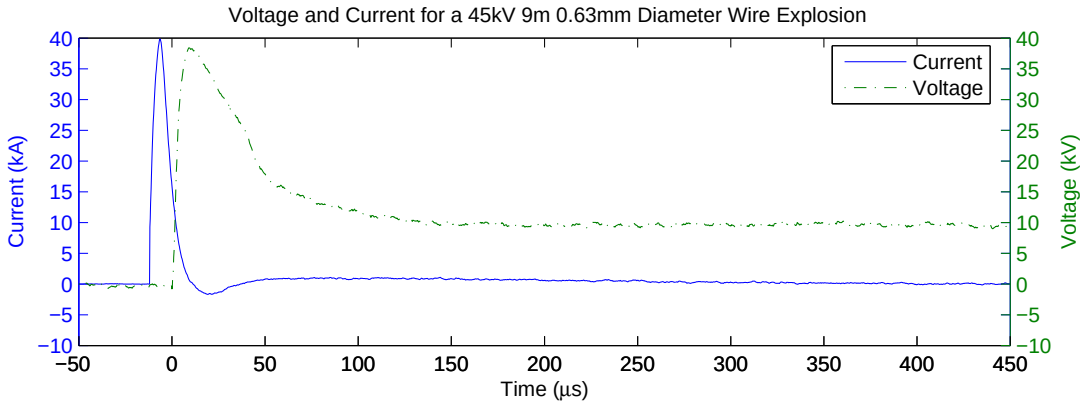
Voltage and Current for a 45kV 9m 0.63mm Diameter Wire Explosion
Current
Voltage
Current (kA)
Voltage (kV)
Time (µs)
40
35
30
25
20
15
10
5
0
−5
−10
−50
0
50
100
150
200
250
300
350
400
450

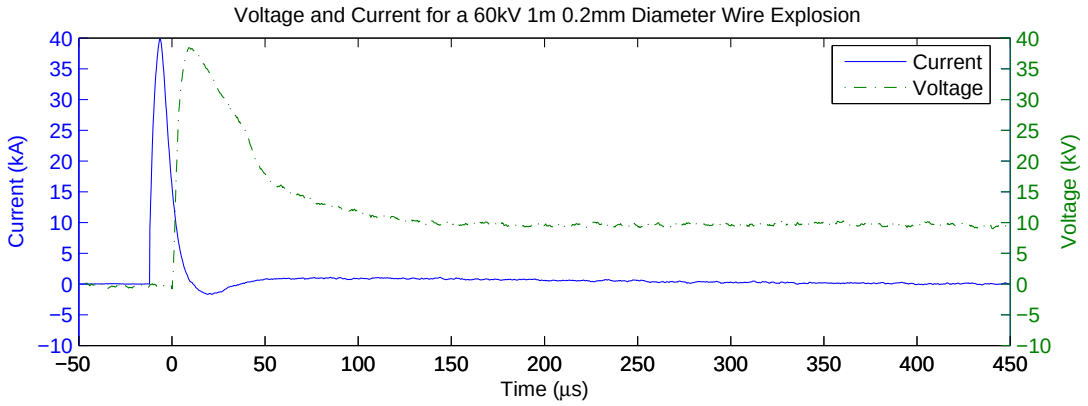
Voltage and Current for a 60kV 1m 0.2mm Diameter Wire Explosion
Current
Voltage
Current (kA)
Voltage (kV)
Time (µs)
40
35
30
25
20
15
10
5
0
−5
−10
−50
0
50
100
150
200
250
300
350
400
450

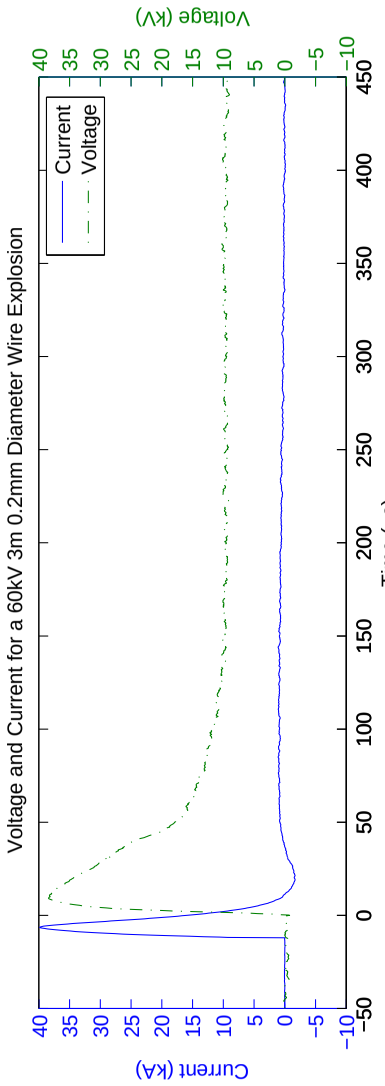
Voltage and Current for a 60kV 3m 0.2mm Diameter Wire Explosion
Current
Voltage
Current (kA)
Voltage (kV)
Time (µs)
40
35
30
25
20
15
10
5
0
−5
−10
−50
0
50
100
150
200
250
300
350
400
450

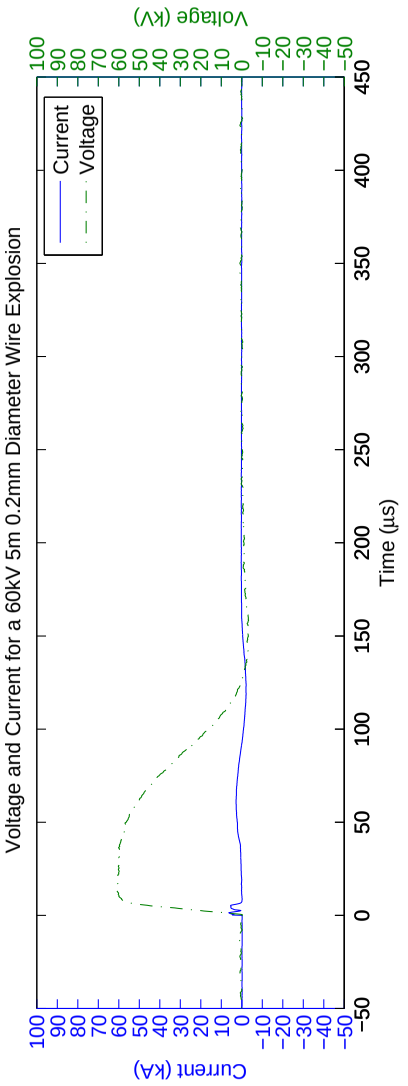
Voltage and Current for a 60kV 5m 0.2mm Diameter Wire Explosion
Current
Voltage
Current (kA)
Voltage (kV)
Time (µs)
100
90
80
70
60
50
40
30
20
10
0
−10
−20
−30
−40
−50
0
50
100
150
200
250
300
350
400
450

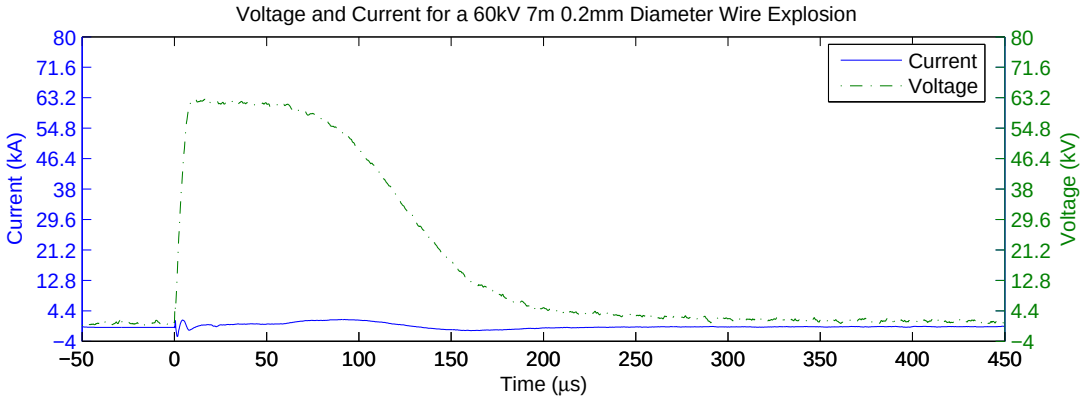
Voltage and Current for a 60kV 7m 0.2mm Diameter Wire Explosion
Current
Voltage
Current (kA)
Voltage (kV)
Time (μs)
80
71.6
63.2
54.8
46.4
38
29.6
21.2
12.8
4.4
−4
−50
0
50
100
150
200
250
300
350
400
450

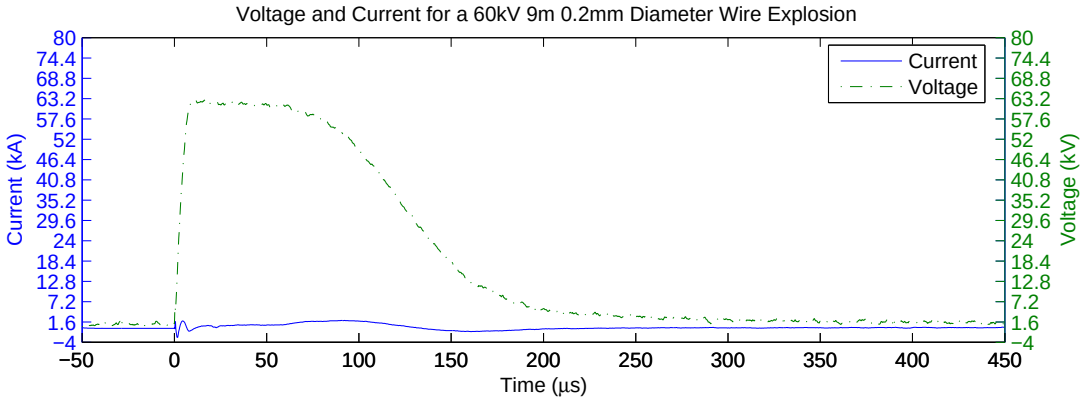
Voltage and Current for a 60kV 9m 0.2mm Diameter Wire Explosion
Current
Voltage
Current (kA)
Voltage (kV)
Time (μs)
80
74.4
68.8
63.2
57.6
52
46.4
40.8
35.2
29.6
24
18.4
12.8
7.2
1.6
−4
−50
0
50
100
150
200
250
300
350
400
450

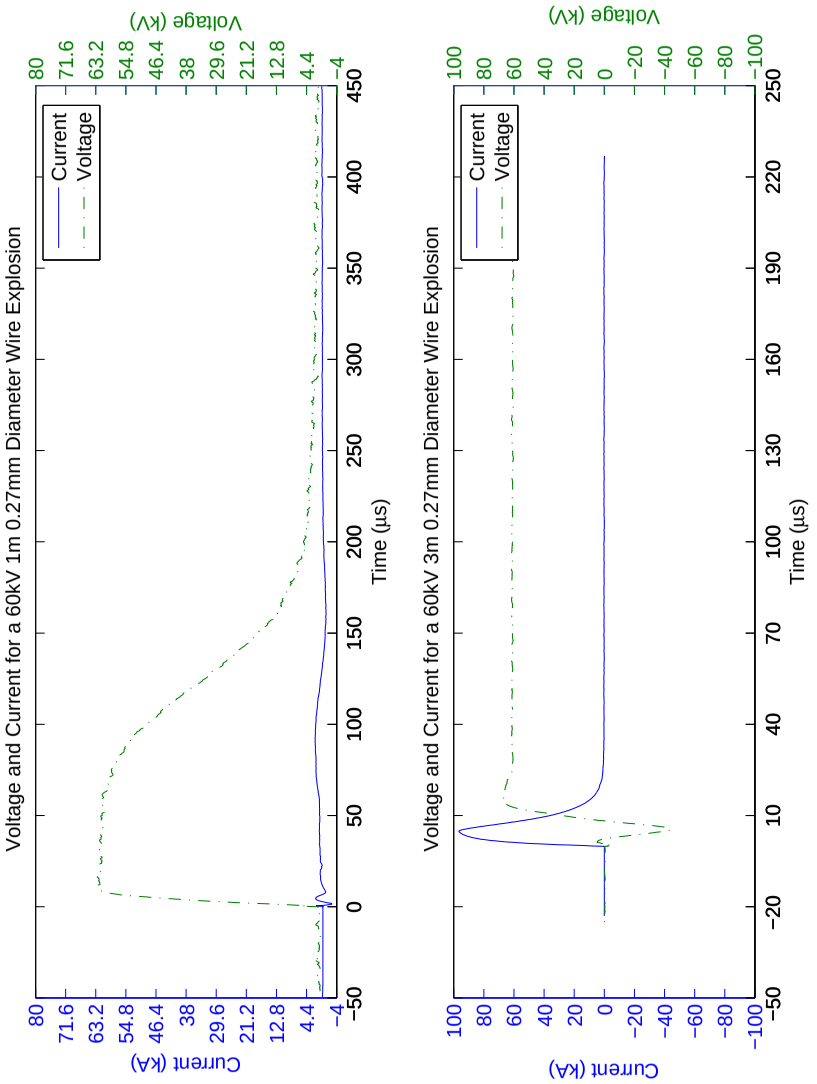
Voltage and Current for a 60kV 1m 0.27mm Diameter Wire Explosion
Current
Voltage
Current (kA)
Voltage (kV)
Time (µs)
80
71.6
63.2
54.8
46.4
38
29.6
21.2
12.8
4.4
−4
−50
0
50
100
150
200
250
300
350
400
450
Voltage and Current for a 60kV 3m 0.27mm Diameter Wire Explosion
Current
Voltage
Current (kA)
Voltage (kV)
Time (µs)
100
80
60
40
20
0
−20
−40
−60
−80
−100
−50
−20
10
40
70
100
130
160
190
220
250

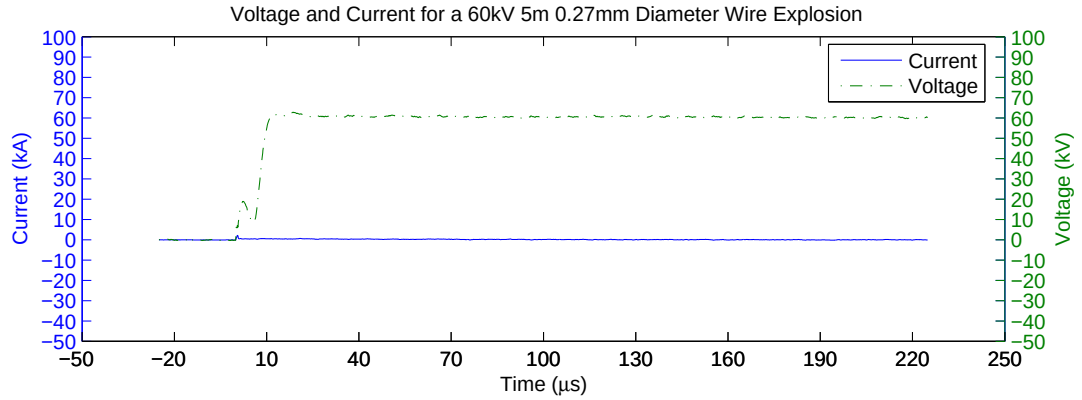
Voltage and Current for a 60kV 5m 0.27mm Diameter Wire Explosion
Current
Voltage
Current (kA)
Voltage (kV)
Time (μs)
100
90
80
70
60
50
40
30
20
10
0
−10
−20
−30
−40
−50
−50
−20
10
40
70
100
130
160
190
220
250

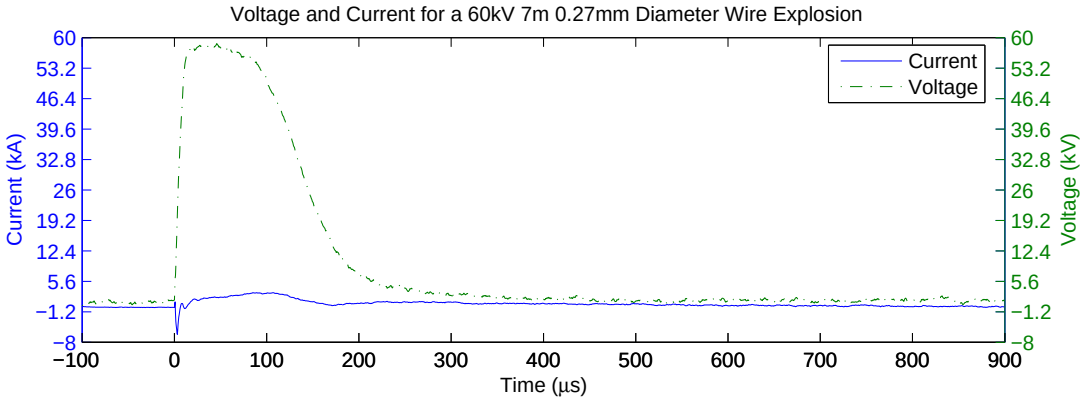
Voltage and Current for a 60kV 7m 0.27mm Diameter Wire Explosion
Current
Voltage
Current (kA)
Voltage (kV)
Time (μs)
60
53.2
46.4
39.6
32.8
26
19.2
12.4
5.6
−1.2
−8
−100
0
100
200
300
400
500
600
700
800
900

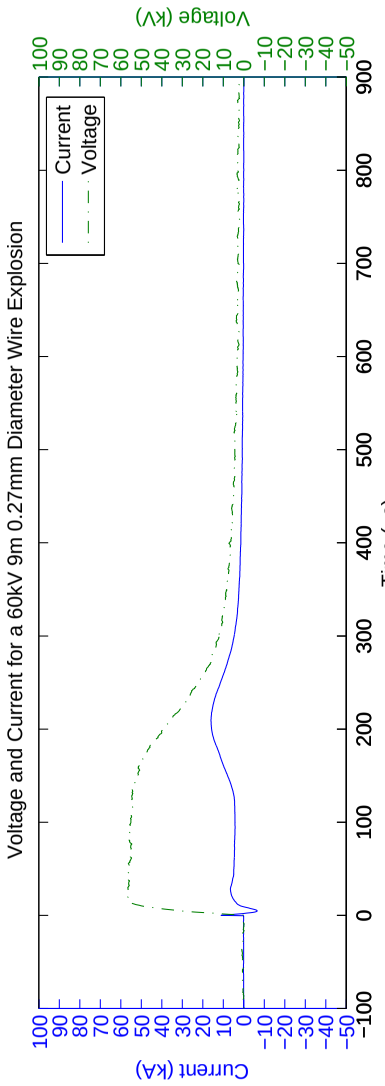
Voltage and Current for a 60kV 9m 0.27mm Diameter Wire Explosion
Current
Voltage
Current (kA)
Voltage (kV)
Time (µs)
100
90
80
70
60
50
40
30
20
10
0
−10
−20
−30
−40
−50
−100
0
100
200
300
400
500
600
700
800
900

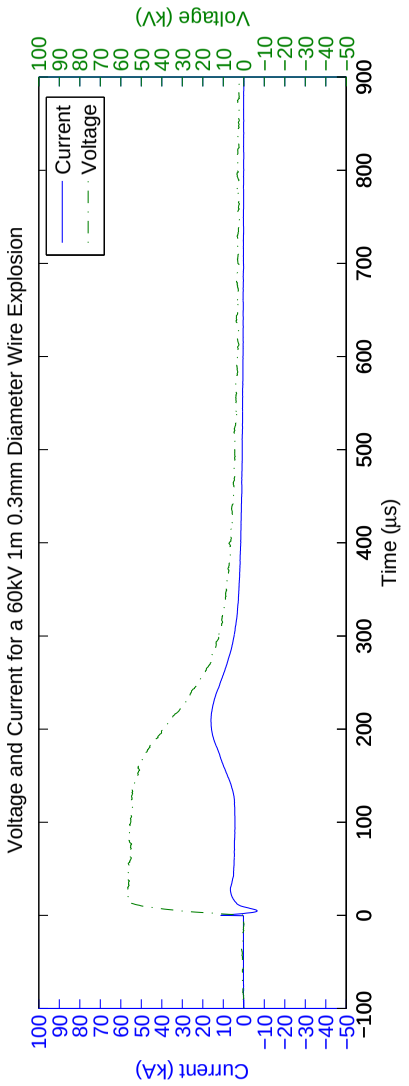
Voltage and Current for a 60kV 1m 0.3mm Diameter Wire Explosion
Current
Voltage
Current (kA)
Voltage (kV)
Time (µs)
100
90
80
70
60
50
40
30
20
10
0
−10
−20
−30
−40
−50
−100
0
100
200
300
400
500
600
700
800
900

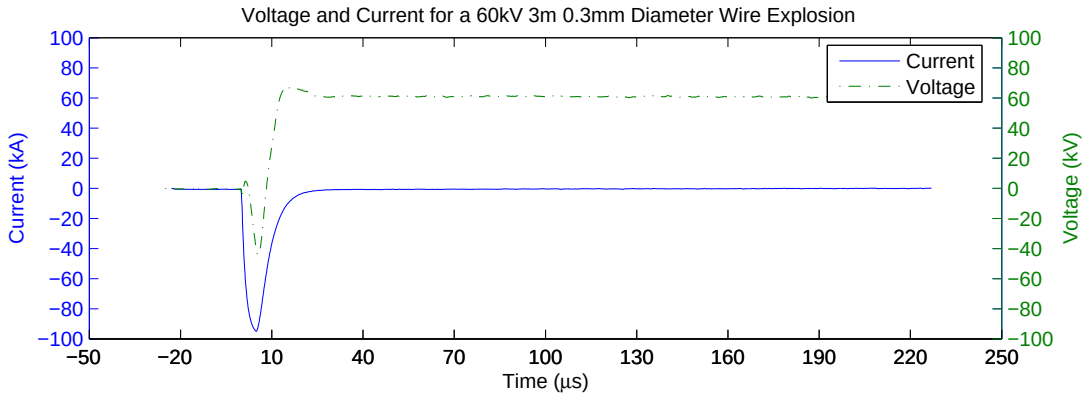
Voltage and Current for a 60kV 3m 0.3mm Diameter Wire Explosion
Current
Voltage
Current (kA)
Voltage (kV)
Time (μs)
100
80
60
40
20
0
−20
−40
−60
−80
−100
−50
−20
10
40
70
100
130
160
190
220
250

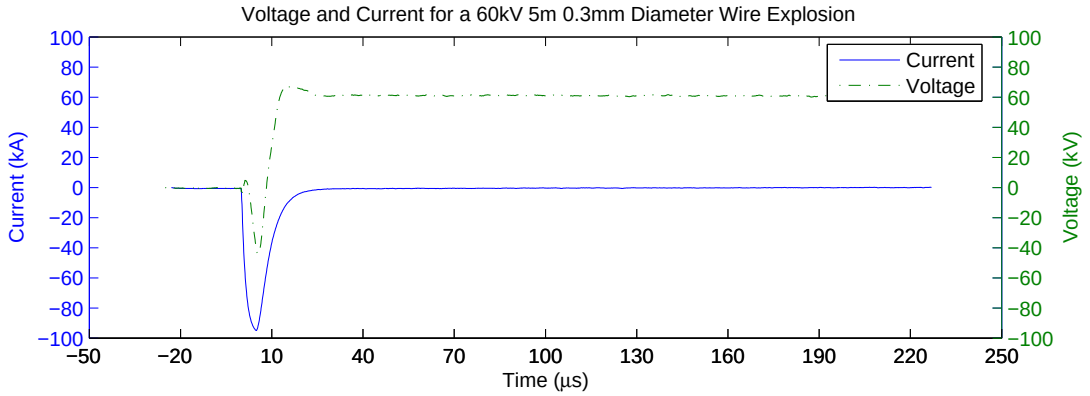
Voltage and Current for a 60kV 5m 0.3mm Diameter Wire Explosion
Current
Voltage
Current (kA)
Voltage (kV)
Time (μs)
100
80
60
40
20
0
−20
−40
−60
−80
−100
−50
−20
10
40
70
100
130
160
190
220
250

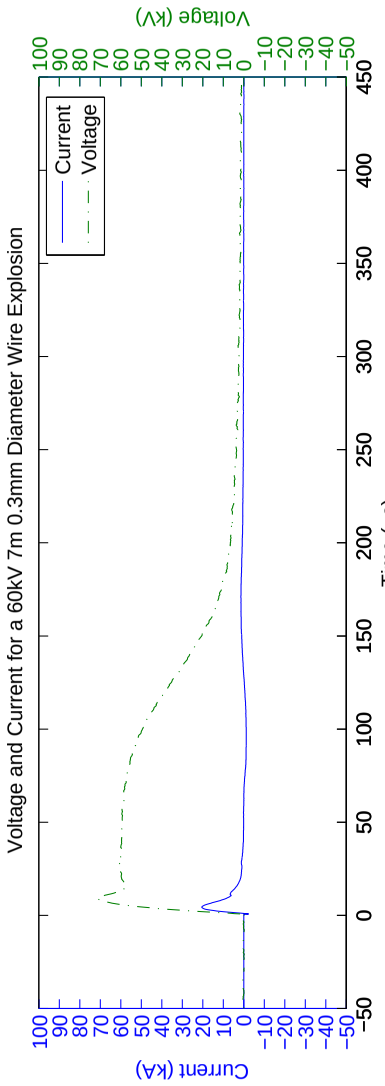
Voltage and Current for a 60kV 7m 0.3mm Diameter Wire Explosion
Current
Voltage
Current (kA)
Voltage (kV)
Time (µs)
100
90
80
70
60
50
40
30
20
10
0
−10
−20
−30
−40
−50
−50
0
50
100
150
200
250
300
350
400
450

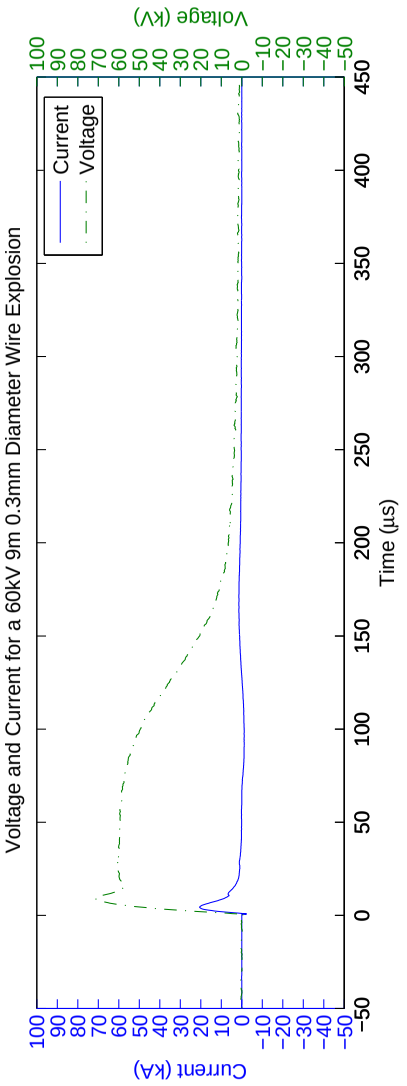
Voltage and Current for a 60kV 9m 0.3mm Diameter Wire Explosion
Current
Voltage
Current (kA)
Voltage (kV)
Time (µs)
100
90
80
70
60
50
40
30
20
10
0
−10
−20
−30
−40
−50
−50
0
50
100
150
200
250
300
350
400
450

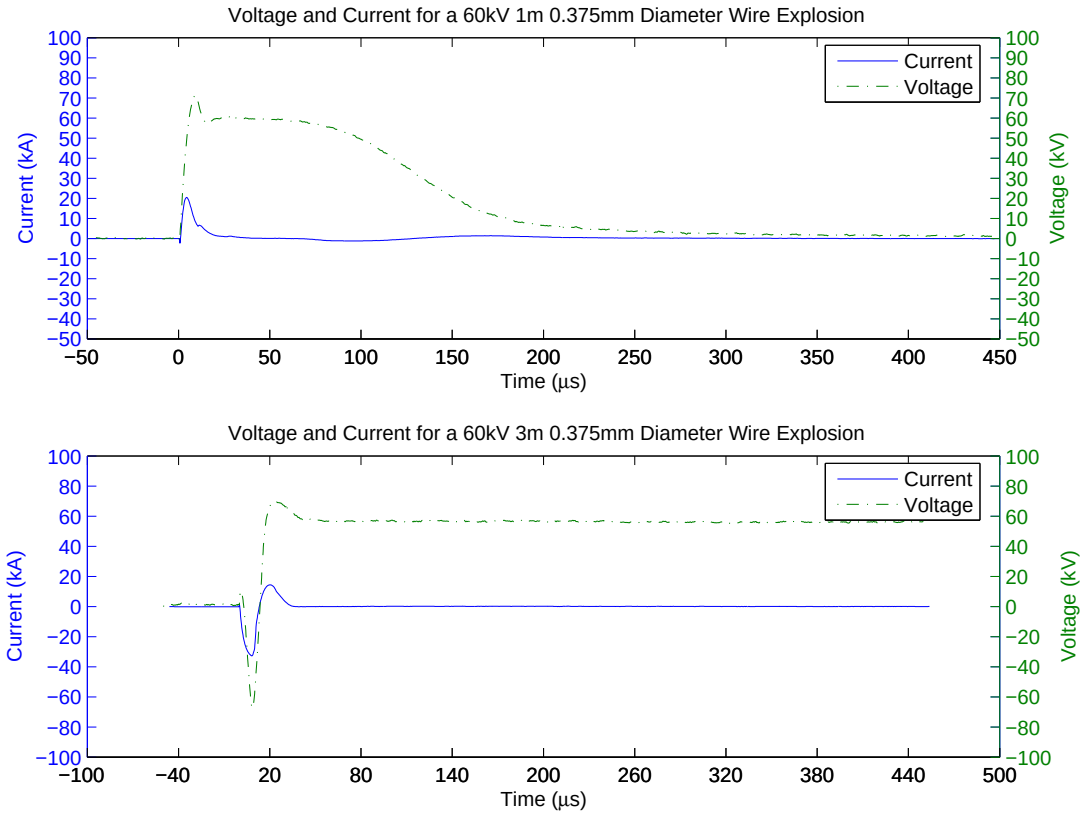
Voltage and Current for a 60kV 1m 0.375mm Diameter Wire Explosion
Current
Voltage
Current (kA)
Voltage (kV)
Time (μs)
Voltage and Current for a 60kV 3m 0.375mm Diameter Wire Explosion
Current
Voltage
Current (kA)
Voltage (kV)
Time (μs)

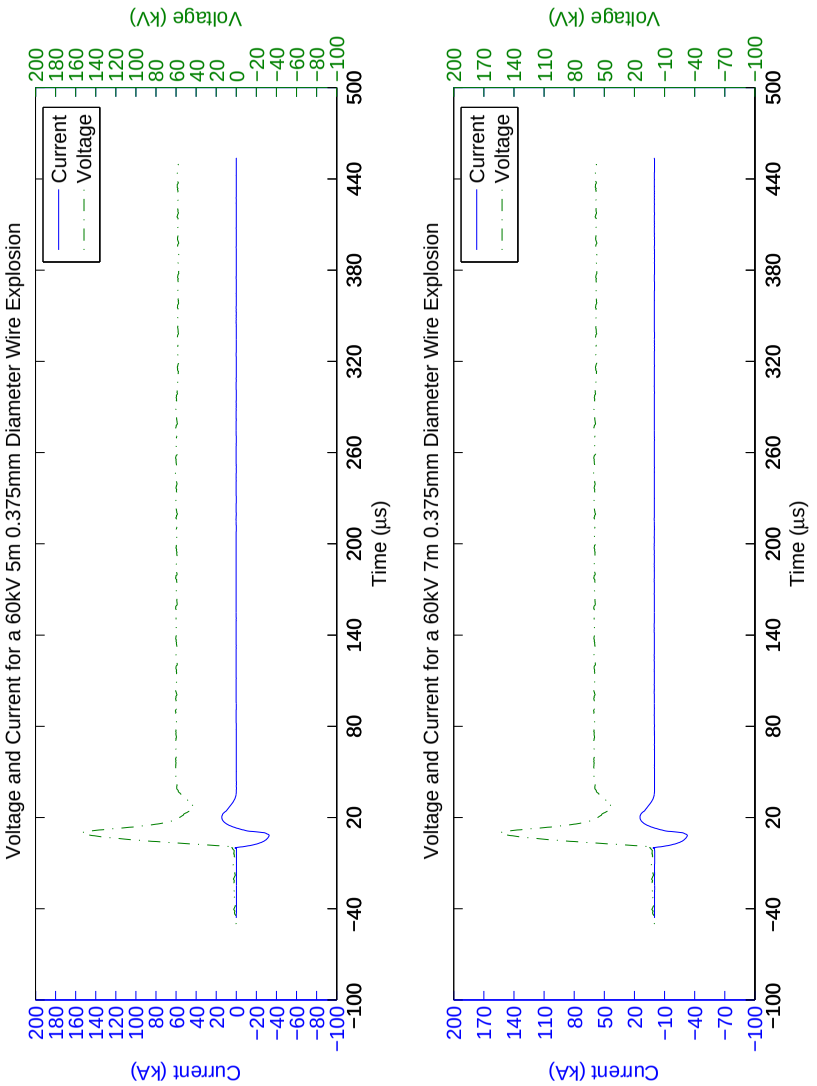
Voltage and Current for a 60kV 5m 0.375mm Diameter Wire Explosion
Current
Voltage
Current (kA)
Voltage (kV)
Time (µs)
200
180
160
140
120
100
80
60
40
20
0
−20
−40
−60
−80
−100
−100
−40
20
80
140
200
260
320
380
440
500

Voltage and Current for a 60kV 7m 0.375mm Diameter Wire Explosion
Current
Voltage
Current (kA)
Voltage (kV)
Time (µs)
200
170
140
110
80
50
20
−10
−40
−70
−100
−100
−40
20
80
140
200
260
320
380
440
500

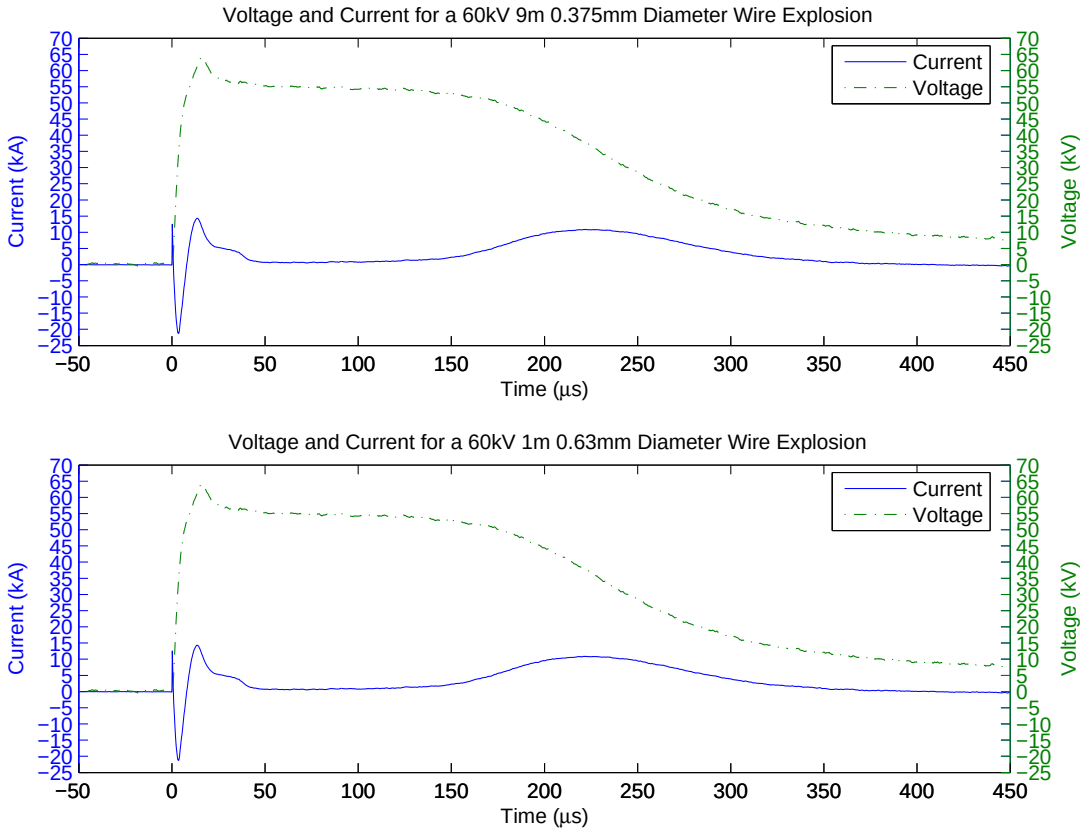
Voltage and Current for a 60kV 9m 0.375mm Diameter Wire Explosion
Current
Voltage
Current (kA)
Voltage (kV)
Time (μs)
Voltage and Current for a 60kV 1m 0.63mm Diameter Wire Explosion
Current
Voltage
Current (kA)
Voltage (kV)
Time (μs)

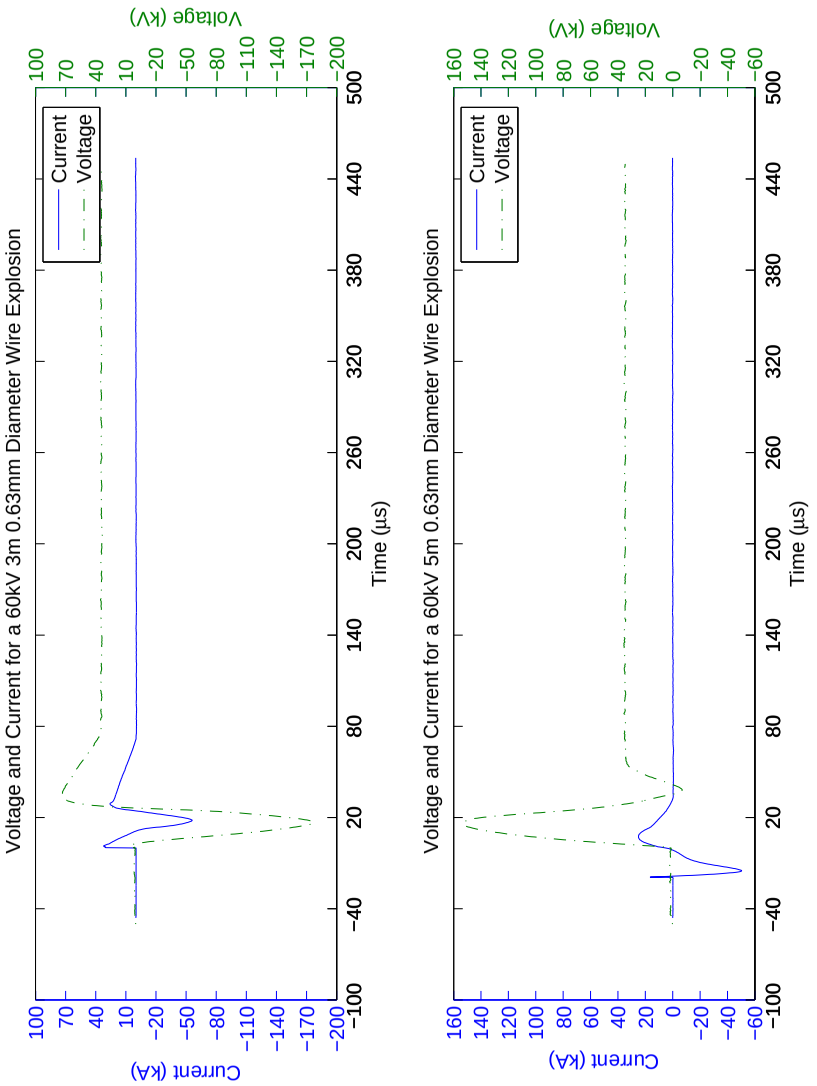
Voltage and Current for a 60kV 3m 0.63mm Diameter Wire Explosion
Current
Voltage
Time (µs)
Current (kA)
Voltage (kV)
100
70
40
10
−20
−50
−80
−110
−140
−170
−200
−100
−40
20
80
140
200
260
320
380
440
500

Voltage and Current for a 60kV 5m 0.63mm Diameter Wire Explosion
Current
Voltage
Time (µs)
Current (kA)
Voltage (kV)
160
140
120
100
80
60
40
20
0
−20
−40
−60
−100
−40
20
80
140
200
260
320
380
440
500

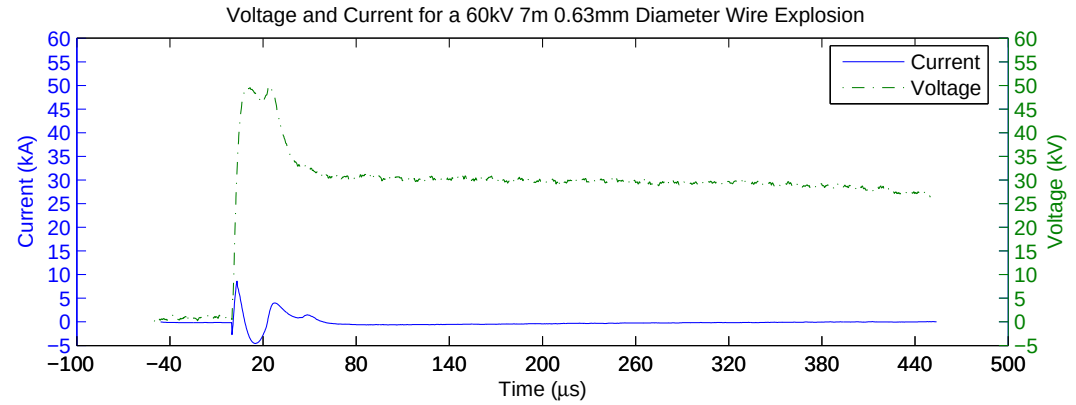
Voltage and Current for a 60kV 7m 0.63mm Diameter Wire Explosion
Current
Voltage
Current (kA)
Voltage (kV)
Time (μs)
60
55
50
45
40
35
30
25
20
15
10
5
0
−5
−100
−40
20
80
140
200
260
320
380
440
500

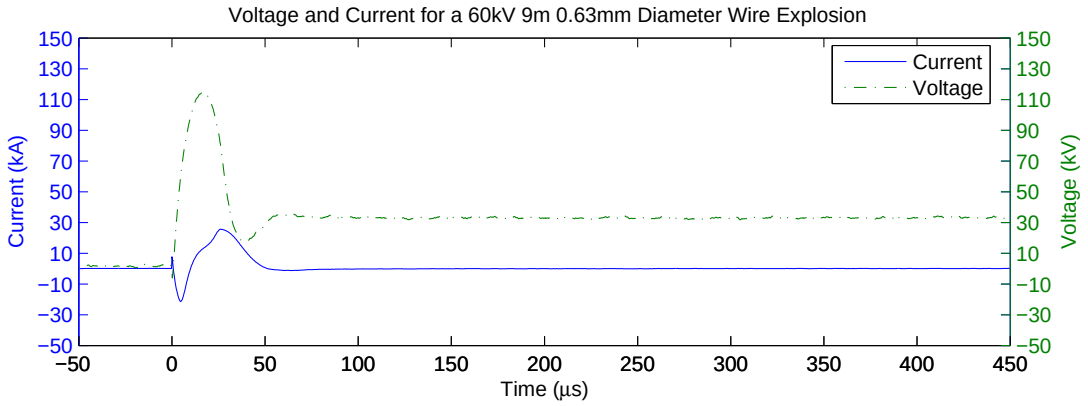
Voltage and Current for a 60kV 9m 0.63mm Diameter Wire Explosion
Current
Voltage
Current (kA)
Voltage (kV)
Time (μs)
150
130
110
90
70
50
30
10
−10
−30
−50
−50
0
50
100
150
200
250
300
350
400
450

REFERENCES

[1] Ieee guide for field testing power apparatus insulation, 1978.

[2] Ieee guide for in-service maintenance and electrical testing of live-line tools, 1984.

[3] Ieee standard test code for high-voltage air switches, 1995.

[4] Ieee std 4-1995 (revision of ieee std 4-1 978) ieee standard techniques for high-voltage testing, 1995.

[5] *Safety Manual - Electricity Industry*. Electricity Engineers' Association of New Zealand, Wellington, 2004 edition, 2004.

[6] Mazen Abdel-Salam. *High-Voltage Engineering: Theory and Practice*. Marcel Dekker, Inc., New York, 2 edition, 2000.

[7] E. Abdi-Jalebi and R. McMahon. High-performance low-cost rogowski transducers and accompanying circuitry. *IEEE Transactions on Instrumentation and Measurement*, 56(3):753–759, 2007.

[8] Andr-Marie Ampre. *Memoir on the Mathematical Theory of Electrodynamic Phenomena, Uniquely Deduced from Experience*. 1827.

[9] F. D. Bennett, H. S. Burden, and D. D. Shear. Expansion of superheated metals. *Journal of Applied Physics*, 45(8):3429–3438, 1974.

[10] B. K. Bhat and I. B. Jordan. Explosion of bare and insulated copper wires. *Journal of Applied Physics*, 42(2):809–814, 1971.

[11] Kenneth H. Carpenter. On the nonexistence of 'ampere tension' in electric conductors. *IEEE Transactions on Magnetics*, MAG-20(6):2159–2160, 1984.

[12] William George Chace, Howard K. Moore, Air Force Cambridge Research Laboratories (U.S.). Geophysics Research Directorate., Air Force Cambridge Research Center (U.S.). Geophysics Research Directorate., and Lowell Technological Institute Research Foundation. *Exploding wires*, volume v. [1]- 1959-. Plenum Press [etc.], New York [etc.], 1959.

[13] David R. Lide (ed). *CRC Handbook of Chemistry and Physics*. CRC Press, Boca Raton, Florida, 84th edition, 2003.

[14] Peter Graneau. Ampere tension in electric conductors. *IEEE Transactions on Magnetics*, MAG-20(2):444–455, 1983.

[15] Peter Graneau. Longitudinal magnet forces. *Journal of Applied Physics*, 55(6 pt 2B):2598–2600, 1983.

[16] D.A. Hammer and D.B. Sinars. Single-wire explosion experiments relevant to the initial stages of wire array z pinches. *Laser and Particle Beams*, 19(3):377–391, 2001.

[17] C.E. Hollandsworth, J.D. Powell, M.J. Keele, and C.R. Hummer. Electrical conduction in exploded segmented wires. *Journal of Applied Physics*, 84(9):4992–5000, 1998.

[18] H. Ja?ger and U. Seydel. Coatings of metallic surfaces by electrical explosions of wires. *Applied Physics*, 2(6):345–347, 1973.

[19] M. Keidar and I. I. Beilis. Vacuum arc plasma jets and their applications. In *IEEE International Conference on Plasma Science*, page 138, 2003.

[20] F.W. Lindner, W. Rudolph, G. Brumme, and Heinz Fischer. Laser initiated spark development in an air gap. *Applied Optics*, 14(9):2225–2228, 1975.

[21] A. Lukyanov and S. Molokov. Flexural vibrations induced in thin metal wires carrying high currents. *Journal of Physics D: Applied Physics*, 34(10):1543–1552, 2001.

[22] A. Lukyanov and S. Molokov. Flexural magneto-elastic vibrations of thin metal wires. *Journal of Physics D: Applied Physics*, 37(5):784–793, 2004.

[23] S. Molokov and J.E. Allen. Theoretical study of wire fragmentation due to high pulsed currents. In *IEE Colloquium (Digest)*, 1996.

[24] S. Molokov and J.E. Allen. The fragmentation of wires carrying electric current. *Journal of Physics D: Applied Physics*, 30(22):3131–3141, 1997.

[25] Edward Nairne. An account of the effect of electricity in shortening wires. by mr. edward nairne, f. r. s. *Philosophical Transactions of the Royal Society of London (1776-1886)*, 70(-1):334–337, 1780.

[26] Edward Nairne. A letter from mr. edward nairne, f. r. s. to sir joseph banks, bart. p. r. s. containing an account of wire being shortened by lightning. *Philosophical Transactions of the Royal Society of London (1776-1886)*, 73(-1):223–225, 1783.

[27] J Nasilowski. Unduloids and striated disintegration of wires. *Exploding Wires*, 3, 1964.

[28] W. F. Ray, W. F. Ray, and C. R. Hewson. High performance rogowski current transducers high performance rogowski current transducers. In C. R. Hewson, editor, *Industry Applications Conference, 2000. Conference Record of the 2000 IEEE*, volume 5, pages 3083–3090 vol.5, 2000.

[29] J. Sekikawa, T. Kitajima, T. Endo, and T. Kubono. Observation of arc-emitted light between slowly opening electrical contacts using a high-speed camera. In *Electrical Contacts, 2004. Proceedings of the 50th IEEE Holm Conference on Electrical Contacts and the 22nd International Conference on Electrical Contacts*, pages 47–52, 2004.

[30] N.M. Shaheen. A simple triggerable spark gap switch for nitrogen lasers. *Measurement Science and Technology*, 1(7):659–661.

[31] D.B. Sinars, T.A. Shelkovenko, S.A. Pikuz, J.B. Greenly, and D.A. Hammer. Exploding aluminum wire expansion rate with 1-4.5 ka per wire. *Physics of Plasmas*, 7(5 I):1555–1563, 2000.

[32] M.J. Taylor. Formation of plasma around wire fragments created by electrically exploded copper wire. *Journal of Physics D: Applied Physics*, 35(7):700–709, 2002.

[33] J. G. Ternan. Equivalence of the lorentz and ampere force laws in magnetostatics. *Journal of Applied Physics*, 57(5):1743–1745, 1985.

[34] D.P. Wall and J.E. Allen. Further studies of the fragmentation of wires due to pulsed currents. *IEE Colloquium (Digest)*, (156):119–122, 2001.

[35] D.P. Wall, J.E. Allen, and S. Molokov. The fragmentation of wires by pulsed currents: Beyond the first fracture. *Journal of Physics D: Applied Physics*, 36(22):2757–2766, 2003.

[36] D. A. Ward, D. A. Ward, and J. La T. Exon. Using rogowski coils for transient current measurements using rogowski coils for transient current measurements. *Engineering Science and Education Journal*, 2(3):105–113, 1993.

[37] C. Zhang, J. Yang, and X. Chi. Research on plasma explosion of metal wire in water. In *Conference Record of IEEE International Symposium on Electrical Insulation*, pages 257–260, 2004.